



## **D4.22: Methods for performing scale-tests for method and model validation of floating wind turbines**

**Edited by: Andreas Manjock**

**With the contribution of:**

**Jose Azcona, Henrik Bredmose, Filippo Campagnolo, Ricardo Pereira and Frank Sandner**

Agreement n.:	308974
Duration	November 2012 – October 2017
Co-ordinator:	DTU

Support by:



---

### **PROPRIETARY RIGHTS STATEMENT**

This document contains information, which is proprietary to the “INN WIND.EU” Consortium. Neither this document nor the information contained herein shall be used, duplicated or communicated by any means to any third party, in whole or in parts, except with prior written consent of the “INN WIND.EU” consortium.

---



## Document information

Document Name:	Methods for performing scale-tests for method and model validation
Document Number:	Deliverable D4.22
Authors:	Jose Azcona, Henrik Bredmose, Filippo Campagnolo, Andreas Manjock, Ricardo Pereira, Frank Sander
Document Type	Report
Dissemination level	PU
Review:	Andreas Manjock, DNV GL Energy, Renewables Certification
Date:	22-08-2014
WP:	WP 4 Offshore Foundations and Support Structures
Task:	4.2 Verification and Validation of Design Methods for Floating Structures
Approval:	Approved by Author



## DESCRIPTION OF THE DELIVERY D4.22

<b>-Deliverable No:</b> 4.22	<b>Title:</b> Methods for performing scale-tests for method and model validation
<b>Month Due:</b> 22	<b>Participants:</b> USTUTT, CENER, DNV GL-Energy
<b>Brief Description (3 lines):</b> The deliverable will consist on a document gathering guidelines and recommendations relating the methodology for the testing of scaled models of floating wind turbines at wave tanks. This good practices manual will include a review of existing recommendations and methodologies described in bibliography and will also include recommendations based in the partner's experience. The document will discuss scaling laws, building of scaled models, testing load cases definition, aerodynamic loading integration, post processing of measurements, etc.	
<b>Specific targets:</b> <ol style="list-style-type: none"> <li>1) Discussion of the scaling laws and model building techniques</li> <li>2) Development and discussion of methodologies for the inclusion of the aerodynamic thrust during the wave tank testing</li> <li>3) Recommendations on testing procedures, test cases definition and processing of the results</li> </ol>	
<b>Measure of success:</b> The document shall include comparative analysis of the methodologies for testing, the scaling laws and the procedures, identifying the advantages and disadvantages and discussing the adequacy to the test type, concept of wind turbine and characteristics of the facility. The document will include a series of recommendations for the test campaign definition and the test execution and for the selection of the different methodologies of scaling, the building techniques and the aerodynamic thrust integration.	
<b>Participant contributions:</b> USTUTT: Procedures for scaling and testing floating wind turbines at water tank. Define guidelines for scale model building of specific floating platform concepts. CENER: Testing load cases definition and integration of aerodynamic rotor thrust on the testing. DNV GL-Energy: Methods for scale testing under consideration of mooring lines, and recommendations for scaling including testing procedures and load case definition.	

1	INTRODUCTION	9
1.1	Literature review	9
1.1.1	Commercial Projects	10
1.1.2	Publicly funded projects	11
1.1.3	Aerodynamic Scaling	13
1.1.4	Summary	14
1.2	Overview table of literature review	15
2	SCALING LAWS FOR FLOATING WIND TURBINE TESTS	20
2.1	Froude scaling	20
2.1.1	Scaling of water and air velocities	20
2.1.2	Aerodynamic loads	21
2.1.3	Scaling of structural properties	22
2.1.4	Scaling of external climate	22
2.1.5	Summary of scaling	22
2.1.6	Dimensionless numbers conserved and not conserved with the modified Froude scaling	23
2.2	Scaling of wind and wave conditions	24
2.2.1	Design basis for offshore wind turbines	24
2.2.2	Basic parameters of wind-wave climates	24
2.2.3	Wave climate	28
2.3	Existing wind-wave climate descriptions	31
2.3.1	Full met-ocean data bases from hind-cast modelling	31
2.3.2	The UpWind design basis	31
2.3.3	Joint probability distributions for wind and wave climate	31
2.3.4	Fatigue averaged wind-wave climates	32
2.3.5	Extreme conditions	33
2.4	Scaling of wind-wave conditions for laboratory tests	33
	References to Section 2.2 to 2.4	34
2.5	Model building experience	34
2.5.1	Materials and strength calculations	35
2.5.2	Identification of mass properties	35

2.5.3	Sensors and data transmission	36
	References Chapter 1 and 2	37
3	DEFINITION OF TEST MODEL WITH ROTOR THRUST INTEGRATION (NANTES)	43
3.1	Introduction	43
3.2	Existing Methods for the Wind Thrust integration in Combined Wave and Wind Tests	43
3.3	Description of the New Ducted Fan/Software-in-the-Loop Method	44
3.4	Control of the Ducted Fan	44
3.5	Implementation of the Software-in-the-Loop System	44
3.6	Experimental Validation of the Software-in-the Loop Method	46
3.7	Description of the Floating Wind Turbine Model Used in the Verification	46
3.8	General Parameters of the Floating Wind Turbine in Full Scale	46
3.9	Description of the Scaled Model	47
3.10	Calibration of the Ducted Fan	47
3.11	Analysis of the Dynamic Response of the Fan	48
3.12	Communication Protocol	48
3.13	Discussion of the Results	48
3.13.1	Static Wind Tests	48
3.13.2	Free Decay Tests	49
3.13.3	Combined Irregular Waves and Turbulent Wind Tests	50
3.13.4	Recommendations on the Testing Using the SIL System	52
3.14	Conclusions	53
	References Chapter 3	54
4	TEST PLAN FOR SEMI-SEMISUBMERSIBLE FWT PLATFORM IN WAVE TANK	55
4.1	Introduction	55
4.1.1	Objectives	55
4.1.2	ECN Infrastructure Specifications:	55
4.1.3	Model Description	56
4.1.4	Scaled Model	58
4.1.5	Reference system	59
4.2	Description of the Experiment setup	59
4.2.1	Scaled Model Setup	59
4.2.2	Aerodynamic thrust	61
4.2.3	Proposed Measurements	62

4.2.4	Estimated Measurements Range	62
4.3	Test Matrix	64
4.3.1	Forced Oscillations	64
4.3.2	Regular Waves with Fixed Hull	66
4.3.3	Free Decay Tests	67
4.3.4	Moored Platform Static Displacement	67
4.3.5	Regular Waves with Moored Hull	68
4.3.6	Environmental Conditions Definition	69
4.3.7	Irregular Waves Cases	70
4.3.8	Wind Loading Characterization	70
4.3.9	Combined Wave and Wind Tests	71
4.4	Practical Recommendations	71
	References Chapter 4	72
	APPENDIX TEST CAMPAIGN 10MW FLOATING WIND TURBINE	73
5	INTEGRATION OF POLIMI AERO-SERVO-ELASTIC SCALED MODEL WITH A FROUDE-SCALED FLOATING PLATFORM	76
6	MOORING LINES: ISSUES FOR DESIGN, MODELLING AND DYNAMIC ANALYSIS	86
6.1	Description of Mooring Lines	86
6.2	Evaluation of Mooring Lines and Anchors for Floating Offshore Wind Turbines	86
6.3	Standards and Guidelines for mooring systems	89
6.4	Definition of Load Cases - Extract from chapter 4 from GL 2012 -Guideline for the Certification of Offshore Wind Turbines	95
	Reference Chapter 6	97
7	CONCLUSIONS	98



## 1 INTRODUCTION

Today only a few full scale prototypes are in operation and measurements of existing floating concepts are rare. Therefore experiments with scaled floating models in wave tanks in combination with wind modelling are a cost effective approach to gather data for referencing and validating the dynamics and loads of Floating Offshore Wind Turbines (FOWT).

The numerical simulation tools for calculating motion and dynamics of FOWT are still under development. Many existing codes of the offshore and oil & gas industry provide approved and validated routines describing the dynamics and loading from waves and currents to floating structures. But they lack a sufficient consideration of the wind loaded part of a FOWT caused by turbulent wind, complex rotor aerodynamics and an own control system on top of the structure. This introduces a fully non-linear loading source to the entire system. Additionally, the influence of second order hydrodynamics and mooring line behaviour is not always modelled in sufficient detail. The state-of-the art of simulation codes and tools for FOWT have been documented in detail in the delivery D4.21 of the Innwind.EU project

This Report collects issues from previous tank test campaigns of scaled FOWT, compare the different scaling methodologies, point out critical aspects and show possible alternatives and recommendations for future tests depending on the specific objective. Furthermore, it gives practical recommendations for the modelling and construction of scaled FOWT.

### 1.1 Literature review

For more than twenty years the idea of installing wind power generators offshore on floating foundations is pursued in research and industry. Within many of the past and present projects wave tank tests have been conducted. Overviews of these projects can be found in (EWEA, 2013), (Henderson & Witcher, 2010), (Consulting Main(e) International, September 2012) and (Wang, Utsunomiya, Wee, & Choo, 2010). This chapter is to be seen as a general summary and extension of previous works.

#### Distinction

A global view on model scale tank tests of floating wind turbine systems presents two major differences in the basic motivation:

Firstly, as the used simulation tools have not yet reached a satisfactory state for all load conditions up to this point, model tests are used for **validation purposes**. The current shortcomings in the state of the art of the numerical design of FOWT require that the calculated results are backed by physical testing. As will be assessed in the literature review a number of physical phenomena are not sufficiently taken into account or not taken into account at all by standard numerical models. For example, Sarpkaya (Sarpkaya & Isaacson, 1981) mentions a general problem working with constant potential flow hydrodynamic coefficients which are part of common hydrodynamic analyses. Since they are varying with water depth, dynamic-response analyses and laboratory tests stay “not only desirable but also necessary for structures built in deeper waters”.

Secondly, as the models implied in state-of-the art simulation tools show the mentioned shortcomings it is crucial to assure that the dynamics of the to-be-built system are fully understood in order to take the step towards prototype and full scale turbine realization model tests. For this, state of the art experiments deliver an adequate solution.

#### The Scaling problem

The presence of two different phases of the surrounding medium (air and water) poses a significant problem to scale the considered system geometrically. The general loads acting on offshore structures within classical marine technology can be found in (Faltinsen, 1993). Figure 1-1 shows a sketch of a scaled FOWT system with the associated relevant non-dimensional numbers. Standard

literature focusing on the design of physical models of floating offshore structures mentions that overall model similitude is ensured through geometric, hydrodynamic and structural similitude (Chakrabarti, 1998). For hydrodynamic similitude this means applying Froude, Strouhal, and Reynolds scaling. While Froude scaling also ensures correct Strouhal scaling, it inevitably leads to an error in scaling of the Reynolds number for both, hydro- and aerodynamics. Although the influence of the hydrodynamic Reynolds number mismatch in FOWT systems is generally disregarded in scaled tests it is yet to be found and quantified. It is mentioned that for offshore structures, where rather oscillatory flow occurs introduced by the waves than steady flow, the Keulegan-Carpenter (KC) number is more in the focus than the Reynolds number. However, for normal operation the scaling which preserves Froude or KC number is considered as conservative (Chakrabarti, 1998). In contrast to the hydrodynamic side, the aerodynamic Reynolds number is of high importance, because of the influence on the flow condition around the airfoil during operation of the wind turbine. This issue is subject of the analyses presented in the following and will be discussed in more detail in the chapter *Scaling laws for floating wind turbine tests*.

The following literature review will show how various institutions have addressed this specific scaling problem along with presenting the numerous attempts to gain insight into the complex dynamics of floating wind turbines in order to build full scale systems and increase fidelity of numerical models. Following the detailed description of the projects an overview table shows a short summary of the findings of each study.

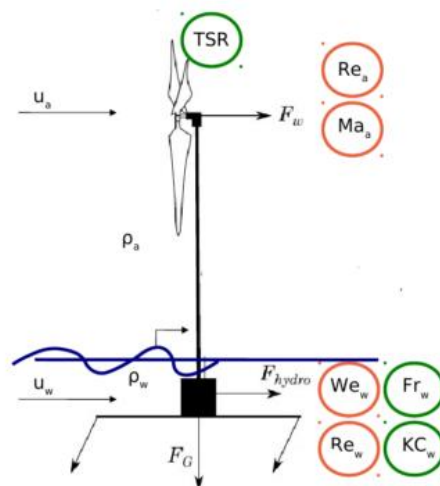


Figure 1-1 Floating wind turbine system and relevant no dimensional numbers, taken from (Bredmose, Larsen, Matha, Rettenmeier, Marino, & Saettran, 2012).

### 1.1.1 Commercial Projects

There have been various commercial projects for the implementation of floating wind energy systems. The projects **Hywind** (Myhr, Maus, & Nygaard, 2011) and **WindFloat** (Roddier, Windfloat: A Floating Foundation For Offshore Wind Turbines Part I: Design Basis And Qualification Process, 2009), (Cermelli, Roddier, & Aubault, 2009), (Aubault, Cermelli, & Roddier, 2009) and (Roddier, Cermelli, Aubault, & Weinstein, 2010), were among the first to gain commercial experience in the years 2009 and 2011, respectively. **Gicon** (Großmann & Dahlhaus, 2013), (Adam, Myland, Dahlhaus, & Großmann, Scale Tests of the Gicon-TLP for Wind Turbines, 2014) and **GustoMSC** with their "Tri-Floater" (Huijs, Mikx, Savenije, & Ridder, 2013), (Courbois, 2013), (Bulder & Henderson, 2002), (Huijs, Ridder, & Savenije, Comparison Of Model Tests And Coupled Simulations For A Semi-Submersible Floating Wind Turbine, 2014) followed in the years after with multiple test campaigns. In Japan the **Fukushima project** (Fukushima Forward) with various phases includes model and prototype tests for a conventional spar concept, a "hybrid spar" and a semi-submersible. The wave

tank tests for the spar concept are documented in (Chujo, Minami, Nimura, & Ishida, 2013). Innovative large-scale offshore floating structures are investigated by **Kyushu University**, (Kyushu University, 2012). Ishihara has developed an innovative multi-turbine foundation and presented model tests in (Ishihara, Phuc, Sukegawa, & Shimada, 2007) and (Ishihara, Waris Bilal, & Sukegawa, A Study On Influence Of Heave Plate On Dynamic Response Of Floating Offshore Wind Turbine System, 2009). The “**Japan Marine United Advance Spar**” was scaled by 1:50 for wave tank tests, (Consulting Main(e) International, September 2012). The large-scale prototype projects in Europe of which tank tests are known are **HiprWind** with a semi-submersible (Quesnel, Bard, & Hanssen, 2011), **BlueH** with a two-bladed semi-submersible concept (Blue H Group, 2012) and the Norwegian **Sway**, which is a tension-leg spar (Sway, 2012). A comparable concept is the **Nautica** wind power layout, for which some information on testing can be found online in (Nautica Windpower, 2012). The multi-turbine concept **WindSea** offers some data on the wave tank tests online, see (Windsea, 2012) and (Scandinavian Oil-Gas Magazine, 2010). Tests were also conducted for the multi-purpose foundation **Poseidon**; see (Floating Power Plant, 2012). This concept was tested in various wave tanks with and without wind and also on site with different prototype scales. The **Pelastar** TLP by Glosten Associates (PelaStar Wind, 2012) was tested but very little information is published. The **Vertiwind** concept by Technip with a vertical-axis wind turbine was tested in a scale of 1:2, see (Pole Mer Paca, 2012). Recently, the **Nautilus** semi-submersible concept, which has also been tested in the Cork wave tank in Ireland, was published in (Aguirre-Suso, et al., 2014). **Iberdrola** is developing a TLP concept and has presented the wave tank test layout in (Amate Lopez, Martín, Marugan García, & Alonso, 2014) with a publication on the most recent test campaign, see (Zamora-Rodríguez, et al., 2014). The University of Maine is involved in a project building the first scaled FOWT prototype in the US called **VolturnUS**; see (Viselli, Goupee, & Dagher, 2014).

### 1.1.2 Publicly funded projects

Various publicly funded research projects have included FOWT wave tank tests. The scope of these tests along with significant findings within the different projects will be presented here.

As part of the **Marinet** project (Bredmose, Larsen, Matha, Rettenmeier, Marino, & Saettran, 2012), state of the art scaling routines were revised and the dynamic-elastic scaling proposed as adequate for scaled FOWT-tests. The **DeepWind** project aimed at an integrated research on vertical-axis floating wind turbine (VFOWT) systems including tests (Paulsen, et al., 2011). A numerical model development of VFOWT together with a wave tank validation is given by (Wang, Moan, & Hansen, 2013).

Within the **Winflo** project (Boulluec, Martin, & Houmard, 2013), 1/40 and 1/25 scale models were developed and tested in order to understand the dynamic behaviour of the concept design and to validate the floater and mooring design. The models included an adapted rotor design, leading to a rotor design with correct scaling of thrust and tip speed ratio. The tests were performed as preparation for building a prototype which is the next step in the project.

The **DeepCwind** (Robertson, et al., 2013) project to this point delivers the most throughout insight available on the capabilities of numerical and experimental investigation of the three major FOWT systems: Tension leg platform (TLP), semi-submersible and spar buoy. Major parts of the research were the assessment of a proper scaling methodology (Martin, Kimball, Viselli, & Goupee, 2012) and its numerical verification, (Robertson A. N., Jonkman, Goupee, Kimball, & Swift, 2012), the realization of a model wind turbine for wave basin testing (Martin H. R., 2011) and the development of thrust scaled blades (Fowler, Iii, Kimball, & Goupee, 2013). Also in the focus were the analysis of the interaction of the mooring dynamics with the global response of the FOWT (Masciola, Robertson, Jonkman, Coulling, & Goupee, 2013) and the calibration and validation of a full scale simulation model within the simulation software FAST (Stewart, Lackner, & Goupee, 2012). In 2013 a new test campaign with the same semi-submersible platform has been performed under improved testing conditions in the MARIN facility in the Netherlands; see (Ridder, Otto, Zondervan, Savenije, & Huijs, 2013). The results together with a comparison to the previous DeepCwind campaign and a model of

a smaller scale (1:130) for a reliability assessment can be found in (Kimball, Goupee, Fowler, Ridder, & Helder, 2014). A code validation of the MLTSIM hydrodynamics code coupled with the FAST software with the same test data can be found in (Koo, Goupee, Lambrakos, & Lim, 2014).

Essential testing experience drawn from DeepCwind can be summarized as follows: Firstly, the blades need to be adequately redesigned in order to produce Froude-scaled thrust forces. This means that new blades with profiles suitable for low Reynolds numbers are needed. The effects of the Reynolds dissimilitude with advanced numerical simulations are shown in (Jain, Robertson, Jonkman, Goupee, Kimball, & Swift, 2012). Also, the presence of consistent wind speed is important for model validation purposes, where aerodynamic interaction between tower and turbine is not considered to full satisfaction, see (Martin, Kimball, Viselli, & Goupee, 2012) and [38]. The instrumentation for the data acquisition of measurements should be of little mass and the cables of negligible stiffness so that the dynamics of the regarded system are not influenced. This could be done by wireless instrumentation. Regarding the fidelity of simulation tools second order hydrodynamics have been found to be an issue for the dynamic behaviour of tested models but are mostly disregarded in custom simulation models. Adding to that, hydrodynamic damping might be incorrectly modelled within simulation tools as well, see (Robertson, et al., 2013). A discussion on the differences of the behaviour of the three different platform concepts can be found in (Goupee, Koo, Lambrakos, & Kimball, 2012).

In another project the development of a spar-type FOWT with significant insight to the design and experimental procedure of FOWT-systems, aiming at the realization of a full scale turbine has been given by **Utsunomiya** (Utsunomiya, Sato, Matsukuma, & Yago, 2009). His tests cover simplified 1/34.5 scale model tests for extreme condition dynamic analysis, see (Utsunomiya, Yoshida, Ookubo, Sato, & Ishida, 2014) and simplified 1/22.5 scale model tests for simulation validation; see (Utsunomiya, Sato, Matsukuma, & Yago, 2009). They reach towards scaled prototype tests in full-scale at-sea-environment (Utsunomiya, et al., 2013) and (Ishida, Kokubun, Nimura, Utsunomiya, Sato, & Yoshida, 2013). His findings include the underestimation of current loads and the response in sway direction by numerical tools in the presence of vortex induced motion; see (Utsunomiya, Yoshida, Ookubo, Sato, & Ishida, 2014). He also documented a negligible effect of a motion suppression device (Utsunomiya, Sato, Matsukuma, & Yago, 2009) and good agreement between prototype measurements and corresponding simulations (Utsunomiya, et al., 2013).

A semi-submersible with a single-point mooring has been tested by **Osaka University** in a scale of 1:100; see (Iijima, Kawai, Nihei, Murai, & Ikoma, 2013). In the tests the behaviour of a weather vane for the assessment of the single-point mooring was analysed.

**Shin** published test results to study the motions of the OC3-Hywind spar as it was also tested by the DeepCwind project and a new spar-type FOWT for 1/128 scaled models in 2D and 3D wave tanks, see (Shin, Model Test of the OC3-Hywind Floating Offshore Wind Turbine, 2011), (Shin & Dam, Model Test of a Floating Offshore Wind Turbine Moored by a Spring-tensioned-leg, 2012). Another investigation with a 1/100 scaled model of a “stepped spar” in a curved wave tank has been presented by **Sethuraman** in (Sethuraman & Venugopal, 2013), with a focus on the validation of OrcaFlex and nonlinear mooring line behaviour comparing the RAOs for pitch, surge and heave motion in regular and irregular waves. They found out that a four point mooring configuration leads to a significant reduction in surge motion. A study with a focus on the derivation of the numerical model comparing computational and experimental results is given in (Matsukuma & Utsunomiya, 2008).

The influence of storm waves on a simplified TLP model was analysed by **Wehmeyer** et al. (Wehmeyer, Ferri, & Frigaard, 2013) with varying tower stiffness's, putting large effort in high wave modelling quality and showing that the inclusion of 2<sup>nd</sup> order waves is essential, especially regarding TLP-specific responses such as ringing and slack line events. His findings include that second order irregular waves are much more likely to be responsible for the ringing response of TLP systems than irregular waves of first order. Another validation of numerical results for a TLP has been done by **Ren**



et al., (Ren, Li, & Ou, 2012), with good performance of their simulation tool. **Olinger et al.** (Olinger, Destefano, Murphy, Naqvi, & Tryggvason, Scale-model experiments on floating wind turbine platforms, 2012) collected information on the dynamic behaviour in pitch, surge and heave direction using simplified models of TLP and spar type FOWT. They found that surge motion of the platform dominates other motions for TLP & Spar and that varying tether pretension has little effect on RAO values.

The impact of the **rotor dynamics** of the wind turbine rotor or the gyroscopic effect on the coupled system dynamics has already been mentioned in various publications. Tests that modelled the rotor merely by a disk with an associated drag coefficient imitated the gyroscopic effect by a rotating body with the same inertia as the wind turbine rotor; see i.e. (Cermelli, Roddier, & Aubault, 2009). In (Karimirad, 2011), an instability of floating wind turbines has been reported with different interpretations regarding the cause: One central cause can be a too aggressively tuned blade-pitch controller of the wind turbine, but also an inappropriate yaw stiffness of the floater yielding large amplitudes in yaw together with large amplitudes in pitch, coupled by the gyroscopic effect. An experimental study on the gyroscopic effect and its impact on FOWT can be found in (Fujiwara, Tsubogo, & Nihei, 2011), where an induced yaw motion due to the gyroscopic effect was both observed and calculated.

### 1.1.3 Aerodynamic Scaling

The geometric downsizing of the wind turbine effectively alters the aerodynamics of the scaled turbine, i.e. the Reynolds number and thus the associated forces on the turbine. A separate aerodynamic scaling of the turbine is therefore necessary in order to keep a correct relationship of the forces acting on the system. An analysis of the aerodynamic scaling of the rotor at the Polytechnic University of Milano can be found in (Bottasso, Campagnolo, & Petrovic, 2014). The research uses a 2-DOF actuator for a wind tunnel model to simulate the motion of a floating wind turbine in waves and its impact on the rotor forces. The paper gives also a good description of a state-of-the art rotor for low Re-numbers, which was designed in order to match tip-speed ratio, thrust force and aerodynamic torque. A scaled rotor of the 5MW NREL reference turbine, see [59] has been built for the InnWind.EU wave tank test. The blade geometry with the identified performance parameters can be found in [60]. A comparable rotor has been designed by the Maritime Institute of the Netherlands (MARIN) as described in (Ridder, Otto, Zondervan, Savenije, & Huijs, 2013). The mentioned institution performs floating wind turbine tests in combined wind and wave environments for individual platforms by placing the standard wind turbine on top. Another study on the aerodynamics has been done by Make (Make, 2014). He numerically investigated the effects of scaling with and without adjusted blade geometry and found that Reynolds dissimilitude of the blade aerodynamics causes a poor match of power and thrust coefficients between model and full scale turbine due to separated flow and separation bubbles. A new blade design aimed to match the performance of the turbine is presented, resulting in a satisfactory scaling for the thrust coefficient  $c_T$  and large differences for the power coefficient  $c_p$ . The new blade design includes an increase of blade chord length by 25% over the full span and an altered pitch distribution to resemble the attached region of the full scale turbine. More optimization through an alternative pitch angle distribution is possible. For more information, see (Hansen, Laugesen, Bredmose, Mikkelsen, & Psychogios, 2014).

Alternative approaches for the modelling of the aerodynamic kinetics in a wave tank have come up recently. A method that aims at reproducing the Froude scaled thrust force by a real-time controlled fan even avoids the need of a wind generator in the wave tank. Such an approach will be also tested in the InnWind.EU model tests. The hardware and software setup as well as the identification procedure is outlined in (Azcona, et al., 2014). Another approach is to realize the hydrodynamic or aerodynamic kinetics completely through a real-time controlled actuator. Such an approach can have various advantages over a full wave tank model test. At Politecnico di Milano a real-time controlled actuator that imitates the hydrodynamic forcing on a FOWT has been implemented. Thus, a high-quality closed-circuit wind tunnel can be used, see (Bayati, Belloli, Ferrari, Fossati, & Giberti, 2014).

The inverse approach of using an actuator imitating the aerodynamic loads while using an experimental wave tank for the hydrodynamic loads is being investigated by (Hall, Moreno, & Thiagarajan, 2014).

#### 1.1.4 Summary

As shown in the previous review, model tests of FOWT systems can have different purposes. The models, load cases and experimental environments are therefore distinctly tailored for each research project in the field. This has two reasons: While some projects are concentrating on the validation and verification of their numerical simulation procedure others are aiming at the realization of full scale turbines and use the model tests together with the numerical tools for verification of the dynamic behaviour. It is clear at this point that physical testing of Floating Offshore Wind Turbine (FOWT) systems provides an essential step towards the realization of full scale prototypes.

The literature review showed that physical phenomena not sufficiently taken into account or not taken into account at all by standard simulation procedures include second order hydrodynamics, dynamic mooring line behaviour and vortex induced motion. Without taking vortex induced motions into account for example, sway and roll responses will be underestimated and yaw responses overestimated, see (Utsunomiya, Yoshida, Ookubo, Sato, & Ishida, 2014).

To this point a reasonable number of experiments have been performed. Future tests should build on the experience from the past and provide relevant features to add to the present knowledge of the complex system behaviour and the fidelity of present simulation tools. The most important scaled FOWT test campaigns have been collected in Table 1-1.

Both literature as well as past test experiments show that Froude scaling has and should be used for experimental studies on FOWT system up to a scaling factor of 1/10. In order to scale rotor effects, different approaches are used, the most fidelity is to be expected by a new rotor design that allows for correctly scaled drag, lift and therefore thrust forces acting on the blades. However, other options might be more practical regarding experiment costs. Rotor effects to be modelled in future experiments include for example the implementation of a controller as has been done by MARIN (Cordle & Jonkman, 2011). Also, from the experiences from DeepCwind (Robertson, et al., 2013), attention should be devoted towards a lightweight instrumentation and a high quality wind field. Additionally to the wind, also the waves need careful modelling in order to realize high frequency pitch response.

Finally, it has to be mentioned that due to built-in errors of model tests regarding the Reynolds number, even with physical experiments the correct dynamic behaviour of the FOWT-system cannot be completely modelled but only approximated to a certain extent.

Useful practical information on scale model building can be found in the theses of the University of Worcester, see (Frye, Horvath, & Ndegwa, 2011) and (Berlo, Gabrielson, Hanly, Parzych, Sacco, & Ryan, 2010) and (Naqvi, 2012).

As shown above most of the current tests and simulations covering wind turbine models of full scale wind turbines up to 5MW. Studies and tests with models representing 10MW or above are extremely rarely distributed. Within this report extended scaling approaches are introduced which are especially capable for model tests for the dimensions of 10 – 20MW wind turbines.

## 1.2 Overview table of literature review

Year published	Floater Type	Project	Scaling Factor	Rotor model	Operational cases <sup>1</sup>	Comments
2006	SB <sup>2</sup>	Hywind (Nielsen, Gunnar, Hanson, & Skaare, 2006)	1/47	n.A. / Rotor used	n.A.	– Challenging dynamic aspects – control algorithms
2007	SS <sup>3</sup>	Ishihara et al. (Ishihara, Phuc, Sukegawa, & Shimada, 2007)	1/150	1) No wind: Concentrated mass 2) Operating condition: disk with holes (Froude scaled thrust) 3) Survival condition: equivalent slender plate	SI <sup>4</sup> , DLC 1.x , 6.x	– New floater Design – Verify numerical model (for calculation of eigenmodes) – damping ratio of vertical motion – optical motion measurements
2009	SB	Utsunomiya et al. (Utsunomiya, Sato, Matsukuma, & Yago, 2009)	1/22.5	n.A. / no Rotor used	SI, DLC 6.x	– Validation of simulation method
2009	SS	Ishihara et al. [19]	1/100	Concentrated mass	SI	– investigate influence of heave plates – optical motion measurements
2009	SS	Windfloat (Cermelli, Roddier, & Aubault,	1/105	Thrust scaled drag disk	SI, DLC 1.x ,	– 100 year waves + design wind speed – tower not to scale

<sup>1</sup> IEC design load cases: 1: power production, 2: power production + fault, 3: Start up, 4: normal shut down, 5: emergency shutdown, 6: parked (standing still or idling), 7: parked + fault, 8: Transport, assembly, maintenance and repair

<sup>2</sup> SB: Spar Buoy

<sup>3</sup> SS: Semi-Submersible

<sup>4</sup> SI: System Identification

Year published	Floater Type	Project	Scaling Factor	Rotor model	Operational cases <sup>1</sup>	Comments
		2009)		with motor	DLC 2.x	– test validity of numerical tools
2011	SB, TLP <sup>5</sup>	Myhr et al. (Myhr, Maus, & Nygaard, 2011)	1/100	Concentrated mass	SI	– Comparison between model & experiment
2011	SB	Shin (Shin, Model Test of the OC3-Hywind Floating Offshore Wind Turbine, 2011)	1/128	Froude scaling	SI, DLC 1.x	– Characteristic & significant motions, RAO
2012	Moored by Spring-tensioned-leg	Shin et al. (Shin & Dam, Model Test of a Floating Offshore Wind Turbine Moored by a Spring-tensioned-leg, 2012)	1/128	n.A. / Rotor used	SI	– Preliminary engineering development – Estimate motion characteristics of platform
2012	SB	Utsunomiya et al. (Utsunomiya, Yoshida, Ookubo, Sato, & Ishida, 2014)	1/34.5	– Froude scaled thrust – new blades	DLC 6.x	– Validate dynamic analysis tool results for extreme environmental conditions
2012	SB	Sethuraman et al. (Sethuraman & Venugopal, 2013)	1/100	Concentrated mass	SI	– Validate numerical model – Focus on non linearities from mooring lines
2012	TLP	Ren et al. (Ren, Li, & Ou, 2012)	1/60	Froude scaled thrust	SI, DLC 6.x	– Square buoy – Validate numerical model

<sup>5</sup> TLP: Tension Leg Platform



Year published	Floater Type	Project	Scaling Factor	Rotor model	Operational cases <sup>1</sup>	Comments
2012	TLP, SB	Olinger et al. (Olinger, Destefano, Murphy, Naqvi, & Tryggvason, Scale-model experiments on floating wind turbine platforms, 2012)	1/100	Concentrated mass	SI	<ul style="list-style-type: none"> <li>– Wireless data acquisition</li> <li>– Data acquisition for numerical model validation</li> </ul>
2013	SS	GustoMSC Tri-Floater (Huijs, Mikx, Savenije, & Ridder, 2013)	1/50	<ul style="list-style-type: none"> <li>– Froude scaled thrust</li> <li>– new blades</li> </ul>	n.A.	– Active blade pitch
2013	TLP	Gicon (Großmann & Dahlhaus, 2013)	1/25	n.A. / Rotor used	n.A.	– Analysing eigenmodes
2013	SB	Utsunomiya et al. (Utsunomiya, et al., 2013)	1/10	1 kW, yaw-free wind turbine	SI, DLC 1.x	– Hybrid Spar buoy
2013	SB	Chujo et al. (Chujo, Minami, Nimura, & Ishida, 2013)	1/100	<ul style="list-style-type: none"> <li>– Froude scaled thrust (maintain <math>c_T - \lambda</math>-ratio)</li> <li>– New blades</li> </ul>	DLC 1.x	<ul style="list-style-type: none"> <li>– Blade pitch control</li> <li>– Analyse floater motion and rotor speed fluctuation</li> </ul>
2013	SS	WINFLO (Boulluec, Martin, & Houmard, 2013)	1/40 1/25	<ul style="list-style-type: none"> <li>– Froude scaled thrust (maintain drag and torque)</li> <li>– New blades</li> </ul>	SI, DLC 1.x	<ul style="list-style-type: none"> <li>– Validate numerical modelling</li> <li>– Validate floater and mooring design for prototype</li> <li>– New floater design</li> </ul>
2013	SS	Philippe et al. (Philippe, 2014)	1/50	n.A. / Rotor used	SI, DLC 1.x	<ul style="list-style-type: none"> <li>– Dutch Trifloater</li> <li>– Compare numerical model</li> </ul>

Year published	Floater Type	Project	Scaling Factor	Rotor model	Operational cases <sup>1</sup>	Comments
2013	SS,TLP,SB	DeepCWind (Robertson, et al., 2013)	1/50	Geometric scaling	SI, DLC 1.x	<ul style="list-style-type: none"> <li>– Extensive study on floater behaviour</li> <li>– Generate publicly available data for numerical model validation</li> </ul>
2013	SS	Iijima et al. (Iijima, Kawai, Nihei, Murai, & Ikoma, 2013)	1/100	Froude scaled thrust	SI, DLC 1.x, DLC 6.x	<ul style="list-style-type: none"> <li>– New floater design</li> </ul>
2013	TLP	Wehmeyer et al. (Wehmeyer, Ferri, & Frigaard, 2013)	1/80	Concentrated mass	SI, DLC 6.x	<ul style="list-style-type: none"> <li>– Assess behaviour of mooring lines</li> </ul>
2013	SS	Ishida et al. (Ishida, Kokubun, Nimura, Utsunomiya, Sato, & Yoshida, 2013)	1/2	100 kW turbine	GPD <sup>6</sup>	
2014	SS	VolturnUS, (Viselli, Goupee, & Dagher, 2014)	1/8	Modified 20 kW pitch regulated commercial turbine to apply peak scaled thrust	GPD	<ul style="list-style-type: none"> <li>– concrete semi-submersible hull and composite tower</li> <li>– demonstrate full-scale design, materials, construction techniques and deployment methods</li> <li>– validate numerical design tools for near full-scale floating turbines</li> </ul>
2014	SS	SAEMar, (Guanche, Meneses, Sarmiento, Vidal, & Losada, 2014)	1/60	Concentrated mass	SI	<ul style="list-style-type: none"> <li>– mooring line design methodology</li> </ul>

<sup>6</sup> GDP: Global performance data

Year published	Floater Type	Project	Scaling Factor	Rotor model	Operational cases <sup>1</sup>	Comments
2014	TLP	GICON, (Adam, Myland, Dahlhaus, & Großmann, Scale Tests of the Gicon-TLP for Wind Turbines, 2014)	1/37	MARIN rotor	SI, DLC 1.x	<ul style="list-style-type: none"> <li>– Froude scaled tower bending frequency</li> <li>– Mismatch of platform and rotor scaling</li> <li>– Preparation of prototype tests</li> </ul>
2014	SS	GustoMSC Tri-Floater, (Huijs, Ridder, & Savenije, Comparison Of Model Tests And Coupled Simulations For A Semi-Submersible Floating Wind Turbine, 2014)	1/50	MARIN rotor	DLC 1.x, 6.x	<ul style="list-style-type: none"> <li>– numerical model validation</li> <li>– active blade pitch control</li> </ul>
2014	SS	Azcona et al., (Azcona, et al., 2014)	1/40	Ducted fan	SI, 1.x	<ul style="list-style-type: none"> <li>– validating rotor model</li> </ul>

**Table 1-1 Scaled FOWT testing overview**

## 2 SCALING LAWS FOR FLOATING WIND TURBINE TESTS

When Floating Offshore Wind Turbines (FOWT) are tested in wave tanks, the requirement of a true scaling of the wave forcing leads to application of Froude scaling. This determines the scaling of time and mass relative to the length scale ratio and thereby defines the scaling of force, elasticity and structural dimensions. Froude scaling, however, does not preserve the Reynolds number which will be smaller than at full scale. While the Reynolds-number dependence of the hydrodynamic force is often neglected, the associated change of aerodynamic Reynolds number leads to a need for a modified blade design in order to achieve the correct rotor thrust. A correct reproduction of the rotor thrust is thus an important aspect for tank testing of floating wind turbines.

The present chapter is based on the work of (Bredmose, Schløer, & Paulsen, 2012) which is here extended to include a modified scaling of the wind speed. First, the Froude scaling and its rationale is summarized. Next the scaling of water and air velocities is derived and the modified air speed scaling is introduced in terms of an additional free parameter. The consistent scaling aerodynamic loads, structural properties and the external wind-wave climate are then discussed followed by a summary of the scaling relations.

Obviously some physical effects will not scale correctly when the Froude scaling is applied. This is reflected in a scale dependence of their associated dimensionless numbers. The matched and non-matched numbers are outlined in section 2.1.6.

### 2.1 Froude scaling

Froude scaling results from the requirement that the balance between inertia forces and gravitational forces must be preserved between prototype scale and model scale. Let the length scale ratio  $\lambda$  be defined as First, define the length scale ratio  $\lambda$  by

$$\lambda = \frac{L_p}{L_m} \quad 2-1$$

where subscripts 'p' and 'm' denote prototype scale and model scale, respectively and  $L$  is a representative length. Now, consider some force  $F$  that leads to an acceleration  $a$  of a structural or fluid element of mass  $M$ . Next require that the ratio of this force to the gravitational force is preserved between prototype scale and model scale

$$\frac{F_p}{M_p g} = \frac{F_m}{M_m g} \quad \Rightarrow \quad \frac{M_p a_p}{M_p g} = \frac{M_m a_m}{M_m g} \quad \Rightarrow \quad a_p = a_m \quad 2-2$$

Now as the dimensions of acceleration are  $L/T^2$  the above result implies that

$$\frac{L_p}{T_p^2} = \frac{L_m}{T_m^2} \quad \Rightarrow \quad \frac{T_p}{T_m} = \sqrt{\lambda} \quad 2-3$$

This determines the ratio of the prototype and model-scale time scale.

Scaling of mass is obtained by the requirement of a fixed ratio of structural mass to fluid mass for the water. Consider a volume  $\text{Vol}$  and require that the mass ratio to a structural element is preserved

$$\frac{M_p}{\rho_{wp} \text{Vol}_p} = \frac{M_m}{\rho_{wm} \text{Vol}_m} \quad \Rightarrow \quad \frac{M_p}{M_m} = \frac{\rho_{wp}}{\rho_{wm}} \lambda^3. \quad 2-4$$

Here  $\rho_w$  is the density of water and we have utilized that volume scales by the length ratio cubed.

#### 2.1.1 Scaling of water and air velocities

The scaling of length and time defines the scaling of water velocities as

$$\frac{u_{wp}}{u_{wm}} = \sqrt{\lambda} \quad 2-5$$

The same scaling applies for velocities in the air,  $u_{ap}/u_{am} = \sqrt{\lambda}$ . Hereby the ratio of air-to-water velocity is preserved between prototype scale and model scale. In some situations, limitations of the wind generation system might impose a need for a modified scaling of the air velocities. Also, at small lab scale, the target air velocities may become so small that they are vulnerable to disturbances in the lab. In such situations a modified air-scaling can be obtained by choosing

$$\frac{u_{ap}}{u_{am}} = \frac{\sqrt{\lambda}}{\beta} \quad 2-6$$

where  $\beta$  is a free parameter. For  $\beta = 1$  strict Froude scaling is achieved, while  $\beta > 1$  leads to larger model scale velocities than Froude scaling. The modified air scaling further leads to a change of the tip speed ratio by

$$\frac{TSR_p}{TSR_m} = \frac{\omega_p R_p}{u_{ap}} \frac{u_{am}}{\omega_m R_m} = \beta. \quad 2-7$$

Hence for  $\beta \neq 1$  the tip speed ratio is not conserved. This will affect the aerodynamic wake and in experiments that involves multiple floating wind turbines and their wake-induced interaction this may be important. While a choice of  $\beta \neq 1$  may seem inconsistent, it should be noted that the low Reynolds numbers at model scale necessitates a modified rotor design anyway. Hence, the detailed aerodynamics around the rotor will not be preserved from prototype to model scale. Further for  $\beta > 1$  the Reynolds number mismatch is mitigated.

### 2.1.2 Aerodynamic loads

The ultimate goal of floating wind turbine experiments is to provide an accurate reproduction of the real loads and the associated structural response. While the hydrodynamic loads and mooring loads can often be reproduced with good approximation by Froude scaled experiments, the aerodynamics will be quite different due to the change in Reynolds number:

$$Re = \frac{u_a D}{\nu} \Rightarrow \frac{Re_p}{Re_m} = \frac{v_m \lambda^{3/2}}{v_p \beta} \quad 2-8$$

Thus for a scale ratio of  $\lambda = 40$ , identical viscosity and strict Froude scaling ( $\beta = 1$ ), a Reynolds number ratio of  $Re_p/Re_m = 40^{3/2} \approx 253$  is obtained. This generally leads to a reduced lift-to-drag ratio for the blades which in turn necessitates a larger blade chord; see e.g. (Hansen, Laugesen, Bredmose, Mikkelsen, & Psychogios, 2014). The model-scale rotor therefore needs to be re-designed for the low Reynolds number, and the detailed aerodynamic flow around it will not resemble the full-scale flow. The main dynamic behaviour, though, will be reproduced as long as the rotor thrust is reproduced. This leads to the following scaling requirement for the thrust coefficient  $C_T$ :

$$F_T = \rho_a C_T A u_a^2 \simeq \frac{\rho_w}{\lambda^3} \Rightarrow \frac{C_{Tp}}{C_{Tm}} = \frac{\rho_{wp}}{\rho_{wm}} \beta^2 \quad 2-9$$

Strict Froude scaling will thus lead to (almost) unchanged  $C_T$  values, while  $\beta > 1$  will reduce the  $C_T$  values in model scale.

Further to the mean rotor loads, also the fluctuating loads are of interest. The magnitude of the turbulent fluctuations in a single point is characterized by the turbulence intensity  $TI = \sigma_{ua}/\bar{u}_a$ . We may now consider the thrust force for the mean wind speed plus one times its standard deviation:

$$F_T^+ = \rho_a C_T A (\bar{u}_a (1 + TI))^2 = \rho_a C_T A \bar{u}_a^2 (1 + TI)^2 \quad 2-10$$

This result shows that as long as the product of  $C_T$  and  $\bar{u}_a^2$  scales correctly, the turbulent contributions (at least in a single point) will scale correctly too. It is worth to note that in cases where  $\beta \neq 1$ e, and where the turbulence intensity is a function of the mean wind speed, the turbulence intensity should be based on the prototype value of  $\bar{u}_a$ .

A next target for the rotor design is to reproduce the right aerodynamic torque. The reason for this is that the torque is absorbed by the floating platform. Hence torque fluctuations will induce dynamic roll motion.

### 2.1.3 Scaling of structural properties

Once the scaling of mass, length and time are defined, the scaling of structural properties follows directly. Structural dimensions scale with  $\lambda$ . Further, the consistent scaling of other properties can be derived from their composition of primary physical units of length, time and mass. For the mass moment of inertia  $J$  (here around the  $x$  axis as one example) we obtain:

$$J_{xx} = \int_M x^2 dM \quad \Rightarrow \quad \frac{J_p}{J_m} = \frac{\rho_{wp}}{\rho_{wm}} \lambda^5 \quad 2-11$$

For a correct elastic scaling, Young's modulus and the cross sectional areal moment of inertia is of interest. Again from the physical units,

$$[E] = \frac{M}{LT^2} \quad \Rightarrow \quad \frac{E_p}{E_m} = \frac{\rho_{wp}}{\rho_{wm}} \lambda \quad 2-12$$

and

$$I_{xx} = \int_A x^2 dA \quad \Rightarrow \quad [I] = L^4 \quad \Rightarrow \quad \frac{I_p}{I_m} = \lambda^4 \quad 2-13$$

It should be noted here that (2-12) implies that the material must be changed along with the scale. Often for a structural beam, it is sufficient that the product of  $E$  and  $I$ ,  $EI$ , scales correctly. Further, if the beam itself does not attract any loads from the surrounding air or water, the outer dimensions can also be changed with no effect on the dynamics. This gives some freedom in choosing a beam for the model with the right scaled values of  $EI$ . The mass distribution must also be correct — here additional mass can be added to meet this requirement.

### 2.1.4 Scaling of external climate

Representative wind-wave climates have been outlined in chapter 2.2. Here, the scaling of these climates for model scale tests is discussed. For the wave climate, the scaling is straightforward as the length scale ratio is  $\lambda$  and the time scale ratio is  $\sqrt{\lambda}$ . This implies that depth and wave heights scale with  $\lambda$ , wave periods with  $\sqrt{\lambda}$  and current speeds with  $\sqrt{\lambda}$ . For the JONSWAP wave spectrum, the shape parameter  $\gamma$  will apply directly as it is dimensionless.

The prototype scale wind climate is usually described by 2-parameter Weibull distribution with scaling parameter  $A$  and shape parameter  $k$ . This allows determination of probabilities of wind speeds in prototype scale. Further, the turbulence intensity is specified as function of mean wind speed. For a given mean wind speed, the turbulence intensity  $TI$  can be applied directly also in model scale as it is a dimensionless number. The wind speeds will scale like specified in (6). It is emphasized that the turbulence intensity should be taken from the prototype scale and applied directly at model scale; no matter what value of  $\beta$  is used.

### 2.1.5 Summary of scaling

The scaling is summarized as follows. The Table 2-1 and Table 2-2 are adopted from [1].

Property	Scaling factor
Length	$\lambda$
Mass	$(\rho_{wp}/\rho_{wm}) \lambda^3$
Mass moment of inertia (J)	$(\rho_{wp}/\rho_{wm}) \lambda^5$
Area moment of inertia (I)	$\lambda^4$
Water velocity	$\lambda^{1/2}$
Air velocity	$\lambda^{1/2} \beta^{-1}$

Acceleration	1
Time	$\lambda^{1/2}$
Frequency	$\lambda^{-1/2}$
Angle	1
Force	$(\rho_{wp}/\rho_{wm}) \lambda^3$
Moment	$(\rho_{wp}/\rho_{wm}) \lambda^4$
Stiffness (E)	$(\rho_{wp}/\rho_{wm}) \lambda$
Stress	$(\rho_{wp}/\rho_{wm}) \lambda$
Power	$(\rho_{wp}/\rho_{wm}) \lambda^{7/2}$
Thrust coefficient ( $C_T$ )	$(\rho_{wp}/\rho_{wm}) \beta^2$

**Table 2-1 Scaling factors FOWT**

Property	Scaling factor
Geometric height (z)	$\lambda$
Wind speed (V)	$\lambda^{1/2}\beta^{-1}$
Turbulent wind frequency (f)	$\lambda^{-1/2}$
Turbulence intensity	1
Wind profile power coefficient ( $\alpha$ )	1
Water depth	$\lambda$
Velocity	$\lambda^{1/2}$
Significant wave height	$\lambda$
Peak period	$\lambda^{1/2}$
Wind-wave misalignment	1

**Table 2-2 Scaling factors Wind and Waves**

### 2.1.6 Dimensionless numbers conserved and not conserved with the modified Froude scaling

The proposed scaling conserves the following dimensionless numbers:

- $Fr = u_w/\sqrt{gL}$ , the Froude number, measures the ratio of water particle velocity to wave velocity.  $u_w$  is a representative water particle velocity,  $L$  is a representative length scale and  $g$  is gravity.
- $KC = u_{w,max}T_w/D$ , the Keulegan-Carpenter number. Measures the relative excursion of a water particle during a wave cycle, relative to the diameter of a structural element. Flows with  $KC \ll 20 - 30$  are inertia dominated while flows with  $KC \gg 20 - 30$  are drag dominated, see (Sumer & Fredsøe, Volume 12, 2006).
- $Lo$ , the aerodynamic Lock number. The Lock number measures the ratio of the aerodynamic forces and the inertia forces. This is conserved in the modified Froude scaling, both for the aerodynamic and hydrodynamic forces.

Other dimensionless numbers are not conserved. These are

- $Re$ , the Reynolds number in the air and in the water. As already discussed, the mismatch of the hydrodynamic Reynolds number will lead to changes in the hydrodynamic force coefficients. For the air-flow, the smaller Reynolds number will lead to the need for a re-designed rotor.
- $We$ , the Weber number. This number measures the balance of surface tension to inertial loads. It is not expected to have importance, except at very small scales.
- $St$ , the Strouhal number in water and air. This number is rather invariant to the Reynolds number until the critical range at  $Re = 2 \cdot 10^5$ . For preserved Strouhal number and strict Froude scaling  $\beta = 1$ , the vortex shedding frequency will scale as  $\lambda^{-1/2}$  which is consistent with the time scaling.

- Ma, the Mach number in water and air. The air-flow for wind turbines is usually below the compressible Mach number range and a mismatch in Mach number is therefore not considered critical.
- TSR, the tip speed ratio. The tip speed ratio will scale as implied by (2-7) and will thus only be conserved for strict Froude scaling with  $\beta = 1$ .

Besides the dimensionless numbers, a couple of effects will also not scale automatically. A careful rotor and nacelle design, however, may help on this. The following topics are thus open for future research

- the aero- and hydro-dynamic Reynolds numbers.
- the aerodynamic torque
- the aerodynamic power
- the generator torque and its contribution to roll-forcing
- 3P forcing from the tower shadow

## 2.2 Scaling of wind and wave conditions

### 2.2.1 Design basis for offshore wind turbines

The design of bottom-fixed offshore wind turbines is based on numerical evaluation of a number of load cases as described by the IEC norm [1] and the interpretation of DNV-GL. Recently, design norms for floating offshore wind turbines have been proposed by DNV and GL. The load cases all refer to the met-ocean design basis, which is site and project specific. The major part of the design basis is the combined wind, wave and current data, which are usually determined from long-term hind-cast modelling, calibrated against available measured data. In the present chapter, a brief overview of the variables that describe a wind-wave climate is given, along with examples of openly available design bases and descriptions. The scaling methodology for the wind-wave parameters is outlined at the end of the chapter with reference to chapter 2.1 where the Froude scaling is derived and where a free parameter for further adjustment of the wind speed is included.

### 2.2.2 Basic parameters of wind-wave climates

#### 2.2.2.1 Statistical variation of mean wind speed

The most important description of a wind climate at a site is the long-term statistical distributions of the 10 minute mean wind speed for fixed vertical height. The distribution is often well fitted by a Weibull distribution. An example is shown in

Figure 2-1. The cumulative density function of the Weibull distribution is given by

$$P(V \leq v) = 1 - \exp \left\{ - \left( \frac{v}{A} \right)^k \right\} \quad 2-14$$

where A is the scale parameter and k is the shape parameter. The Weibull representation makes it possible to represent the wind climate in large regions simply by maps or data bases of the Weibull parameters (A,k). Examples of such data bases are the Wind Atlas [4] and output of the EU NORSEWIND project [5]. An example from the latter is shown in Figure 2-2.



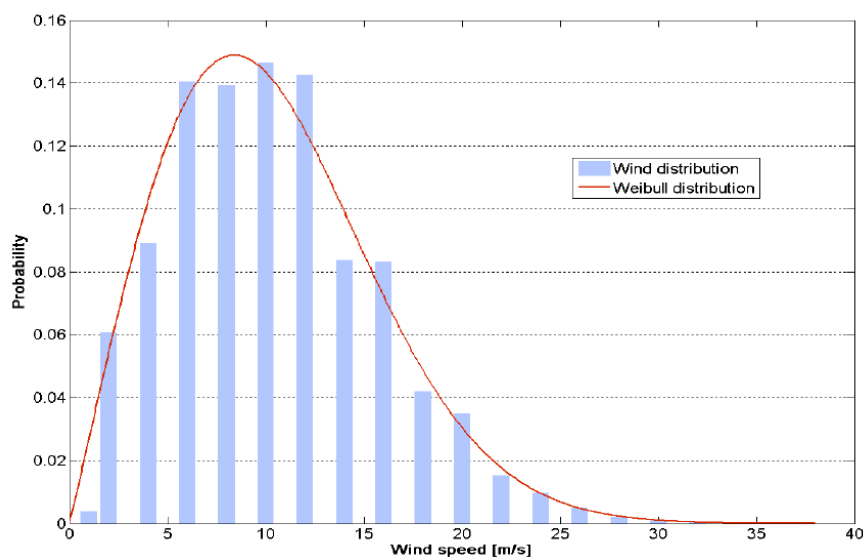


Figure 2-1 Example of a Weibull wind distribution at hub height. From the UpWind design basis [6].

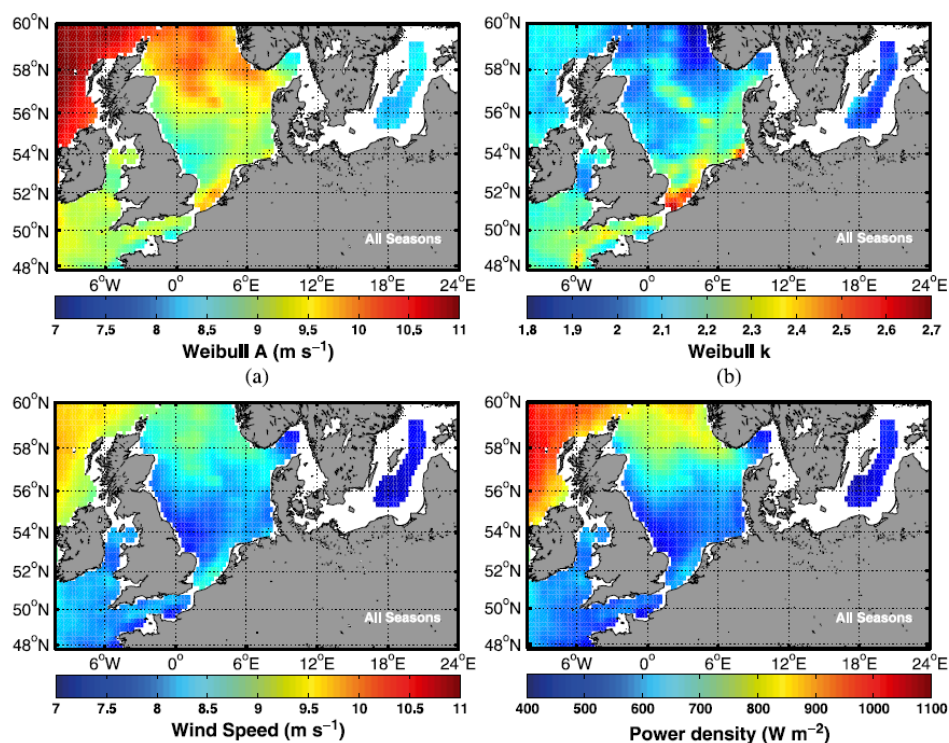


Figure 2-2 The 10 meter marine wind climate across the North Western European seas. The white areas correspond to lack of data, mainly due to precipitation. From [5].

### 2.2.2.2 Vertical variation of mean wind speed

The vertical profile of the mean wind speed is usually well described by the log profile

$$V(z) = \frac{u^*}{\kappa} (\ln(z/z_0) - \psi) \quad 2-15$$

which can be derived from physical principles. Here  $u^*$  is the frictional velocity,  $\kappa=0.4$  is the von Karman constant,  $z$  is the measurement height and  $z_0$  is the roughness length. The function  $\psi$  represents the effect of varying atmospheric stability. Negative values of correspond to stable

conditions while  $\phi > 0$  corresponds to unstable conditions. As the proper determination of  $\phi$  is still under active research,  $\phi = 0$  is often used.

The roughness length  $z_0$  can be determined from the Charnock relation

$$z_0 = C(u^*)^2/g \quad 2-16$$

where  $C = [0.01; 0.015]$  is constant which depends on the distance to the coast and  $g$  is the acceleration of gravity. Over water,  $z_0$  is a small quantity, of the order of 0.1-0.3mm.

As an alternative to the log-profile, the power law profile

$$V(z) = V(z_{10}) \left( \frac{z}{z_{10}} \right)^\alpha \quad 2-17$$

is often used. Here  $\alpha$ , the power coefficient is often taken equal to 0.14, see e.g. [1], and  $(z_0, u_0)$  is a reference height and a reference velocity. While (2-17) is perhaps more straightforward to use than (2-15), we note that (

2-16) is based on empirical fitting while (2-15) can be derived from physical principles.

Equation (2-2) and (2-15) describe the wind shear and clearly shows that the Weibull parameter  $A$  changes with height  $z$ . Actually, also the  $k$ -parameter has a height dependence. However, it is common practice to assume a constant  $k$  over all heights.

### 2.2.2.3 Turbulence intensity and turbulence spectrum

The turbulence intensity is defined as the ratio of the standard deviation of the turbulent fluctuations to the mean wind speed

$$TI = \frac{\sigma_v}{\bar{V}} \quad 2-18$$

The turbulence intensity thus measures the strength of the wind fluctuations. It is a function of wind speed and a number of formulas exist to describe this variation. Figure 2-3 shows a graph from [6] where several of these are depicted. Here we will cite the turbulence intensity formula from the UpWind project

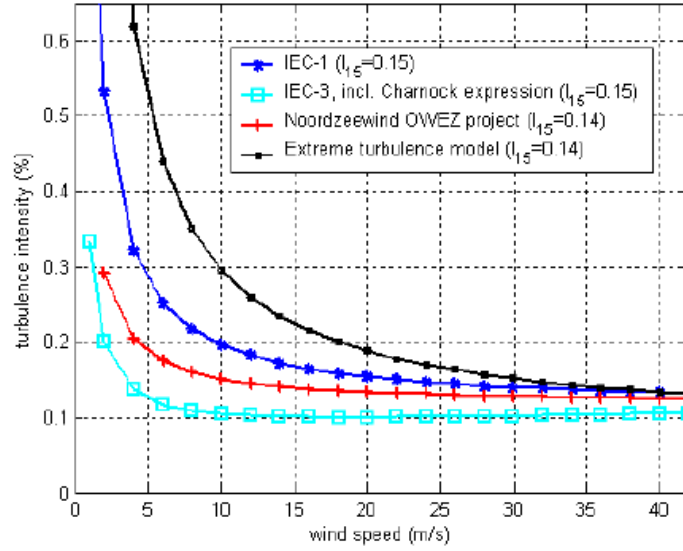


Figure 2-3 Turbulence intensity as function of wind speed. Various formula give different results. From the UpWind project [6].

$$TI(v) = \frac{15 + av}{(1 + a)v} I_{15} \quad 2-19$$

where  $a$  is a coefficient around 5.

The frequency distribution of the turbulent fluctuations is described by the turbulence spectrum. The Kaimal spectrum [7]

$$f S_v(f) = \sigma_v^2 \frac{4 \frac{Lf}{V_{10}}}{\left(1 + 6 \frac{Lf}{V_{10}}\right)^{5/3}} \quad 2-20$$

is widely used. In this formula  $f$  is the frequency,  $v_{10}$  is the 10 minute mean wind speed and  $L$  is a length scale given as

$$L = \begin{cases} 5.67z & \text{for } z < 60 \text{ m} \\ 340.2 & \text{for } z > 60 \text{ m} \end{cases} \quad 2-21$$

Due to the spatial variation of turbulence, the instantaneous wind speed also varies between points in space. This is described through the coherence function of the Kaimal spectrum

$$\text{Coh}(r, f) = \exp \left\{ -12 \left[ \left( \frac{fr}{V_{\text{hub}}} \right)^2 + \left( 0.12 \frac{r}{L_c} \right)^2 \right]^{1/2} \right\} \quad 2-22$$

In this formula  $r$  is the distance between the projection of the position vectors of the two points considered onto a plane perpendicular to the mean wind direction and  $L_c$  is the coherence scale parameter, see [8].

Another example of a wind spectrum is the von Karman spectrum, see e.g. [9]. The Kaimal and von Karman models give the correct statistical distributions for the wind speed in space and time and can thus be used to form the numerical input for aero-elastic computations with distributed blade loads. There is however, no guarantee that the synthesized wind fields are solutions to the Navier-Stokes equations which describe the basic mass and momentum conservation for a wind field. A solution to this problem is offered by the Mann turbulence model [10] which enables computation of a 'box' of turbulent wind in three directions. The model is widely used as input for aero-elastic computations.

#### 2.2.2.4 Directional wind spectra

Similarly to the variation of mean wind speed, the mean wind direction also varies over time. This is usually represented by a two-parameter probability function of wind speed and direction

$$p(v = V^*, \theta = \theta^*)$$

2-23

which is further often depicted as a wind rose. An example is given in Figure 2-4.

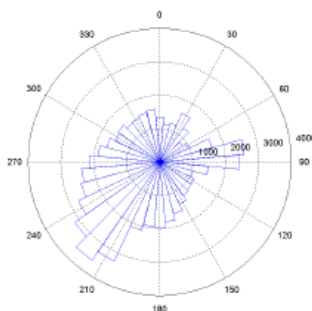


Figure 2-4 Example of a wind rose. From the UpWind project [6].

#### 2.2.3 Wave climate

The wave climate in a certain point is usually characterized by the significant wave height  $H_s$  and the peak period  $T_p$ . While the wind climate is defined for a 10 minute duration, the standard duration for wave record and wave statistics is three hours. The two lengths of time emerge for two different reasons: for the wind speed, there is no lower limit on the period – for example the Kaimal spectrum goes to infinity as the frequency approaches zero. It has however been found that 10 minutes is short enough for the wind speed variation to be considered as statistically stationary. The statistical properties can be described as function of the mean value. For waves, the three hour duration is chosen to obtain sufficient length for a simulation or lab test to give statistically representative results. For wind, this is obtained by performing multiple 10 minute simulations or sometimes, simulations with longer duration.

The significant wave height is defined as the average wave height of the one third largest fraction of waves in a wave record. This is typically based on 3 hour record. A more practical definition is  $H_{m0}$ , which is based on the standard deviation  $\sigma$  of the free surface elevation

$$H_{m0} = 4\sigma_\eta = 4\sqrt{(\eta - \bar{\eta})^2} = 4\sqrt{m_0}$$

2-24

where  $m_0$  is defined below. Practically  $H_s$  is often calculated by (2-24) due to its simplicity.

The distribution of energy over frequencies in a wave field is described by the frequency spectrum  $S_{\eta}(f)$  which is simply the power spectrum of the free surface elevation time series. Therefore  $S_{\eta}(f)$  satisfies

$$m_0 = \int_{f=0}^{\infty} S_{\eta}(f) df = \sigma_{\eta}^2 \quad 2-25$$

Further, it can be shown that at least for small amplitude wave motion, the time averaged local energy density in a spatial point in a wave field is

$$E = \rho g \sigma_{\eta}^2 \quad 2-26$$

(see e.g. [11]). Here  $\rho$  is the water density and  $g$  is gravity. Hereby, the zeroth moment of the spectral function  $S_{\eta}$  is, apart from the  $\rho g$  factor, equal to the local energy density.

A Wave spectrum generally varies with location, time and significant wave height. For deep water conditions, however, several standard spectral shapes have been devised. Here the Pierson-Moskowitz spectrum [12] is widely used:

$$S_{PM}(f) = 0.3125 H_s^2 f_p^4 f^{-5} \exp \left\{ -\frac{5}{4} \left( \frac{f}{f_p} \right)^{-4} \right\} \quad 2-27$$

Here  $f_p$  is the peak frequency, i.e. the frequency that contains most spectral energy.

Through the Joint North Sea Wave Project [13], this spectrum was modified to match observations of the sea states in the North Sea. The resulting spectrum, the JONSWAP spectrum can be written as [1]

$$S_{JONSWAP} = 0.3125 H_s^2 T_p \left( \frac{f}{f_p} \right)^{-5} \exp \left\{ -\frac{5}{4} \left( \frac{f}{f_p} \right)^{-4} \right\} (1 - 0.287 \ln \gamma) \gamma^{\exp \left\{ -\frac{1}{2} \left( \frac{f/f_p - 1}{\sigma} \right)^2 \right\}} \quad 2-28$$

where  $T_p = 1/f_p$  is the peak period,  $\sigma$  is defined by

$$\sigma = \begin{cases} 0.07 & \text{for } f \leq f_p \\ 0.09 & \text{for } f > f_p \end{cases} \quad 2-29$$

and  $\gamma$ , the peak enhancement parameter can be expressed from  $H_s$  and  $T_p$  by

$$\gamma = \begin{cases} 5 & \text{for } T_p/\sqrt{H_s} \leq 3.6 \\ \exp \{ 5.75 - 1.15 T_p/\sqrt{H_s} \} & \text{for } 3.6 \leq T_p/\sqrt{H_s} \leq 5 \\ 1 & \text{for } 5 < T_p/\sqrt{H_s} \end{cases} \quad 2-30$$

The two spectra are shown in Figure 2-5 where it can be seen that the JONSWAP spectrum has a sharper peak than the Pierson-Moskowitz spectrum.

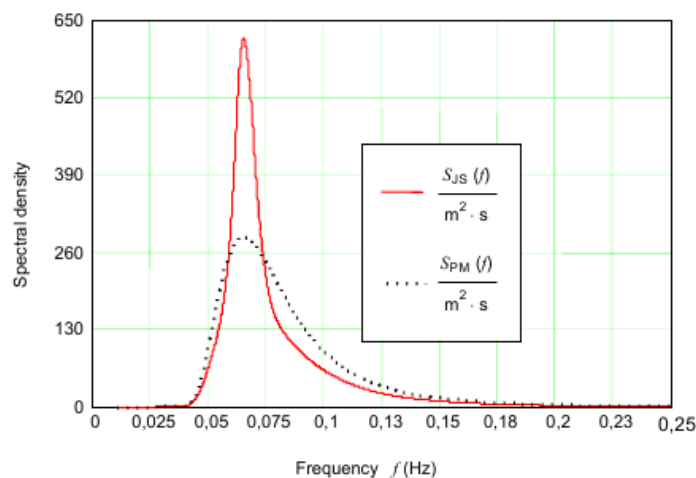


Figure 2-5 The Pierson-Moskowitz and JONSWAP wave spectra. From [1].

Additionally to the significant wave height, the wave spectrum is characterized by a wave period measure. Here  $T_p = 1/f_p$  is the most commonly used, which is simply the wave frequency where the spectral function  $S_\eta(f)$  has its maximum. Alternative measures are the average zero up-crossing period  $T_z$  and the peak to peak period  $T_c$  which can both be expressed from moments of the wave spectrum. For the JONSWAP spectrum,  $T_z$  and  $T_p$  are further related by

$$T_z = T_p \sqrt{\frac{5 + \gamma}{11 + \gamma}} \quad 2-31$$

Like wind, waves are not unidirectional. The directional spreading is described by the direction spectrum  $S_\eta(f, \theta)$  which defines the power spectral density as function of frequency and direction  $\theta$ . Often this combined frequency and directional spectrum is factored as

$$S_\eta(f, \theta) = S_\eta(f) D(f, \theta) \quad 2-32$$

where  $D(f, \theta)$  is then the directional spreading function, which also has a number of generic distributions, for example the cos<sup>2n</sup> spectrum. These spectral shapes are useful if the information on directional spreading for a certain location is sparse.

#### Current

Current also affects the hydrodynamic loads and are thus an important part of the design basis. The IEC 61400-3 norm [1] distinguishes between three types of current namely sub-surface current, wind-induced current and current induced by breaking waves in the surf zone.

The sub-surface current can be described by a simple power-law profile

$$U_{SS}(z) = U_{SS}(0) \left( \frac{z + d}{d} \right)^{1/7} \quad 2-33$$

where  $d$  is the depth and  $z$  is the vertical coordinate, running upwards from the mean sea level.

The wind induced current can be described by the linear profile

$$U_W(z) = U_W(0) \left(1 + \frac{z}{20}\right) \quad 2-34$$

which is valid from  $z=-20\text{m}$  to  $z=0$  at the mean sea level. Both current formulations require knowledge of  $U_W(0)$  and  $U_W(z)$ . This is part of the met-ocean design basis and associated extreme value analysis.

## 2.3 Existing wind-wave climate descriptions

### 2.3.1 Full met-ocean data bases from hind-cast modelling

For real offshore wind farm projects, the detailed design is based on a comprehensive met-ocean data base that collect detailed information on the external wind and wave climate, current, icing, soil properties etc. Usually the data base results from numerical hind-cast modelling, where a large area has been simulated for typically 50 years and where the model has been calibrated against measurements at the specific site and long-term measurements at other points that are more distant but still within the modelling area. Given the model output, statistical information on the simultaneous occurrence of mean wind speed, wind direction, significant wave height, peak period and wave direction can be extracted.

### 2.3.2 The UpWind design basis

Often the full met-ocean design basis is proprietary to each project. An openly available design basis, however, was established in the UpWind project [6]. Here wind and wave data for three sites are collected. One site, Ijmuiden, has a depth of 21.4 m, while another site, K13, has a depth of 25m. The third site is a deep-water (50 m) version of the K13 site, where the extreme wave properties were adjusted to reflect the larger depth. The general wind wave climate, however, were found to be nearly unaffected by the depth change and are therefore identical. The design basis is described in a report of Fischer et al [6] and includes wind roses, wave roses, scatter diagrams for significant wave height and peak period and scatter diagrams for the simultaneous direction of wind and waves. All the information is parameterized in terms of wind speed. The design basis further includes 1, 5, 10, 50 and 100-year values for  $H_s$ ,  $T_p$  and the maximum wave height.

### 2.3.3 Joint probability distributions for wind and wave climate

Johannessen et al [14] provided a statistical model for the combined wind-wave climate in the Northern North Sea. The model describes the combined probability of mean wind speed, significant wave height and peak period through the

$$f_{V,H_{m0},T_p}(v, h, t) = f_V(v) f_{H_{m0}|V}(h|v) f_{T_p|H_{m0},V}(t|h, v) \quad 2-35$$

The wind distribution  $f_V(v)$  is a Weibull distribution;  $f_{H_{m0}|V}$  is also a Weibull distribution where the scale and shape parameters are linear functions of the wind speed. Finally, the peak period distribution  $f_{T_p|H_{m0},V}$  is modelled by a log normal distribution where the mean and standard deviations are functions of  $v$  and  $H_s$ . All the parameters in the model are determined by least squares fits to simultaneous values of wind and wave properties from 1973-1999 from the Northern North Sea.

The combined model is useful as it provides a closed-form representation of the wind-wave climates, still based on real data. In the paper of Johannessen et al [Jo] it is utilized to derive contour surfaces for the 100-year combination of  $V$ ,  $H_s$  and  $T_p$ .



### 2.3.4 Fatigue averaged wind-wave climates

For simplified calculations of life time fatigue, a single string of wind-wave climates is useful, that is, for each wind speed, one representative wave climate with fixed  $(H_s, T_p)$ . Representative here means a wave climate that yields the same fatigue damage as all the climates in the  $(H_s, T_p)$  scatter diagram weighted with their probabilities. Kühn [15] proposed a method to calculate such a climate, by a fatigue-based averaging of the wave properties. For each wind speed, the averaging process is done in two stages:

1) First, by assumption of inertia dominated loads, the stresses will depend linearly on the wave height. Hence the wave height that gives the same damage as all the climates in the  $(H_s, T_p)$  scatter diagram is found similarly to the equivalent stress range i.e.

$$H_s^* = \left( \frac{\sum_j p_j H_{s,j}^m}{\sum_j p_j} \right)^{1/m} \quad 2-36$$

where  $m$  is the Wöhler exponent which is a material property. For steel,  $m$  is usually between 3 and 5.

Further, as the fatigue damage is proportional to the number of stress cycles which from the linear properties of the inertia dominated loads must equal the number of waves, the inverse period must be weighted directly with their probability

$$\frac{1}{T_z^*} = \frac{\sum_j p_j (1/T_{z,j})}{\sum_j p_j} \quad 2-37$$

2) by full computation of the wave induced stresses of the structure for the full scatter matrix, the „true“ fatigue damage from the waves can be calculated and the provisional values of  $(H_s, T_p)$  of step (1) can be adjusted to yield the same fatigue damage.

It should be noted that step (2) in the averaging procedure is specific to the structure considered as it is based on a response calculation. Often only step (1) is carried out which is not structure specific.

The UpWind design basis [6] provides such 1-parameter wind-wave climates for the three sites of Ijmuiden, K13 shallow and K13 deep. Further, in the Marinet report of Bredmose et al (2012) [16] further two 1-parameter climates are given, one associated with the Beatrice jacket wind turbines and one for the Södra Midsjöbanken. Bredmose et al [16] compared the five climates and found that the correlation between  $V$  and  $H_s$  was very similar for the five data sets. The function

$$\frac{H_s}{H_0} = 1 + \frac{2.6 \left( \frac{v_{10}}{v_0} \right)^3}{1 + \left( \frac{v_{10}}{v_0} \right)^2} \quad 2-38$$

was found to represent the correlation well, as can be seen in Figure 2-6. Here  $v_{10}$  is the wind speed 10 m above mean sea level. It should be noted that the data are fatigue averaged and that the sites are for bottom fixed wind turbines, and thus more shallow than for typical floating wind turbine concepts. Nevertheless, the correlation seems quite general and may thus be relevant also for floating wind turbine climates.



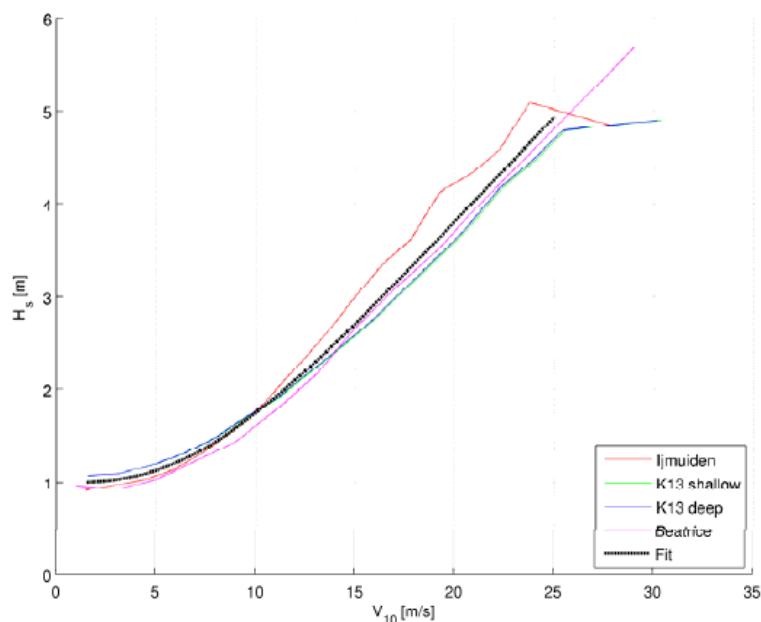


**Figure 2-6 Correlation between fatigue averaged value of significant wave height  $H_s$  and wind speed 10 meter above mean sea level,  $v_{10}$ . From [16].**

Further in [16] it was found that the correlation of  $H_s$  and  $T_p$  showed some more variation, although still being within the proposed bands of the IEC 61400-3 norm [1].

$$11.1\sqrt{H_s/g} \leq T \leq 14.3\sqrt{H_s/g} \quad 2-39$$

Here it should be noted that the formula describe limits for the wave period of extreme *single* waves occurring in a sea state with significant wave height  $H_s$ , and not peak periods. Strictly speaking, it thus cannot be used for  $T_p$  values. The observation that the values fell within the bands of 2-39 is still valid, though.

### 2.3.5 Extreme conditions

Additionally to the broad statistics of wave climates conditional to a given wind speed and averaged one-parameter climates, data for extreme conditions are needed to design for ULS loads. Traditionally, the 1- and 50-year quantiles of the marginal distributions of  $V$  and  $H_s$  are used along with the maximum single wave height within the 1- and 50-year sea states. The UpWind design basis [6] gives several examples of this.

An alternative approach to the marginal distributions is the environmental contour method, where the joint probability distribution of  $(V, H_s, T_p)$  is utilized to define a surface in the  $(V, H_s, T_p)$ -space with a probability associated with a 50-year return period. This method is applied in Johannesen et al [14]. Further examples for five sites in the North Sea and the Atlantic are provided in [17].

## 2.4 Scaling of wind-wave conditions for laboratory tests

When a structure is to be modelled in the lab with simultaneous wind and wave loads, the dominance of gravity as the restoring force for the waves implies that Froude scaling is the relevant scaling law. Given a length scale ratio of  $\lambda$  between prototype scale and model scale, the forces will scale like  $(\rho_{wp}/\rho_{wm})\lambda^3$ , where the first factor is the ratio of water density at prototype and lab conditions.

To achieve dynamic similarity, i.e. that all forces scale consistently, the aerodynamic loads must follow the same scaling. This is the basis for the Froude scaling for wind-wave conditions which is derived and discussed in chapter 2.2. Strict application of this principle leads to a scaling of wind speeds like  $\lambda^{1/2}$ . This may, however, not be possible in all lab settings. Therefore a free parameter  $\beta$  is introduced to allow for an adjustment of the lab wind speed beyond strict Froude scaling.

The scaling law and associated scaling of structural properties and external wind-wave climate parameters is described in chapter 2.2.

### References to Section 2.2 to 2.4

- [1] IEC 61400-3: Wind turbines- Part 3: Design of offshore wind turbines, 2009.
- [2] DNV-OS-J101: Design of offshore wind turbine structures. May 2014.
- [3] DNV-OS-J103: Design of floating wind turbine structure. June 2013.
- [4] [www.windatlas.dk](http://www.windatlas.dk) and [www.wasp.dk](http://www.wasp.dk)
- [5] Karagali, A. Pena, M. Badger and C.B. Hasager, Wind characteristics of the North Sea and the Baltic Seas from QuickScatt satellite. Wind Energy. 2012
- [6] UpWind: Fisher, T., W. deVries and B. Schmidt: UpWind deliverable, Design Basis WP4: Offshore Foundations and Support Structures - UpWind Project. University Stuttgart, 2010.
- [7] Kaimal J.C., Wyngaard J.C., Izumi Y. and Coté O.R. (1972). "Spectral Characteristics of Surface-Layer Turbulence". Quart. J. Royal Meteorology Soc., 98, pp 563 – 589.
- [8] IEC 61400-1, Design requirements, 2008.
- [9] Burton, T., Jenkins, N., Sharpe, D. and Bossanyi, E. (2011) Wind Energy Handbook. Second Edition. Wiley.
- [10] J.Mann, Wind field simulation, Prob. Engng. Mech. Volume 14, no 4, 269-282, 1998
- [11] Svendsen, I.A. and Jonsson, I.G. (1976) Hydrodynamics of Coastal Regions. Den Private Ingeniørfond, Technical University of Denmark.
- [12] Pierson, W. J. and Moskowitz, L. 'A proposed spectral form for fully developed wind seas based on the similarity theory of S. A. Kitaigorodskii' (1964). J. Geophys. Res. 69(24), pp 5181-5190.
- [13] Hasselmann K., T.P. Barnett, E. Bouws, H. Carlson, D.E. Cartwright, K. Enke, J.A. Ewing, H. Gienapp, D.E. Hasselmann, P. Kruseman, A. Meerburg, P. Miller, D.J. Olbers, K. Richter, W. Sell, and H. Walden (1973). 'Measurements of wind-wave growth and swell decay during the Joint North Sea Wave Project (JONSWAP)'. *Ergänzungsheft zur Deutschen Hydrographischen Zeitschrift Reihe, A*(8) (Nr. 12), p.95.
- [14] K. Johannessen. Joint distribution for wind and waves in the northern North Sea. In Proceedings of the Eleventh International Offshore and Polar Engineering Conference, 2001.
- [15] M Kühn, "Dynamics and design optimisation of offshore wind energy conversion systems," PhD Thesis, Delft University of Technology, Delft, The Netherlands, 2001.
- [16] Bredmose, H., Larsen, S.E., Matha, D., Rettenmeier, A., Marino, E. and Sætran, L. (2012). Collation of offshore wind-wave dynamics. Deliverable D4.2 of the EU Marinet project.
- [17] Li, L., Gao, Z. and Moan, T. (2013) Joint Environmental Data at Five European Offshore Sites for Design of Combined Wind and Wave Energy Devices. Proc. ASME 32nd Int. Conf. Ocean, Offshore and Arctic Engng., Nantes, France, June 2013.

### 2.5 Model building experience

A model of the OC4-DeepCWind semi-submersible, (Robertson, et al., 2013), has been built at the University of Stuttgart for the wave tank tests scheduled within the InnWind.EU project, Figure 2-7.

The generic model has been chosen in order to provide an additional test series in a different wave tank than the previous test with the aim of making the data public for the research community. The numerical codes of the project partners shall be validated and additionally special load cases and controller settings shall be analysed. This section will give an insight into the practical aspects of the choice of materials, strength calculations, the mass distribution and design considerations for the joints. Afterwards the identification process of the mass and inertia properties is outlined. Finally, the applied sensor technology with wireless data transmission is shown.

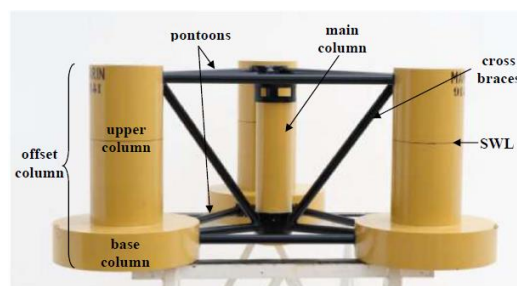


Figure 2-7 Scaled OC4-DeepCWind model at the University of Stuttgart (left) and model description by (Robertson A. , et al.) (right).

### 2.5.1 Materials and strength calculations

The original full scale model is made of steel and ballasted with water in the offset columns. This design is unsuitable for the scaled model due to small wall thickness and the resulting lack of stiffness. Therefore the upper columns and the main column are made out of PVC tubes where the central column has been reinforced by braided carbon-fiber-reinforced polymers in order to strengthen the connection to the tower which is the bottleneck in terms of material stresses. The struts are also carbon-fiber-reinforced polymers. The base columns are fabricated as solid parts out of laminated timber, which has been afterwards sealed by spar varnish. They include part of the ballast and are convenient to shape and assemble. The main ballast is implemented as dumbbell disks to be flexible and to lower the centre of gravity.

The integrity of the structure has been proven by static hand calculations assuming that the ballast disks are preassembled and the highest load occurs during transport, when the platform is suspended at the tower-base connection and the columns are hanging loose producing a high sectional moment at the joints of the struts at the main column. The safety factor for this calculation was assumed as 10.

### 2.5.2 Identification of mass properties

The exact measurement of the centre of gravity, the mass and the mass moment of inertia of the scaled model is highly important in order to properly evaluate the discrepancies between the physical results and the numerical simulations. While scaling mass and moments of inertia, the water density has to be considered, since the tests are performed in freshwater rather than salt water. The lengths and diameters of all parts, as well as the overall mass match to their scale. During the construction and building process, the masses and the moments of inertia were frequently monitored within the CAD system. This includes weighing all manufactured parts and updating their mass in the CAD system. Especially the heavier than scaled main column reduces all

three moments of inertia and lifts the centre of gravity. To compensate this mismatch, additional weights are placed at the bottom outer side of the wooden base columns, see Figure 2-8.

The final centre of gravity and moment of inertia are determined by pendulum tests as was proposed by NACA, see (Gracey, 1948). This method is easy to reproduce wherever there is a crane, e.g. with a new wind turbine mounted at the platform.

### 2.5.3 Sensors and data transmission

The sensors on the platform measure the acceleration in all six (translational and rotational) degrees of freedom as well as the mooring line forces. The mooring forces are measured at the fairleads on top of the base columns, see Figure 2-8. The force sensor is firmly fixed at the base column, so its own weight doesn't affect the mooring line behaviour. The drawback is that the angle of the measured force is fix and independent of the real mooring line angle.

As was shown by (Robertson, et al., 2013) it is important to avoid cables for data transmission going from the floating platform to the stationary data logger. Therefore an onboard storage system has been built saving the platform measurement data on an SD card on the platform and sends it via a wireless connection to a PC at the rate of 100Hz. The measurement equipment is powered by a lithium-ion battery and safely stowed in one of the offset columns. Therefore it is easily accessible, even if the platform is in the water.

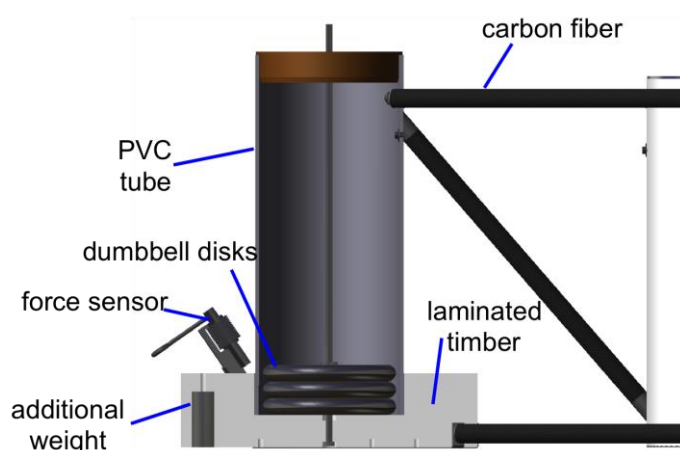


Figure 2-8 Sketch of the outer column of the OC4 semi-submersible

## References Chapter 1 and 2

- Pole Mer Paca. (2012). Retrieved May 3, 2014, from <http://www.polemerpaca.com/Ressources-energetiques-marines/Energies-marines-renouvelables/VERTIWIND>
- Adam, F., Myland, T., Dahlhaus, F., & Großmann, J. (2014). Scale tests of the Gicon-TLP for wind turbines.
- Adam, F., Myland, T., Dahlhaus, F., & Großmann, J. (2014). Scale Tests of the Gicon-TLP for Wind Turbines. *Proceedings of the ASME 2014 33rd International Conference on Ocean, Offshore and Arctic Engineering*. San Francisco, USA.
- Aguirre-Suso, G., Pérez-Morán, G., Sánchez-Lara, M., Lopez-Mendia, J., Fernández, J., Laidler, A., et al. (2014). Nautilus: Design Considerations For A 5mw Wind Turbine Semisubmersible Platform. *Proceedings of the EWEA*.
- al., A. M. (2014). Model test of a 1:8 scale floating wind turbine offshore in the gulf of maine. *Proceedings of the ASME 2014 33rd International Conference on Ocean, Offshore and Arctic Engineering*.
- Amate Lopez, J., Martín, V. d., Marugan García, L., & Alonso, P. (2014). Iberdrola Ingeniería Tipwind: "A smart way to drive costs down ". *Proceedings of the EWEA*, (p. 24089).
- Aubault, A., Cermelli, C., & Roddier, D. (2009). Windfloat: A Floating Foundation For Offshore Wind Turbines Part iii: Structural Analysis.
- Azcona, J., Bouchotrouch, F., González, M., Garciandá, J., Munduate, X., Kelberlau, F., et al. (2014, #jun#). Aerodynamic Thrust Modelling in Wave Tank Tests of Offshore Floating Wind Turbines Using a Ducted Fan. *Journal of Physics: Conference Series*.
- Bayati, I., Belloli, M., Ferrari, D., Fossati, F., & Giberti, H. (2014). Wind Tunnel Tests On Floating Offshore Wind Turbines : Design Of A 6-DOD Robotic Platform For Floating Motion Simulation. *Proceedings of the EWEA*. Barcelona.
- Berlo, D., Gabrielson, C., Hanly, S., Parzych, M., Sacco, M., & Ryan, S. (2010). *Design Of Scale-Model Floating Wind Turbine Platforms*. Ph.D. dissertation, Worcester Polytechnic Institute.
- Blue H Group. (2012). Retrieved November 15, 2012, from <http://www.bluehgroup.com/>
- Blue H Group. (2012). Retrieved November 15, 2012, from <http://www.bluehgroup.com/>
- Bottasso, C., Campagnolo, F., & Petrovic, V. (2014, #apr#). Wind tunnel testing of scaled wind turbine models: Beyond aerodynamics. *Journal of Wind Engineering and Industrial Aerodynamics*, 127, 11-28.
- Boulluec, M. L., Martin, A., & Houmard, A. (2013). Tank Testing Of A New Concept Of Floating Offshore Wind Turbine. *Proceedings of the 22nd International Conference on Offshore and Polar Engineering*.
- Bredmose, H., Larsen, S. E., Matha, D., Rettenmeier, A., Marino, E., & Saettran, L. (2012). *MARINET D2.4: Collation of offshore wind-wave dynamics*. Tech. rep.
- Bredmose, H., Schløer, S., & Paulsen, B. (2012). Higher-harmonic response of a cantilever beam to fully nonlinear regular wave forcing.
- Bulder, B., & Henderson, A. (2002). *Studie Naar Haalbaarheid Van en Randvoorwaarden Voor Drijvende Offshore Windturbines*. TNO-Bouw.



- Campagnolo, F., Bottasso, C. L., & Bettini, P. (2014). Design, manufacturing and characterization of aero-elastically scaled wind turbine blades for testing active and passive load alleviation techniques within a ABL wind tunnel.
- Cermelli, C., Roddier, D., & Aubault, A. (2009). Windfloat: A Floating Foundation For Offshore Wind Turbines Part II: Hydrodynamics Analysis. *Proceedings of the ASME 28th International Conference on Ocean, Offshore and Arctic Engineering*.
- Chakrabarti, S. (1998). Physical Model Testing of Floating Offshore Structures.
- Chujo, T., Minami, Y., Nimura, T., & Ishida, S. (2013). Experimental Study For Spar Type Floating Offshore Wind Turbine With Blade-Pitch Control., (pp. 1-7).
- Consulting Main(e) International, L. (September 2012). *Floating Offshore Wind Foundations: Industry Consortia and Projects in the United States, Europe and Japan - An Overview*. Bremen ME 04551, USA.
- Cordle, A., & Jonkman, J. (2011). *State of the Art in Floating Wind Turbine Design Tools*. unpublished.
- Courbois, A. (2013). *Étude expérimentale du comportement dynamique d ' une éolienne offshore flottante soumise à l'action conjuguée de la houle et du vent*. Ph.D. dissertation, \{E}cole Centrale de Nantes.
- EWEA. (2013). *Deep water - The next step for offshore wind energy*. Tech. rep.
- Faltinsen, O. M. (1993). *Sea loads on ships and offshore structures*. Cambridge [u.a.]: Cambridge University Press.
- Floating Power Plant. (2012). Retrieved April 20, 2014, from <http://www.floatingpowerplant.com/>
- Fowler, M., Iii, D. A., Kimball, R., & Goupee, A. (2013). Wave Basin Model Tests Of Floating Offshore Wind Turbines., (pp. 1-11).
- Frye, J., Horvath, N., & Ndegwa, A. (2011). *Design Of Scale-Model Floating Wind Turbine: Spar Buoy*. Ph.D. dissertation, Worcester Polytechnic Institute.
- Fujiwara, H., Tsubogo, T., & Nihei, Y. (2011). Gyro Effect of Rotating Blades on the Floating Wind Turbine Platform in Waves. *Proceedings of the Twenty-first (2011) International Offshore and Polar Engineering Conference*, 8, pp. 399-406.
- Fukushima Forward*. (n.d.). (The University of Tokyo) Retrieved from <http://www.fukushima-forward.jp/pdf/pamphlet3.pdf>
- Goupee, A. J., Koo, B. J., Lambrakos, K. F., & Kimball, R. W. (2012). Model Tests for Three Floating Wind Turbine Concepts. *Offshore Technology Conference*. Houston, TX/USA.
- Gracey, W. (1948). *The Experimental Determination of the Moments of Inertia of Airplanes by a Simplified Compound-Pendulum Method*. Washington.
- Großmann, J., & Dahlhaus, F. (2013). Gicon-Tlp For Floating Wind Turbines Experimental And Numerical Investigations. *Proceedings of the EWEA Offshore*, (pp. 1-8).
- Guanche, R., Meneses, L., Sarmiento, J., Vidal, C., & Losada, Í. (2014). Methodology to obtain the life cycle mooring loads on a semisubmersible wind platform. *Proceedings of the ASME 2014 33rd International Conference on Ocean, Offshore and Arctic Engineering*.
- Hall, M., Moreno, J., & Thiagarajan, K. (2014). Performance Specifications For Real-Time Hybrid Testing Of 1:50-Scale Floating Wind Turbine Models. *Proceedings of the ASME 2014 33rd International Conference on Ocean, Offshore and Arctic Engineering*. San Francisco, USA.

- Hansen, A. M., Laugesen, R., Bredmose, H., Mikkelsen, R., & Psychogios, N. (2014). Small scale experimental study of the dynamic response of a tension leg platform wind turbine. *Submitted for journal publication*.
- Henderson, A. R., & Witcher, D. (2010, #jan#). Floating Offshore Wind Energy - A Review of the Current Status and an Assessment of the Prospects. *Wind Engineering*, 34(1), 1-16.
- Huijs, F., Mikx, J., Savenije, F., & Ridder, E.-J. D. (2013). Integrated design of floater , mooring and control system for a semi-submersible floating wind turbine. *Proceedings of the EWEA Offshore*.
- Huijs, F., Ridder, E.-J. D., & Savenije, F. (2014). Comparison Of Model Tests And Coupled Simulations For A Semi-Submersible Floating Wind Turbine. *Proceedings of the ASME 2014 33rd International Conference on Ocean, Offshore and Arctic Engineering*. San Francisco, USA.
- Iijima, K., Kawai, M., Nihei, Y., Murai, M., & Ikoma, T. (2013). Conceptual Design Of A Single-Point-Moored Fowt And Tank Test For Its Motion Characteristics., (pp. 1-8).
- Ishida, S., Kokubun, K., Nimura, T., Utsunomiya, T., Sato, I., & Yoshida, S. (2013). At-sea experiment of a hybrid spar type offshore wind turbine. *ASME 2013 32nd International Conference on Ocean, Offshore and Arctic Engineering*.
- Ishihara, T., Phuc, P. V., Sukegawa, H., & Shimada, K. (2007). A study on the dynamic response of a semi-submersible floating offshore wind turbine system Part 1 : A water tank test. *Proceedings of the 12th International Conference on Wind Engineering*. Cairns, Australia.
- Ishihara, T., Waris Bilal, M., & Sukegawa, H. (2009). A Study On Influence Of Heave Plate On Dynamic Response Of Floating Offshore Wind Turbine System. *The 3rd European Offshore Wind (EOW) Conference*.
- Jain, A., Robertson, A., Jonkman, J., Goupee, A., Kimball, R., & Swift, A. H. (2012). FAST Code Verification of Scaling Laws for DeepCwind Floating Wind System Tests., 4, pp. 355-365.
- Jonkman, J., Butterfield, S., Musial, W., & Scott, G. (2009). Definition of a 5-MW Reference Wind Turbine for Offshore System Development Definition. (February).
- Karimirad, M. (2011). *Stochastic Dynamic Response Analysis of Spar-Type Wind Turbines with Catenary or Taut Mooring Systems*. Ph.D. dissertation, NTNU.
- Kimball, R., Goupee, A. J., Fowler, M. J., Ridder, E.-J. D., & Helder, J. (2014). Wind/wave basin verification of a performance-matched scale-model wind turbine on a floating offshore wind turbine platform. *Proceedings of the ASME 2014 33rd International Conference on Ocean, Offshore and Arctic Engineering*. San Francisco, USA.
- Koo, B., Goupee, A. J., Lambrakos, K., & Lim, H.-J. (2014). Model Test Data Correlations with Fully Coupled Hull/Mooring Analysis For A Floating Wind Turbine On A Semi-Submersible Platform. *Proceedings of the ASME 2014 33rd International Conference on Ocean, Offshore and Arctic Engineering*. San Francisco, USA.
- Kyushu University. (2012). Retrieved April 2014, from [www.riam.kyushu-u.ac.jp/ship/indexe.html](http://www.riam.kyushu-u.ac.jp/ship/indexe.html) (30)
- Make, M. (2014). *Predicting scale effects on floating offshore wind turbines*. Ph.D. dissertation, University of Delft.
- Martin, H. R. (2011). *Development Of A Scale Model Wind Turbine For Testing Of Offshore Floating Wind Turbine Systems*. Ph.D. dissertation, University of Maine.

- Martin, H. R., Kimball, R. W., Viselli, A. M., & Goupee, A. J. (2012, #jul#). Methodology for Wind/Wave Basin Testing of Floating Offshore Wind Turbines. *Proceedings of the 31st International Conference on Ocean, Offshore and Arctic Engineering OMAE2012* (pp. 445-454). Asme.
- Masciola, M., Robertson, A., Jonkman, J., Coulling, A., & Goupee, A. (2013). Assessment of the Importance of Mooring Dynamics on the Global Response of the DeepCwind Floating Semisubmersible Offshore Wind Turbine. *Proceedings of the Twenty-third (2013) International Offshore and Polar Engineering*. Anchorage/Alaska.
- Matsukuma, H., & Utsunomiya, T. (2008, #nov#). Motion analysis of a floating offshore wind turbine considering rotor-rotation. *The IES Journal Part A: Civil & Structural Engineering*, 1(4), 268-279.
- Myhr, A., Maus, K. J., & Nygaard, T. A. (2011). Experimental and Computational Comparisons of the OC3-HYWIND and Tension-Leg-Buoy ( TLB ) Floating Wind Turbine Conceptual Designs. *Proceedings of the Twenty-first (2011) International Offshore and Polar Engineering Conference*, 8, pp. 353-360.
- Naqvi, S. K. (2012). *Scale model experiments on floating offshore wind turbines*. Ph.D. dissertation, Worcester Polytechnic Institute.
- Nautica Windpower. (2012). Retrieved May 16, 2014, from <http://www.nauticawindpower.com>
- Nielsen, F., Gunnar, T., Hanson, D., & Skaare, B. (2006). Integrated dynamic analysis of floating offshore wind turbines.
- Olinger, D. J., Destefano, E., Murphy, E., Naqvi, S. K., & Tryggvason, G. (2012). Scale-model experiments on floating wind turbine platforms. *50th AIAA Aerospace Sciences Meeting including the New Horizons Forum and Aerospace Exposition*, (pp. 1-11).
- Olinger, D. J., Destefano, E., Murphy, E., Naqvi, S. K., Tryggvason, G., Introduction, I., et al. (2012). Scale-model experiments on floating wind turbine platforms. *50th AIAA Aerospace Sciences Meeting including the New Horizons Forum and Aerospace Exposition*, (pp. 1-11).
- Paulsen, U. S., Pedersen, T. F., Madsen, H. A., Enevoldsen, K., Nielsen, P. H., Berthelsen, P. A., et al. (2011). Deepwind- An innovative wind turbine concept for offshore. *Proceedings of the EWEA*. Brussels, Belgium.
- PelaStar Wind. (2012). Retrieved May 3, 2014, from [www.pelastarwind.com/](http://www.pelastarwind.com/)
- Philippe, M. e. (2014). Comparison of simulation and tank test results of a semi-submersible floating wind turbine under wind and wave loads. *ASME 2013 32nd International Conference on Ocean, Offshore and Arctic Engineering*.
- Quesnel, L., Bard, J., & Hanssen, J. E. (2011). Introducing Hiprwind high power, high reliability offshore wind technology. *Proceedings of the EWEA*.
- Ren, N., Li, Y., & Ou, J. (2012). The Wind-Wave Tunnel Test of a New Offshore Floating Wind Turbine with Combined Tension Leg-Mooring Line System. *Proceedings of the Twenty-second (2012) International Offshore and Polar Engineering Conference*, 4, pp. 255-261.
- Ridder, E.-J. D., Otto, W., Zondervan, G.-J., Savenije, F., & Huijs, F. (2013). State of the art model testing techniques for floating wind turbines. *Proceedings of the EWEA Offshore*.
- Robertson, A. N., Jonkman, J. M., Goupee, A. J., Kimball, R. W., & Swift, A. H. (2012). FAST Code Verification of Scaling Laws for DeepCwind Floating Wind System Tests Preprint Anant Jain. *Proceedings of the 22nd International Conference on Offshore and Polar Engineering*. Rhodes, Greece.



- Robertson, A., Goupee, A., Jonkman, J., Prowell, I., Molta, P., Coulling, A., et al. (2013). Summary Of Conclusions And Recommendations Drawn From The Deepwind Scaled Floating Offshore Wind System Test Campaign., (pp. 1-13).
- Robertson, A., Jonkman, J., Masciola, M., Song, H., Goupee, A., Coulling, A., et al. (n.d.). *Definition of the Semisubmersible Floating System for Phase II of OC4*. Tech. rep.
- Roddier, D. (2009). Windfloat: A Floating Foundation For Offshore Wind Turbines Part I: Design Basis And Qualification Process. *Proceedings of the ASME 28th International Conference on Ocean, Offshore and Arctic Engineering*.
- Roddier, D., Cermelli, C., Aubault, A., & Weinstein, A. (2010). WindFloat: A floating foundation for offshore wind turbines. *Journal of Renewable and Sustainable Energy*, 2(3), 033104.
- Sarpkaya, T., & Isaacson, M. (1981). *Mechanics of wave forces on offshore structures*. Van Nostrand Reinhold Co.
- Scandinavian Oil-Gas Magazine. (2010). Windsea - Next generation Floating Wind Farm. *Scandinavian Oil-Gas Magazine*(7/8 2010).
- Sethuraman, L., & Venugopal, V. (2013, #apr#). Hydrodynamic response of a stepped-spar floating wind turbine: Numerical modelling and tank testing. *Renewable Energy*, 52, 160-174.
- Shin, H. (2011). Model Test of the OC3-Hywind Floating Offshore Wind Turbine. *Proceedings of the Twenty-first (2011) International Offshore and Polar Engineering Conference*, 8, pp. 361-366.
- Shin, H., & Dam, P. T. (2012). Model Test of a Floating Offshore Wind Turbine Moored by a Spring-tensioned-leg. 4, 287-291.
- Stewart, G., Lackner, M., & Goupee, A. (2012). Calibration and Validation of a FAST Floating Wind Turbine Model of the DeepCwind Scaled Tension-Leg Platform. *Proceedings of the 22nd International Conference on Offshore and Polar Engineering*. Rhodes, Greece.
- Sumer, B. M., & Fredsøe, J. (Volume 12, 2006). *Hydrodynamics Around Cylindrical Structures. Advanced Series on Ocean Engineering, World Scientific*.
- Sway. (2012). Retrieved April 16, 2014, from <http://www.sway.no/>
- Utsunomiya, T., Matsukuma, H., Minoura, S., Ko, K., Hamamura, H., Kobayashi, O., et al. (2013, #jun#). At Sea Experiment of a Hybrid Spar for Floating Offshore Wind Turbine Using 1/10-Scale Model. *Journal of Offshore Mechanics and Arctic Engineering*, 135(3), 8.
- Utsunomiya, T., Sato, T., Matsukuma, H., & Yago, K. (2009). Experimental Validation for Motion of a SPAR-Type Floating Offshore Wind Turbine Using 1/22.5 Scale Model. pp. 951-959.
- Utsunomiya, T., Yoshida, S., Ookubo, H., Sato, I., & Ishida, S. (2014, #mar#). Dynamic Analysis of a Floating Offshore Wind Turbine Under Extreme Environmental Conditions. *Journal of Offshore Mechanics and Arctic Engineering*, 136(2).
- Viselli, A., Goupee, A., & Dagher, H. (2014). Model Test Of A 1:8 Scale Floating Wind Turbine Offshore In The Gulf Of Maine. *Proceedings of the ASME 2014 33rd International Conference on Ocean, Offshore and Arctic Engineering*. San Francisco, USA.
- Wang, C. M., Utsunomiya, T., Wee, S. C., & Choo, Y. S. (2010). Research on floating wind turbines: a literature survey. *The IES Journal Part A: Civil & Structural Engineering*, 3, pp. 267-277.
- Wang, K., Moan, T., & Hansen, M. O. (2013). A Method For Modeling Of Floating Vertical Axis Wind Turbine. *Proceedings of the ASME 2013 32nd International Conference on Ocean, Offshore and Arctic Engineering*, (pp. 1-10).

Wehmeyer, C., Ferri, F., & Frigaard, P. B. (2013). Experimental Study of an Offshore Wind Turbine TLP in ULS Conditions. *Proceedings of the Twenty-third (2013) International Offshore and Polar Engineering*, 9, pp. 301-308.

Windsea. (2012). Retrieved April 19, 2014, from [www.windsea.no](http://www.windsea.no)

Zamora-Rodriguez, R., Gomez-Alonso, P., Amate-Lopez, J., De-Siego-Martin, V., Dinoi, P., Simos, A., et al. (2014). Model Scale Analysis Of A Tip Floating Offshore Wind Turbine. *Proceedings of the ASME 2014 33rd International Conference on Ocean, Offshore and Arctic Engineering*. San Francisco, USA.

## 3 DEFINITION OF TEST MODEL WITH ROTOR THRUST INTEGRATION (NANTES)

### 3.1 Introduction

Reliable recreation of the dynamics of a full scale floating wind turbine by a scaled model in a basin requires the precise scaling of the masses and inertias and also the relevant forces and its frequencies acting on the system. The scaling of floating wind turbines based on the Froude number is customary for basin experiments. This method preserves the hydrodynamic similitude, but the resulting Reynolds number is much lower than in full scale. The aerodynamic loads on the rotor are therefore out of scale. Several approaches have been taken to deal with this issue, like using a tuned drag disk or redesigning the scaled rotor. These methods have several drawbacks, as will be discussed in section 3.2, and the cost can be high.

In this chapter we describe the work of development and experimental validation of an alternative method based on the use of a ducted fan located at the model tower top in the place of the rotor. The fan can introduce a variable force that represents the total wind thrust by the rotor. A system controls this force by varying the rpm, and a computer simulation of the full scale rotor provides the desired thrust to be introduced by the fan. This simulation considers the wind turbine control, gusts, turbulent wind, etc. The simulation is performed in synchronicity with the test and it is fed in real time by the displacements and velocities of the platform captured by the acquisition system. Thus, the simulation considers the displacements of the rotor within the wind field and the calculated thrust models the effect of the aerodynamic damping. The system is not able currently to match the effect of gyroscopic momentum.

The method has been applied to the testing of a semisubmersible platform with full catenary mooring lines for a 6MW wind turbine in scale 1/40 at École Centrale de Nantes. Several tests including pitch free decay under constant wind and combined wave and wind cases have been performed. Data from the experiments are compared with aero-servo-hydro-elastic computations with good agreement showing the validity of the method for the representation of the scaled aerodynamics. The new method for the aerodynamic thrust scaling in basin tests is very promising considering its performance, versatility and lower cost in comparison with other methods.

The development and validation has been performed by CENER within the INN WIND.EU project. The access to the ECN wave tank has been granted to CENER by the MARINET program financed by the European Commission. The platform model used in the validation was offered by Dr.techn.Olav Olsen AS (OO) and the Institute for Energy Technology (IFE) provided the platform scaled model where the fan was coupled for the demonstration of the new methodology.

This method will be applied in the wave tank tests of scaled 10 MW wind turbine model that will be performed in Nantes in autumn 2014 as part of the activities of the INN WIND.EU task 4.2.

### 3.2 Existing Methods for the Wind Thrust integration in Combined Wave and Wind Tests

Froude scaling has become a standard in the different scaled floating wind turbine test campaigns performed up to date [1]. This methodology has been extensively used in the oil & gas industry, and experience has shown that it is an efficient way of preserving the hydrodynamic similarity. The realistic inclusion of wind for the testing of a floating wind turbine in combination with waves is a technical challenge, because Froude scaling produce low Reynolds numbers. As the lift and drag coefficients of the blade airfoils are very sensitive to the Reynolds number, the aerodynamic forces on the turbine rotor are out of scale when Froude scaling is directly applied.

One method to deal with this issue consists on the use of a drag disk instead of the rotor. If the dimensions and the drag of the disk are correctly chosen, the wind flow will produce a representative force of the full scale wind loading. With this system the influence of the control logic over the aerodynamic loading cannot be captured and the aerodynamic torque is not accurately modelled. The gyroscopic effects can be taken into account by installing a motor that rotates a mass

representing the rotor inertia at the adequate speed. This methodology was used in the WindFloat project [2].

A different approach was taken in the DeepCwind test campaign [3]. The wind turbine model was scaled according to the Froude number. To achieve appropriately scaled thrust forces, the wind speeds had to be increased, but the matching of the aerodynamic characteristics was not good enough.

Finally, a more precise alternative consists of redesigning the rotor of the scaled model, so that a representative thrust of the full scaled aerodynamic force is obtained in the new rotor at the low Reynolds regime [1].

### 3.3 Description of the New Ducted Fan/Software-in-the-Loop Method

The basic concept of the new method developed consists of substituting the rotor by a fan driven by an electric motor. The fan thrust is controlled by the fan rotational speed set by the controller, which again depends on the real time simulation of the full scale rotor in a turbulent wind field, with the platform motions measured in real time in the wave tank test. The FAST code developed by NREL [4] was used for the simulation of the rotor thrust. This code has been extensively validated within the IEA Annex 30 (OC3) for the simulation of floating wind turbine including comparisons of the rotor aerodynamic thrust with other software [5]. We refer to the described method as Software-in-the-Loop (SIL).

### 3.4 Control of the Ducted Fan

The fan system used in the tests is composed of a brushless motor integrated with the ducted fan. The motor power electronics is regulated by an Electronic Speed Controller (ESC) card that is powered by an industrial AC/DC power supply. The rpm of the motor is controlled by a Pulse Width Modulation (PWM) signal that is generated with the LabVIEW control software, using servo libraries for Arduino. The demanded force for the fan is provided by the full scale simulation of the rotor's aerodynamic thrust. The PWM signal has a variable period with a range between 1000ms (fan stopped) and 2000ms (fan at maximum power). The ESC model can be configured and fine-tuned by a programming card that allows setting parameters as the timing of the motor, the type of power supply or the PWM-frequency. Figure 3-1 shows the layout of the system hardware.

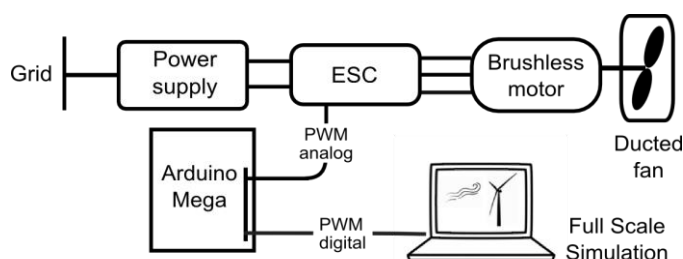


Figure 3-1 Fan Control System Lay Out

The selection of the power of the fan system is based on the range of required thrust during the test. This depends on the nominal power of the wind turbine and the scale factor. In addition, the thermal stability of the fan system has to be considered, in order to run at the required power during the requested time of the test and avoid using a cooling down phase.

### 3.5 Implementation of the Software-in-the-Loop System

The layout of the system is shown in Figure 3-2 Software-in-the-Loop Method Diagram. The left side describes the simulation part of the system, which works in full scale, and the right

side represents the wave tank scaled test. The different magnitudes that are interchanged between both blocks are transformed by the appropriated scaling laws based on the factor scale  $\lambda$ .

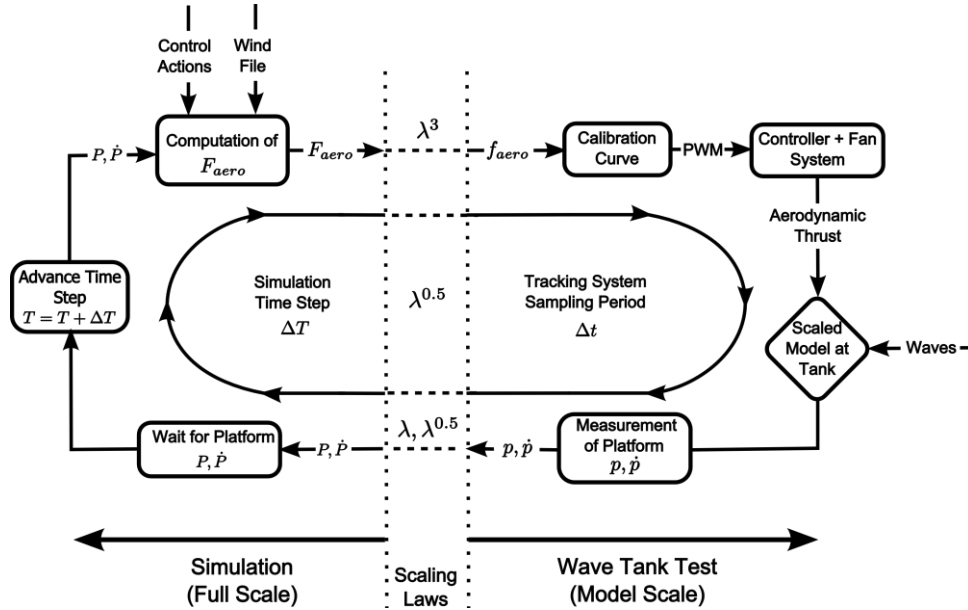


Figure 3-2 Software-in-the-Loop Method Diagram

The simulation tool provides the total aerodynamic force on the shaft  $F_{aero}$  from integration of all the aerodynamic loading at the blade elements. This force in full scale is transformed to the model scale

( $f_{aero}$ ) and the pulse width of the PWM signal needed to produce the force in the ducted fan is provided by a calibration curve (see Section 3.10). The control system regulates the fan speed that introduces the desired force at the model's hub height. The waves produced by the wave maker are also acting over the platform and, together with the aerodynamic thrust, inducing motions. The acquisition system measures the positions and velocities for the 6 degrees of freedom of the platform at a certain sampling period. These measurements are sent to the simulation tool that is waiting for the data to advance one time step and calculate the new value of the aerodynamic thrust. For this reason, the sampling period,  $\Delta t$ , and the simulation time step,  $\Delta T$ , have to be set accordingly (with a factor of  $\lambda^{0.5}$ ).

This approach can obtain a realistic aerodynamic thrust on the scaled model. As the computation of the force takes into consideration the motion of the platform, the effect of the aerodynamic damping is included. In addition, the control actions, the different types of wind (turbulent, constant, gusts) and the operating condition (idling, power production, etc.) are taken into account for the calculation of the thrust at every instant of the test. The simplicity of the method makes it cost effective and flexible because the material is not specific for a certain wind turbine model and it could be used in different tests for different models. It allows the generation of thrust force representation of 10 – 20 MW turbines by varying the set up rotation speed only. The main drawback is that it does not match correctly the gyroscopic momentum or the aerodynamic torque. These effects are considered less important with respect to the global dynamics of floating wind turbines.

### 3.6 Experimental Validation of the Software-in-the Loop Method

The performance of the Software-in-the-Loop system has been applied to a floating semi-submersible platform with a 6 MW turbine model and validated with a test campaign performed in December 2013 at the Ecole Centrale de Nantes (ECN) wave tank in France. The results of this validation are presented in the following sections to show the capabilities of the proposed methodology.

### 3.7 Description of the Floating Wind Turbine Model Used in the Verification

The platform concept that was tested at ECN is called "Concrete Star Wind Floater". It is an innovative semisubmersible design in concrete for a 6MW wind turbine. A sketch of the platform is provided in Figure 3-3. For the wind turbine model, we have scaled the NREL Baseline 5MW wind turbine [6] to be representative of a 6MW wind turbine, according to the public available data of the Siemens SWT-6.0-120 turbine. First, we adjusted the original rotor diameter from 126m to 120m, keeping the same relative radial distribution of chord, twist and airfoils. Then, we increased the rotor speed to obtain the Siemens 6MW nominal tip speed and we also increased the generator torque to match the nominal power. The main characteristics of the floating wind turbine are summarized in Table 3-1.

Property	Value	Comments
Total Weight	10091.5t	Including turbine
RNA mass	310t	-
Tower mass	350t	-
Platform mass	9431.5t	-
Centre of gravity	9.658m	Above Keel. Full system
Centre of buoyancy	7.046m	Above Keel.
Pitch/Roll inertia	7.46E6tm <sup>2</sup>	Referenced to platform centre & waterline. Full system.
Yaw inertia	4.5E6tm <sup>2</sup>	Referenced to platform centre & waterline. Full system.
Platform Draft	20m	-
Rotor diameter	120m	-
Rated wind speed	12.7m/s	-

Table 3-1 Main characteristics of the floating wind turbine

### 3.8 General Parameters of the Floating Wind Turbine in Full Scale

The mooring system is composed by three lines. The fairleads are located at the external cylinders surface, 14m below the Still Water Line (SWL). The anchors are located at a depth of 200m. The main parameters of the mooring system in full scale are shown in Table 3-2. The length of the two downwind lines (lines 2 and 3) has been reduced due to restrictions imposed by the dimensions of the wave tank (50m length, 30m width and 5m depth).

	Line 1	Line 2	Line 3
Anchors radial position	829.23m	580.0m	580.0m
Fairleads radial position	32.5m	32.5m	32.5m
Angular position of anchors	180°	60°	300°
Angular position of fairleads	180°	60°	300°
Depth of anchors	200m	200m	200m
Depth of fairleads	14m	14m	14m
Length	835.5m	835.5m	835.5m
Equivalent line diameter	0.126m	0.126m	0.126m
Mass density	106.77kg/m	106.77kg/m	106.77kg/m



Axial stiffness	7.536E8N	7.536E8N	7.536E8N
-----------------	----------	----------	----------

**Table 3-2 Mooring System Parameters in Full Scale**

### 3.9 Description of the Scaled Model

Froude scaling was applied to the model building using a scale factor of 1/40. The structural stiffness was not scaled, instead, the model can be considered rigid. A complete description of the scaled model is provided in [7]. As has been described in Section 4.33.10, a ducted fan substitutes the whole rotor in the scaled model. For the full scaled rotor of our 6MW wind turbine, we estimated an expected maximum peak of aerodynamic thrust of around 1500kN. Therefore, we chose a fan with a maximum thrust of 3kg (around 1900kN in full scale) that could reproduce the expected force with a comfort margin. The mass of the fan is around 0.5kg which is not enough to represent the 310t that weights the RNA in full scale. Therefore, we included some ballast at the scaled model tower top to match the required weight. Figure 3-4 shows an image of the scaled model in the basin with the ducted fan on top during a test.



**Figure 3-3 Concrete Star Wind Floater**

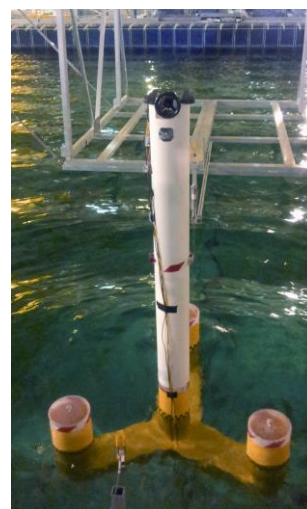


**Figure 3-4 Scaled Model in the Wave Tank**

### 3.10 Calibration of the Ducted Fan

The relationship between the PWM signal and ducted fan thrust was obtained by a static calibration. Figure 3-5 shows the installation of the fan on a cantilevered horizontal steel plate equipped with strain gages. With the fan disconnected, we loaded the plate with a set of weights to obtain a relation between the different weights and the plate deformation. Afterwards, we unloaded the plate, and connected the fan at different powers, measuring the deformation against the pulse width. We established the relationship between the PWM period and the static force of the fan with an error below 0.8% at medium and high power and below 2.5% at low power.





Figure 3-5 Fan Set Up for Calibration

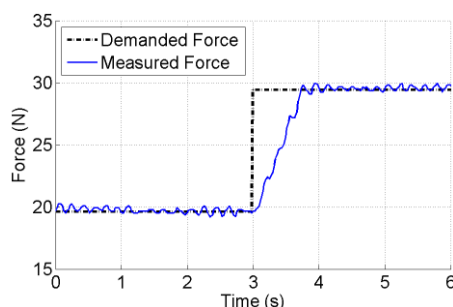


Figure 3-6 Fan Response to Step Demand

### 3.11 Analysis of the Dynamic Response of the Fan

We assessed the capability of the fan system to react to the required changes in thrust by demanding the fan a step change in the force and evaluating the delay in the response. Figure 3-6 shows the response of the fan to a step change in the demanded force of 9.8N (1kg). The noise in the measured force is due to vibrations in the beam/strain gauge setup excited by the fan. The slope of the measured force is 13.43N/s (136 kN/s in full scale). We performed a combined wind and wave simulation of our full scale wind turbine model, using a turbulent wind of 12.7m/s mean wind speed and 19% of turbulence intensity and waves with  $H_s = 2.6\text{m}$  and  $T_p = 7.3\text{s}$ . From the thrust signal (Figure 3-7) we estimated that the maximum rate of change of the thrust is approximately 140kN/s (Figure 3-8). The ducted fan therefore seems to have adequate response in terms of thrust force rate of change, but this is clearly just the first of several required tests, where the next ones will include phase information.

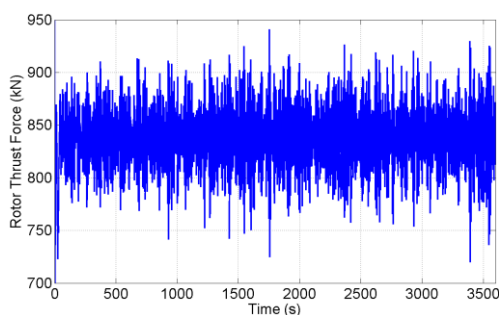


Figure 3-7 Computed Thrust Force

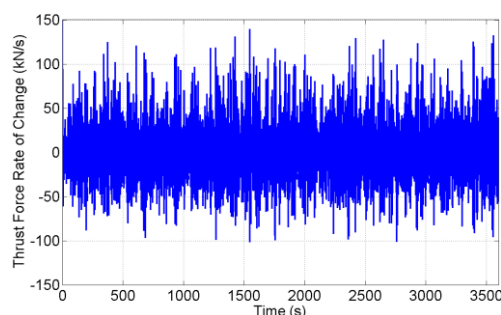


Figure 3-8 Thrust Force Rate of Change

### 3.12 Communication Protocol

We have used the LabVIEW software to acquire the data from the wave tank motion capture system (Qualisys) and to communicate with the wind turbine simulation software during the test execution. A TCP/IP network protocol was selected for the communication between LabVIEW and Qualisys and also between LabVIEW and the simulation code. TCP/IP has been selected because it provides a simple user interface that ensures a reliable network communication.

### 3.13 Discussion of the Results

The results of the experiments are discussed in the next sections in comparison with FAST full scale computations. The results are presented in full scale.

#### 3.13.1 Static Wind Tests

A set of tests in still water with different constant wind speeds were performed. Once all the transients were dissipated, the constant platform surge and pitch displacements were measured. The comparison of these experimental data with computations are presented in Figures 3-9 and

3-10 for different wind speeds. In addition to the rated wind speed (12.7m/s), which produces the maximum thrust, two lower wind speeds (5m/s and 8.5m/s) were chosen and also a higher wind speed of 25m/s. Once the static regime was reached, the rotor speed and blade pitch angle imposed by the controller in the SIL was constant.

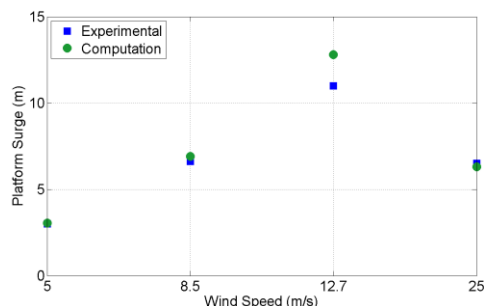


Figure 3-9 Surge Displacement with Constant Wind

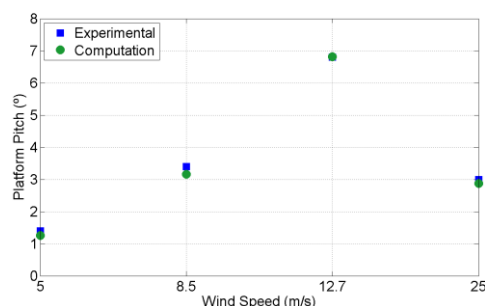


Figure 3-10 Pitch Displacement with Constant Wind

The results show a good agreement between measurements and computations for the surge and pitch displacements with the exception of the surge displacement for the wind speed of 12.7m/s. The computed displacement at this wind speed is 14% higher than the experimental. The surge displacement seems to be sensitive to small changes on the mooring parameters, in particular at rated wind speed. Some uncertainty on the value of some parameters of the mooring system exists that could cause the differences in surge at 12.7m/s. The agreement on the pitch angle between tests and simulations shows that the fan introduced the correct static force.

### 3.13.2 Free Decay Tests

We performed free decay tests of the moored platform in the surge and heave degrees of freedom. Figure 3-11 and 3-12 show a comparison of the experimental results obtained in surge and heave with computations. Quadratic damping has been added in the computations to take into account for viscosity. The agreement between measurements and simulations is very good. The surge oscillation period in the experiment seems to be slightly higher than in the computation. This could be due to small differences in the mooring system modelling resulting in slight differences in the stiffness.

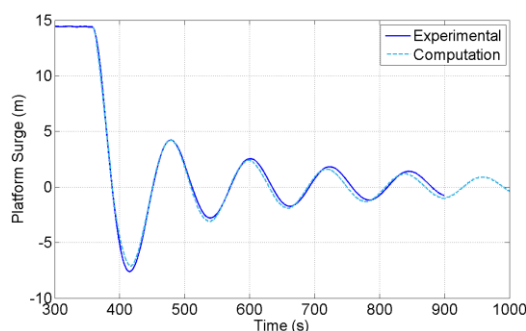


Figure 3-11 Free Decay Tests in Surge

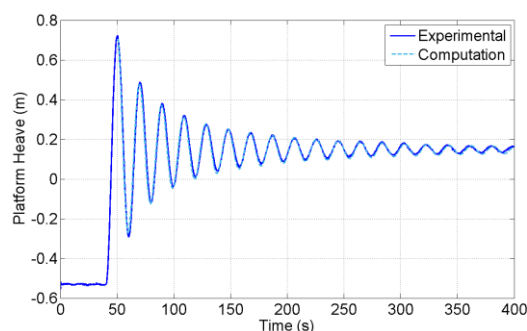
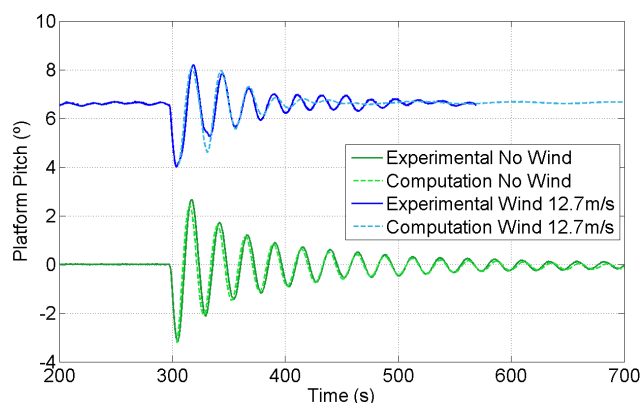


Figure 3-12 Free Decay Test in Heave

For the pitch degree of freedom, in addition to a regular test, we performed a second free decay including the aerodynamic loading of a constant wind of 12.7m/s. This second test allowed assessing the effect of the aerodynamic loading on the pitch behaviour of the platform. The wind speed of 12.7m/s produces the maximum thrust on the rotor and it is just in the transition between the wind turbine control regions 2 and 3. Therefore, pitch control is activated in this case. Figure 3-13 presents a comparison of both platform pitch free decay tests, with and without wind, with computations.



**Figure 3-13 Experimental and Computed Pitch Free Decay with & without Wind Loading**

In the free decay tests with no wind loading, the platform oscillates around the  $0^\circ$  position. The correspondence between measured data and computation is good. The same free decay tests performed with a constant wind of 12.7m/s are represented. In this case, the loading at the rotor produces a pitch on the platform that oscillates around  $6.5^\circ$ . The match between the experimental results and the computation in the free decay case including wind is fairly good. The experiment shows a very good agreement on the damping of the highest oscillations. The difference seen in the second valley is probably due to imperfect pitch excitation in the experiment. The damping ratio of the case with wind loading (0.033) is lower than in the case with no wind (0.086) due to the effect of the pitch control that is simulated by the SIL. A low amplitude oscillation persists in the tests data that is not present in the simulation case. This effect is due to excessive filtering of the motion signal that fed the SIL system during the test, not allowing the fan to respond to low amplitude oscillations. This issue will be improved in future campaigns.

### 3.13.3 Combined Irregular Waves and Turbulent Wind Tests

Two different environmental conditions were defined to test the behaviour of the platform under combined irregular waves and turbulent wind. The first sea state had a significant wave height,  $H_s$ , of 1.96m and a peak period,  $T_p$ , of 6.5s and was combined with a turbulent wind of 8.5m/s mean speed and 23% turbulence intensity. The second state corresponded to a sea with  $H_s = 2.64\text{m}$ ,  $T_p = 7.3\text{s}$  and a mean wind speed of 12.7m/s with 19% turbulence intensity. A JONSWAP spectrum was used for the generation of the irregular waves and the winds followed a Kaimal turbulence model. The wave spectrums used in the simulations were obtained by analysis of the measured wave height time series in the experiment. The resulting  $\gamma$  shape factor for the first sea state is estimated to be 2.87 and 5.0 for the test cases excluding wind and including wind, respectively, and 4.0 for both test cases of the second sea state. The Figures 3-14 and 3-15 show the surge and pitch response for the first sea state with and without the turbulent wind of 8.5m/s. Data from both tests and computations have been included. Figures 3-16 and 3-17 plot the same data for the second environmental state. The duration of the time series to obtain the PSD's was 3800s. The absolute values of the surge and pitch PSD's are not shown for confidentiality reasons. Instead, PSD's have been normalized using as factor the value of the respective PSD (surge or pitch) at  $T_p$  for the second sea state experimental data including wind, where the motion is larger.

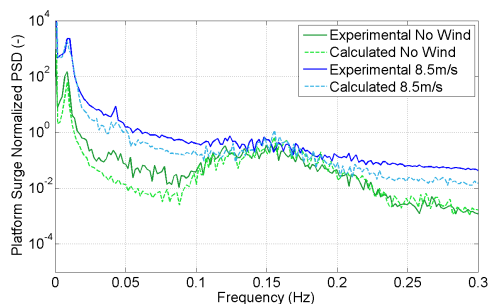


Figure 3-14 Surge PSD Hs=1.96m Tp=6.5s

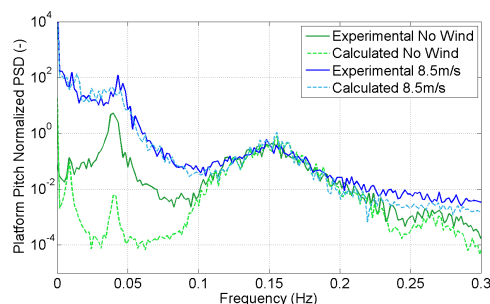


Figure 3-15 Pitch PSD Hs=1.96m Tp=6.5s

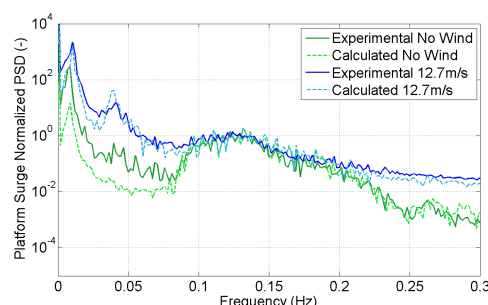


Figure 3-16 Surge PSD Hs=2.64m Tp=7.3s

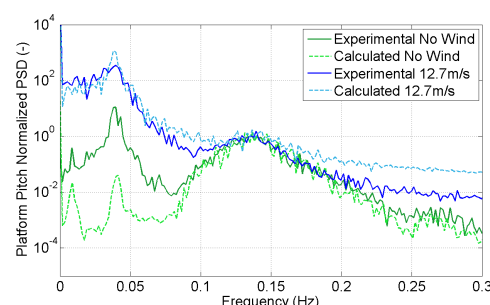


Figure 3-17 Pitch PSD Hs=2.64m Tp=7.3s

Important differences in the magnitude of the motion appear between cases with wind and those excluding it. As the wind has low frequency variations, these differences are more pronounced between 0 and 0.1Hz. They are also more important for the pitch degree of freedom than for the surge. The concordance between tests and simulations for the cases with wind is very good in both environmental conditions and both for surge and pitch, showing the correct performance of the ducted fan and SIL method. Around  $T_p$ , where direct wave loading is more important, the surge and pitch motions are similar in all the series. The wind turbulence excites additional motions away from  $T_p$ , both at higher and lower frequencies, because the turbulence is more important relative to the low wave excitation. Some important disagreements at low frequencies in pitch, but also in surge, appear in the wave only cases between tests and simulations when the aerodynamic loading is not driving the platform motions. As will be discussed later, the reason for this discrepancy could be a difference in the wave energy at low frequencies between the wave tank and our computations and also second order effects that are not captured by FAST.

For the surge displacement in both sea states (Figures 3-14 and 3-15), two main peaks appear in the PSD's. The first one corresponds to the surge natural frequency (0.011Hz) and the second one is located around  $T_p$  of the wave spectrum. The agreement in the peak amplitude between test and simulation is very good both in cases with and without wind. A certain discrepancy exists on the surge energy at low frequency (around 0.05Hz), specially for the 8,5m/s wind speed case.

For the pitch PSD's (Figures 3-16 and 3-17) two main peaks also arise: one at the pitch natural frequency (0.043Hz) and another around  $T_p$  of the wave spectrum. The amplitude of the PSD for all the series matches very well in the proximity of  $T_p$ , where more direct wave loading exist, but around the natural frequency the amplitude for the no wind case is much lower in the computation than in the results obtained in the wave tank. This is the main discrepancy found between experiments and computations. When the wind loading is introduced, the magnitude of the peak

matches very well between tests and simulation, because the wind loading influences the pitch motion more than waves.

Figure 3-18 compares the PSD of the wave height for the experimental and computational time series to illustrate the differences in the wave energy between the wave tank and our computations. The wave generated in the tank presents more energy at low frequencies than the computation, and this could excite more the pitch natural frequency and also the surge, explaining in part the mentioned discrepancies in the motions between the no wind tested and computed cases. Second order slow-drift hydrodynamic effects are not captured by the simulation software that we have used and this can also contribute to the differences.

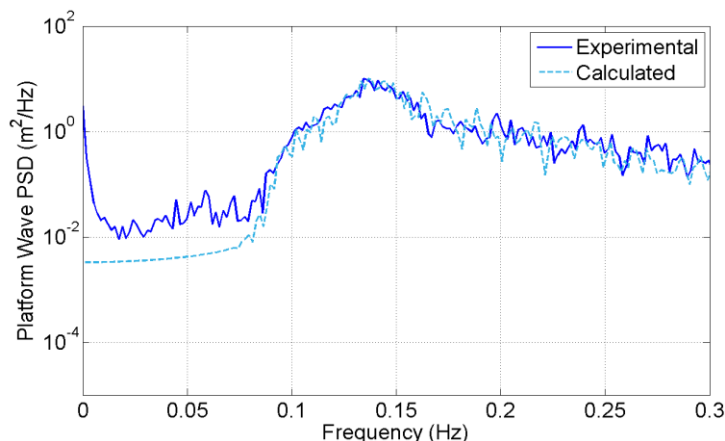


Figure 3-18 Experimental and Computed Wave Spectrum  $H_s=2.64\text{m}$   $T_p=7.3\text{s}$

### 3.13.4 Recommendations on the Testing Using the SIL System

The selection of the adequate ducted fan is one of the most critical decisions to be made when defining the scaled model to make the tests. Several commercial fans can be found with different force ranges. As an example, typical force ranges can be 4-17N or 10-30N depending on the power of the fan. Before choosing the fan, an estimation of the range of forces needed to represent the aerodynamic thrust during the test should be done. This force highly depends on several parameters that have to be defined in advance. The scale factor of the tests  $\lambda$  has a great importance, because the force is scaled with a factor of  $\lambda^3$ . The different wind speeds that are going to be tested should be also known, together with the sea condition. A complete description of the floating wind turbine model, including the controller, should be available before selecting the fan, to perform a set of simulations using the same software that will be used as SIL and reproducing the sea and wind conditions that will be tested. These computations will provide a reliable range of the expected thrust.

A fan that can provide the maximum expected thrust with certain margin should be chosen, but it is advisable not to excessively oversize it. Usually, the velocity of response of the fan is lower when it is operating in the lower part of its rpm range. A set of tests with the isolated fan should be carried out to verify the capability of the fan to respond to changes in the force demand. These tests can consist on the measurement of the time delay for a step change in the force demand or the comparison of the force provided by the fan with a force demand corresponding to a wind condition that will be tested.

The use of an intake ring improves the airflow into the fan, eliminating the turbulence generated by the sharp edges of the fan housing. Usually, these intake rings are provided as an accessory to the fan. It is advisable the use of them to improve the efficiency of the fan response.

The time step of the Software-in-the-Loop simulation strongly depends on the scale factor and the acquisition system frequency. Typical data acquisition frequencies range between 50Hz and 120Hz. Lower frequencies in the acquisition system provides higher time steps in the simulations, reducing



the computational effort required to simulate the case and thus increasing the reliability of the real time performance of the SIL system. But, on the other hand, a time step too large can lead the simulation to not converge. Therefore, a compromise has to be found when selecting the data acquisition frequency.

The communication between the wave tank acquisition system and the SIL can be a source of last minute trouble, furthermore because it has to be done "in situ" and any loss of time when working at the testing facility is important. Therefore, tests on the communication should be made in advance, if possible in the wave tank system. If this is not possible, using a temporary license and installing the acquisition software in a different computer should be considered. This would allow making tests with the system in advance, in a different location than the wave tank.

If possible, a simulation of the cases that are going to be performed in the test campaign should be done in advance using the same software that will be used as SIL. This will contribute to avoid any unforeseen event as convergence problems, or excessive displacements of the platform that could lead it out of the generated wind field, etc.

The output data of the simulations of the SIL should be carefully configured before the tests. In particular some parameters as the rotor thrust can have special importance for verification purposes. A force sensor should be located in the scaled model, to measure the force. These measurements should be compared with the thrust demand provided by the SIL after the tests. It should be kept in mind that the accelerations and displacements of the platform can affect the measurements of the force sensor making difficult to isolate the force coming from the fan.

The test cases to be performed including wind loading should be defined in order of increasing complexity, starting with very simple cases. This will allow performing a step by step verification of the ducted fan and SIL system. It is advisable to perform steady wind-only tests in still water, to verify the static displacements in pitch and surge. Surge and pitch free decay tests under steady wind loading allow checking the aerodynamic damping provided by the system. Different regular wave cases under steady wind and turbulent wind loading in still water should be also tested to characterize the system behaviour. Finally, combined irregular waves and turbulent wind cases must be run.

### 3.14 Conclusions

A new methodology for the scaling of aerodynamic loading during combined wave and wind scaled tests at wave tank has been validated. The method uses a ducted fan governed by a real time computation of the full rotor coupled with the platform motions during the test.

The methodology has been applied to a 6MW semi-submersible floating wind turbine in the ECN wave tank to verify its performance. The experimental results have been compared with computations, in general with good correspondence. Static tests and free decay tests have been useful to verify settings of our computational model: mass and inertia distribution, damping, mooring line stiffness, etc. In addition, the platform pitch displacements under different constant wind loading compare well between tests and computations, showing the correct static performance of the ducted fan system. The free decay test in pitch under a constant wind of 12.7m/s illustrates the capability of the fan to capture the coupling of the aerodynamic thrust with the rotor's relative displacements within the wind field. Finally, the PSD's of the platform surge and pitch motions under irregular waves, without wind loading, present a certain disagreement, due to differences on the wave spectrum and second order hydrodynamics. Nevertheless, when the turbulent wind is included to the irregular wave cases, these differences disappear, and the experimental results match very well the computations. In particular the effect of wind over the pitch motion is very accurately captured, which is important to calculate the correct rotor loads.

The performance of the ducted fan and SIL system has been successfully validated. We plan to apply it in the future test campaigns that will be carried out as part of the INN WIND.EU activities. The results obtained in these future experiments will be useful to further validate the method. The methodology is very promising, furthermore, considering the low cost of the system and its easy

extend to model 10 -20 MW turbines without extensive scaled rotor blade design and its versatility to be used in different test campaigns.

### References Chapter 3

- [1] Matthew J F, Kimball W K, Thomas D A and Goupee A J *Design and Testing of Scale Model Wind Turbines for Use in Wind/Wave Basin Model Tests of Floating Offshore Wind Turbines*, Proc 32nd ASME International Conference on Offshore Mechanics and Arctic Engineering, Nantes, France, 2013.
- [2] Roddier D, Cermelli C, Aubault A and Weinstein A *WindFloat: A Floating Foundation for Offshore Wind Turbines*, Journal of Renewable and Sustainable Energy 2 033104, 2010.
- [3] Robertson A N, Jonkman J M, Goupee A J, Coulling A J, Prowell I, Browning J, Masciola M D and Molta P *Summary of Conclusions and Recommendations Drawn from the DeepCwind Scaled Floating Offshore Wind System Test Campaign*, Proc 32nd ASME International Conference on Offshore Mechanics and Arctic Engineering, Nantes, France, 2013.
- [4] Jonkman J M *Dynamics Modeling and Loads Analysis of an Offshore Floating Wind Turbine*, Technical Report NREL/TP-500-41958, 2007
- [5] Jonkman J, Larsen T, Hansen A, Nygaard T, Maus K, Karimirad M, Gao Z, Moan T, Fylling I, Nichols J, Kohlmeier M, Pascual J and Merino D *Offshore Code Comparison Collaboration within IEA Wind Task 23: Phase IV Results Regarding Floating Wind Turbine Modeling*, European Wind Energy Conference (EWEC), Warsaw, Poland, 2010.
- [6] Jonkman J M, Butterfield S, Musial W and Scott G *Definition of a 5-MW Reference Wind Turbine for Offshore System Development*, Technical Report NREL/TP-500-38060, 2009
- [7] Kelberlau F, Lawerenz M and Nygaard T *A Free Decay Testing of a Semisubmersible Offshore Floating Platform for Wind Turbines in Model Scale*, MSc Thesis, UNI Kassel and the Norwegian University of Life Sciences, 2013.



## 4 TEST PLAN FOR SEMI-SEMISUBMERSIBLE FWT PLATFORM IN WAVE TANK

### 4.1 Introduction

In this chapter, a test campaign to be performed within the task 4.2 of the INNWIND.EU project is described. The tests will take place in the Ecole Centrale de Nantes (ECN) and the duration of the campaign will be 4 weeks.

The purpose of this chapter is to illustrate with a real example how to define a test campaign: scaling laws, scaled model building, lay out of the model, test cases definition, etc.

When a wave tank test campaign for a floating wind turbine is planned, many different persons can be involved in the different tasks that have to be carried out, as the design and building of the scaled model, the installation of the model in the basin, the integration of the aerodynamic loading, the definition of the test cases, the operation of the facility, etc. Therefore it is very important to collect all the information in one document to share the data efficiently and avoid misunderstandings. This chapter aims to give some ideas about the points and the information that should be documented.

The chapter also provides an example of a comprehensive test matrix with a detailed definition of all the cases in a spreadsheet. A description of each group of cases, including the objective of each test and an explanation of how they have been defined is also provided in Section 4.3 of this chapter.

#### 4.1.1 Objectives

Since measurement campaigns for full scale floating wind turbines are still rare it is essential in the development phase of new floating concepts to validate simulations with scaled test models. The objective of the proposed test plan is the validation against experimental data of the different numerical codes that have been developed by the Task 4.2 partners. These tools include CFD codes, potential non-linear hydrodynamics, mooring line dynamics, etc. In addition, these experiments will be useful for the validation of testing methodologies, in particular for the integration of the aerodynamic rotor thrust during combined wave and wind tests and the mooring system modelling. The tools and methods validated in this test campaign will be applied to the design of a floating substructure for a 10MW wind turbine in Task 4.3 of the INNWIND.EU project.

#### 4.1.2 ECN Infrastructure Specifications:

The test campaign described in this document will take place at the ECN wave tank. The main characteristics of this facility are:

- 50m long, 30m wide, 5m deep + central pit 5m x 5m max depth 10m
- 48 flap type paddles, controlled in position mode or force mode (active absorption)
- Periods 0.8 to 5s
- $H_{max} = 1\text{m}$  (regular waves),  $H_s = 0.8\text{m}$  (irregular waves),  $H_{max} = 1.8\text{m}$  (focused waves)
- Uni and multi-directional waves ( $0$  to  $45^\circ$ ), spreading, usual and user-defined wave spectra, crossed and focused waves
- Wind generation system (max.  $3\text{m} \times 3\text{m}$  section, wind speed  $0\text{-}15\text{m/s}$ , usual and user-defined wind spectra)
- Free (anchored) model or captive tests
- Optical aerial and underwater motion tracking systems
- Mooring Control System of 4 computer controlled winches
- Multi-camera recording system
- For installation: 4 tons mobile crane with 7m of clearance, qualified diving team

### 4.1.3 Model Description

No publicly available designs of floating platforms for 10MW wind turbines exist and the direct extrapolation to obtain a 10MW design from already existing platforms for smaller wind turbines may not result in a valid concept, because the dynamic behaviour will change. A redesign of the platform is required and that means an important effort. In fact, the design of a floating platform for a 10MW wind turbine will be carried out in task 4.3. For these reasons, an available 5MW model will be used in this test campaign. This model is adequate to validate the design methods to be applied to the 10MW concept design.

The platform design to be tested is the model used for the Phase II of the IEA Annex 30 (OC4) [1] that was originally defined in the DeepCWind project [2]. It is a semi-submersible design with three legs and 20m draft. The NREL Baseline 5MW wind turbine [3] is installed in the platform. The hub height is 87.6m. As it is explained in [1], the tower of the wind turbine has been modified with respect to the description in [3] to be integrated in the floating platform. The basic geometry of the floating wind turbine is shown in Figure 4-1:

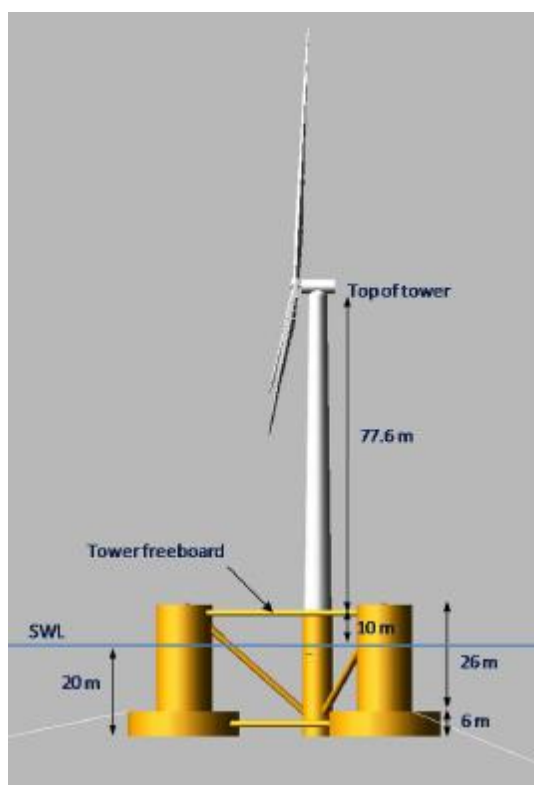


Figure 4-1 Full Scale Semi-submersible [1]

The general mass characteristics of the platform are:

Magnitude	Value	Comments
Weight	13473 t	Including ballast
Centre of Gravity	13.46 m	Below sea water level (SWL)
Inertia Ixx	6.827E+9 kgm <sup>2</sup>	About centre of gravity, exclusive added mass
Inertia Iyy	6.827E+9 kgm <sup>2</sup>	About centre of gravity, exclusive added mass
Inertia Izz	1.226E+10 kgm <sup>2</sup>	About centre of gravity, exclusive added mass

Table 4-1 General Mass Parameters of the Floating Wind Turbine in Full Scale

An overview of the main parameters that define the tower is provided in Table 4-2.

Magnitude	Value	Comments
Tower Base Elevation	10 m	(Platform Top) Above SWL
Tower Top Elevation	87.6 m	(Yaw Bearing) Above SWL
Total Tower Mass	249.718 t	-
Tower centre of Gravity Location	43.4m	Above SWL. Along Tower Centreline
Inertia Izz	1.226E10 kgm <sup>2</sup>	About centre of gravity, exclusive added mass

**Table 4-2 General Parameters of the Tower**

Table 4-3 shows a summary of the main parameters that define the rotor of the wind turbine model.

Magnitude	Value
Total RNA Mass	350 t
Rotor Mass	110 t
Nacelle Mass	240 t
Rotor Diameter	126 m
Rating	5 MW
Hub Height	90 m
Rated Tip Speed	80 m/s

**Table 4-3 General Parameters of the Rotor**

The OC4 mooring lines system is composed by three lines spread symmetrically about the central vertical axis of the platform with the characteristics provided in Table 4-4. The depth of the location is 200m.

Parameter	Line 1	Line 2	Line 3
Anchors radial position	837.6m	837.6m	837.6m
Fairleads radial position	40.868m	40.868m	40.868m
Angular position of anchors	180°	60°	300°
Angular position of fairleads	180°	60°	300°
Depth of anchors	200m	200m	200m
Draft of fairleads	14m	14m	14m
Unstretched length of the lines	835.5 m	835.5 m	835.5 m
Equivalent diameter	0.0766m	0.0766m	0.0766m
Mass density	113.35 kg/m	113.35 kg/m	113.35 kg/m
Equivalent mass density in water	108.63 kg/m	108.63 kg/m	108.63 kg/m
Axial stiffness (EA)	7.536E8 N	7.536E8 N	7.536E8 N
Hydrodynamic drag coefficient	1.1	1.1	1.1
Hydrodynamic added-mass coefficient	1.0	1.0	1.0
Seabed drag coefficient	1.0	1.0	1.0

**Table 4-4 Mooring System Parameters**

The natural frequencies of the system, computed with the FAST code [4], are shown in the next Table 4-5:

Degree of freedom	Frequency (Hz)	Period (s)
Surge	0.00927	107.90
Sway	0.00927	107.92
Heave	0.05814	17.20
Roll	0.03913	25.55
Pitch	0.03916	25.54
Yaw	0.01310	76.35

**Table 4-5 Natural Frequencies**

#### 4.1.4 Scaled Model

The scaling of the model is based on the Froude nondimensional number [5]:

$$F_r = \frac{u^2}{gD} \quad 4-1$$

Where  $u$  is the fluid velocity,  $g$  is the gravitational acceleration and  $D$  is a characteristic dimension of the floating platform. This characteristic dimension (length) is scaled using a factor  $\lambda$ . The gravity cannot be scaled, thus, to keep the Froude similarity between the full scale and the model, the time is affected by a factor of  $\lambda^{0.5}$ . The scale factor to be applied to all the other magnitudes involved in the tests can be easily derived. The scaling laws applied to each magnitude are collected in Table 4-6:

Magnitude	Scale Law
Length	$\lambda$
Time	$\lambda^{0.5}$
Linear Velocity	$\lambda^{0.5}$
Linear Acceleration	1
Angle	1
Angular Velocity	$\lambda^{-0.5}$
Angular Acceleration	$\lambda^{-1}$
Mass	$\lambda^3$
Mass per unit length	$\lambda^2$
Mass moment of inertia	$\lambda^5$
Moment of Inertia (I)	$\lambda^4$
Volume	$\lambda^3$
Force	$\lambda^3$

Tension	$\lambda^3$
---------	-------------

Table 4-6 Scaling Laws

#### 4.1.5 Reference system

The origin of the reference system that is used in this document is located at the water tank centre and at the medium water level. The x direction is the nominal downwind direction and the y axis points to the left when looking downwind. The z axis is positive upwards. The reference system is shown in the Figure 4-2. The rectangle represents the dimensions of the ECN wave tank (30m x 50m).

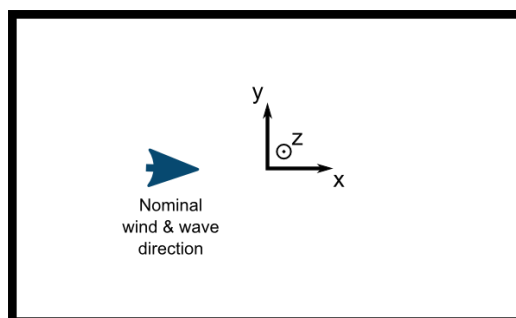


Figure 4-2 Reference System

## 4.2 Description of the Experiment setup

### 4.2.1 Scaled Model Setup

The mooring system (described in full scale in Section 2.3) will required some modifications to be installed at ECN wave tank due to constraints imposed by the basin dimensions.

The basin depth is 5m that, according to the 1/45 scale factor, corresponds to 225m in full scale. This is slightly different to the 200m depth used for the design of the OC4 mooring system. For this reason, the anchor and the portion of the line lying on the seabed will be raised 0.55m from the basin bottom.

In addition, the width of the basin is not enough to locate the anchor points of the two downwind lines (lines 2 and 3). Therefore, they will have to be approached to the basin centre and the line length will have to be reduced accordingly.

For the line 1, aligned with the nominal wind and wave direction, the OC4 configuration can be maintained and the anchor will be located at the basin at a radial distance from the centre of the basin of 18.613m (837.6m in full scale) with a line length of 18.567m (835.5m in full scale) that corresponds to the full scaled OC4 system described in Section 4.1.4.

For lines 2 and 3, the radial distance of the anchors to the basin centre will be reduced to 17.1m (769.5m in full scale) and the length of these lines will be reduced in the same amount to 17.05m (767.25m in full scale). This reduction of the radial distance allows installing the anchors inside the basin at a distance from the tank wall of 0.19m. The geometry of the scaled mooring system is summarized in Table 4-7:

Line	Anchor x	Anchor y	Anchor Z	Length
1	-18.613m	0.0m	-4.44m	18.567m

2	8.55m	14.81m	-4.44m	17.05m
3	8.55m	-14.81m	-4.44m	17.05m

**Table 4-7 Scaled Model Mooring System Setup**

The next two Tables 4-8 and 4-9 allow comparing the original OC4 mooring system geometry and the modified geometry of the mooring system for tests:

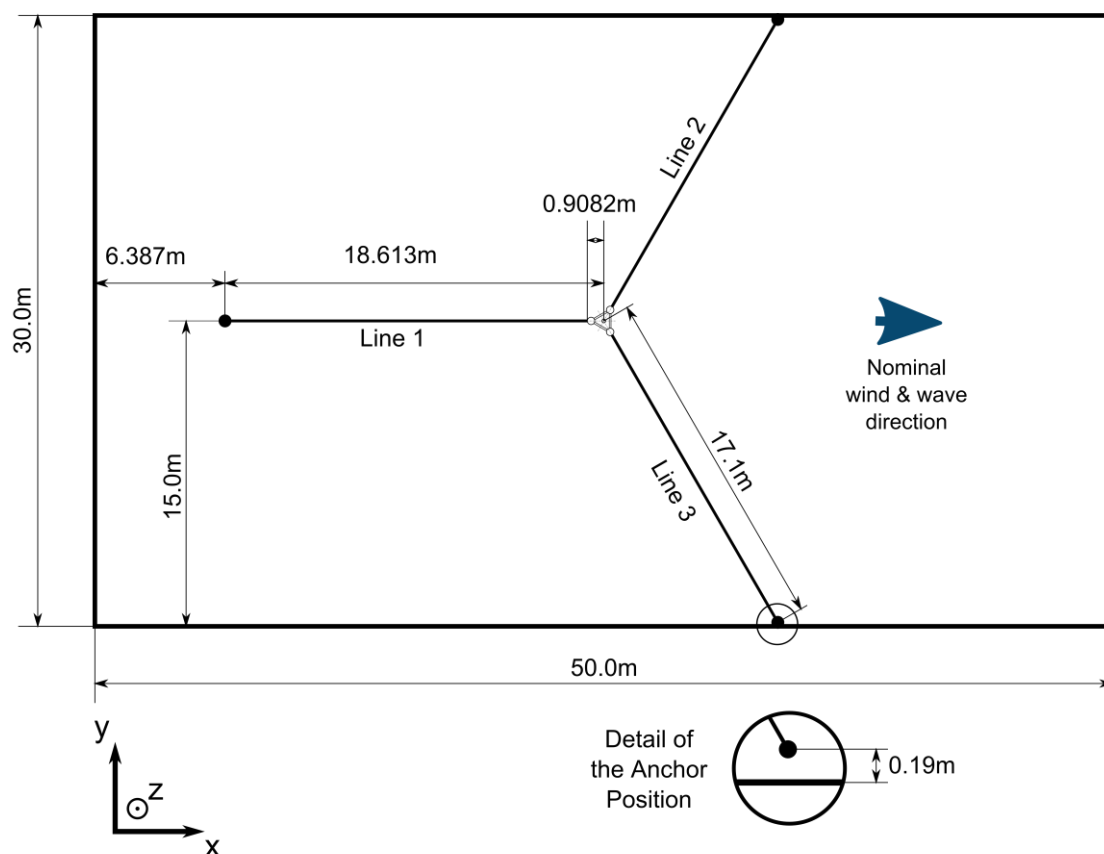
Line	Original OC4 Mooring System				
	Anchor Radial Distance	Fairlead Radial Distance	Depth	Length	Orientation
1	837.6m	40.868m	200m	835.5m	180°
2	837.6m	40.868m	200m	835.5m	60°
3	837.6m	40.868m	200m	835.5m	300°

**Table 4-8 Original Mooring System Geometry in Full Scale**

Line	Modified Mooring System				
	Anchor Radial Distance	Fairlead Radial Distance	Depth	Length	Orientation
1	837.6m	40.868m	200m	835.5m	180°
2	769.5m	40.868m	200m	767.25m	60°
3	769.5m	40.868m	200m	767.25m	300°

**Table 4-9 Modified Mooring System Geometry in Full Scale**

Figure 4-3 shows the lay out of the platform model and the scaled mooring lines in the wave tank. The platform is located at the geometric centre of the basin.



Origin: wave tank center

**Figure 4-3 Platform Tests Lay-Out**

Finding a commercial chain with the adequate characteristics to represent exactly the full scale mooring lines is not an easy task. For this reason, the chain with the closest properties to represent the full scale lines will be searched, but the final characteristics of the scaled mooring system will not match exactly the characteristics described in Table 4-4, in Section 2.3.

The following chain has been proposed for the scaling of the mooring line: [http://www.ostalbketten.de/shop/product\\_info.php?cPath=32&products\\_id=135](http://www.ostalbketten.de/shop/product_info.php?cPath=32&products_id=135) Table 4-10 compares the characteristics of this chain with respect to the objective values based on the OC4 mooring system description in model scale:

	Objective Value	Proposal
Diameter	1.7mm (cable)	1.6mm (link)
Mass/Length	56g/m	59g/m
Mass/Length (in water)	53.6g/m	-

**Table 4-10 Properties of the Objective and Proposed Lines for the Scaled model**

#### 4.2.2 Aerodynamic thrust

The realistic inclusion of wind for the testing of a floating wind turbine in combination with waves is a technical challenge, because Froude scaling produce low Reynolds numbers. This effect has a great



influence on the aerodynamic forces generated in the wind turbine's rotor, because the lift and drag coefficients of the blade airfoils are very sensitive to the Reynolds number. As a consequence, the aerodynamic forces obtained on the turbine's rotor are out of scale when Froude scaling is directly applied on the rotor's geometry.

Two different methods to include the scaled aerodynamic thrust will be used in the test campaign. The first one is the use of a pitch controlled scaled rotor that has been redesign to provide, at low Reynolds number, an aerodynamic thrust representative of the full scale thrust. The second method will be the use of a fan at the tower top, controlled by a "Software-in-the-Loop" system [6]. The basic concept of this method consists of substituting the rotor by a fan driven by an electric motor. The fan thrust is controlled by the fan rotational speed set by the controller, which again depends on the real time simulation of the full scale rotor in a turbulent wind field, with the platform motions measured in real time in the wave tank test.

#### 4.2.3 Proposed Measurements

Depending on the test case, the following measurements are proposed. A short nomenclature (V, Wv, Wi, ML...) has been specified for each group of measurements. This nomenclature is used in the test matrix to specify the data that will be measured at each test case.

V (Video):

- Video from the side, over and under water

Wv (Wave):

- Wave height upstream, downstream and to the side of the platform

Wi (Wind)

- Wind velocity
- Total rotor force

ML (Mooring Lines):

- Tension in mooring lines at fairlead and anchors
- Motion of the underwater line (cameras)

PM (Platform Motions):

- 6 dof's position, velocities and accelerations (laser tracking)
- Accelerometers at tower top

PF (Platform Forces):

- Dynamometer measurements for forced motions tests

#### 4.2.4 Estimated Measurements Range

Several load cases have been run to roughly estimate the expected range of values for the magnitudes that have to be measured during the testing and provide some guidance in the election of the sensors. These cases consider several combinations of wave and wind for different situations: rated wind velocity (maximum thrust), a wind speed of 18m/s and the storm wind velocity, in combination with different waves. The load cases are described in Table 4-11:

Load Case	Wind	Wave	Comments
1	11.4 m/s Turbulent	Still Water	Power production
2	11.4 m/s Constant	Regular H=6m T=10s	Power production

3	11.4 m/s Turbulent	Irregular Hs=6m Tp=10s	Power production
4	18 m/s Constant	Regular H=11.3m T=5.49s	Power production
5	18 m/s Turbulent	Irregular Hs=11.3m Tp=5.49s	Power production
6	47.5m/s Constant	Irregular Hs=17m Tp=5.24s	Idling Dynamic mooring lines
7	47.5m/s Turbulent	Irregular Hs=17m Tp=5.24s	Idling Dynamic mooring lines

**Table 4-11 Load Cases for the Sensor Range Estimation**

According to the results of the simulations run with the FAST code in full scale, the expected range for the magnitudes to be measured in the experiment are shown in Table 4-12 (in model scale):

Magnitude	Units	Max	Min
Force Rotor-Twr	(N)	11.621	-3.152
Fairlead 1Tension	(N)	18.107	7.505
Fairlead 2Tension	(N)	28.587	3.136
Fairlead 3Tension	(N)	16.505	7.471
Fairlead 1 Angle	(deg)	40.760	31.239
Fairlead 2 Angle	(deg)	39.173	22.680
Fairlead 3 Angle	(deg)	41.050	32.039
Anchor 1Tension	(N)	15.906	5.479
Anchor 2Tension	(N)	26.403	0.552
Anchor 3Tension	(N)	14.419	5.502
Anchor 1 Angle	(deg)	0.000	0.000
Anchor 2 Angle	(deg)	2.725	0.000
Anchor 3 Angle	(deg)	0.000	0.000
Surge	(m)	0.365	-0.004
Sway	(m)	0.103	-0.140
Heave	(m)	0.026	-0.029
Roll	(deg)	3.435	-2.003
Pitch	(deg)	5.223	-0.451
Yaw	(deg)	5.598	-10.100
Twr Top X Acceleration	(m/sec <sup>2</sup> )	3.488	-3.380
Twr Top Y Acceleration	(m/sec <sup>2</sup> )	0.506	-0.441
Twr Top Z Acceleration	(m/sec <sup>2</sup> )	0.530	-0.599
Twr Top X Rot Acceleration	(deg/sec <sup>2</sup> )	1.209	-1.291
Twr Top Y Rot Acceleration	(deg/sec <sup>2</sup> )	5.460	-5.746
Twr Top Z Rot Acceleration	(deg/sec <sup>2</sup> )	2.246	-2.427

**Table 4-12 Estimation of the Measurements Range in Model Scale**

### 4.3 Test Matrix

The detailed tentative test matrix can be found in a datasheet attached to this document. The test schedule starts with cases where the mooring system is not installed (forced oscillations, regular waves with fixed hull and free decay tests with free hull) and then continues with the cases where the platform is moored. The cases including wind are presented in the last part of the test matrix, first with simple cases for the characterization of the wind loading, and then in combined wave and wind cases. For every case, the importance of the case has been indicated with a number between 1 and 3 (1: high priority; 3: low priority). This will help to decide which cases could be skipped in case of delays on the time schedule during the test execution.

All the magnitudes defining the test cases in this document are presented in full scale, but in the test matrix datasheet they are provided also in the scaled model. The first sheet of the excel file attached is called "Parameters" and collects all the parameters that define the test campaign: scale, sea state conditions, winds, initial displacements for the free decay tests, frequencies and amplitudes of the forced oscillations cases, etc. The sheet called "Platform Test Matrix" details all the test cases of the campaign, based on these parameters. Therefore, if any of the data in "Parameters" is changed, all the affected cases in the test matrix will automatically update.

In the following subsections, the different groups of cases of the test matrix are described and commented. A complete compilation of the test matrix for the 10 MW wind turbine (scale factor 1/60) is given in the appendix of this chapter.

#### 4.3.1 Forced Oscillations

The group of cases A consists of prescribed forced oscillations of the platform on the 6 rigid body degrees of freedom at different frequencies. The frequencies have been chosen based on computations using the WAMIT software [7], based in potential hydrodynamic theory. Figures 4-4, 4-5, 4-6 and 4-7 show the computed added mass and potential damping for the different degrees of freedom of the platform. The added mass and damping values at the chosen frequencies for the forced oscillations experiments are shown in the figures as black dots.

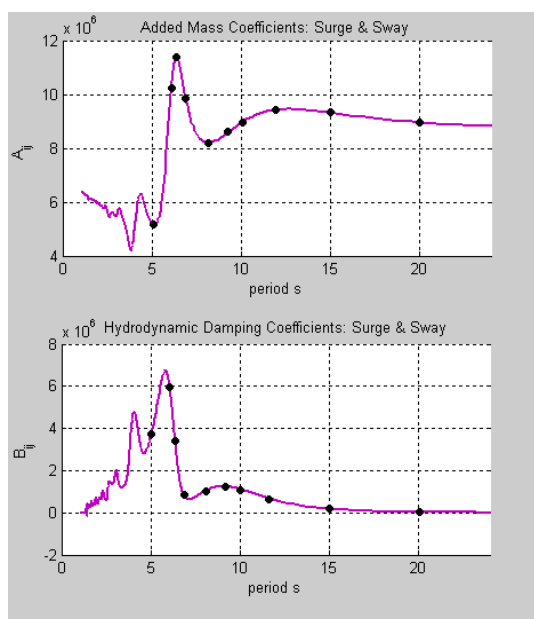


Figure 4-4 Surge & Sway Added Mass and Damping

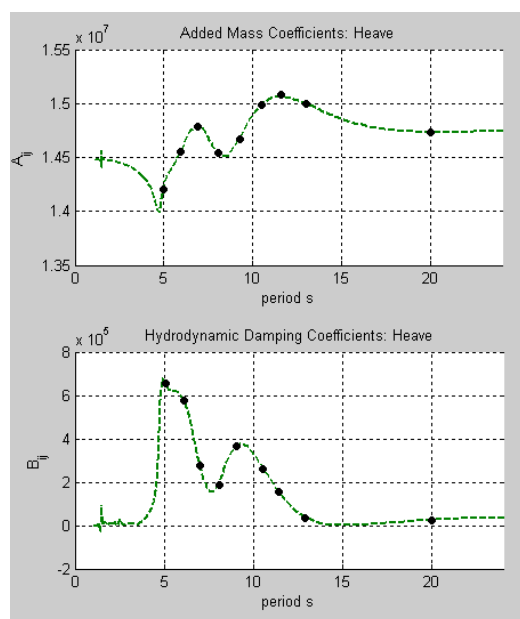


Figure 4-5 Heave Added Mass and Damping

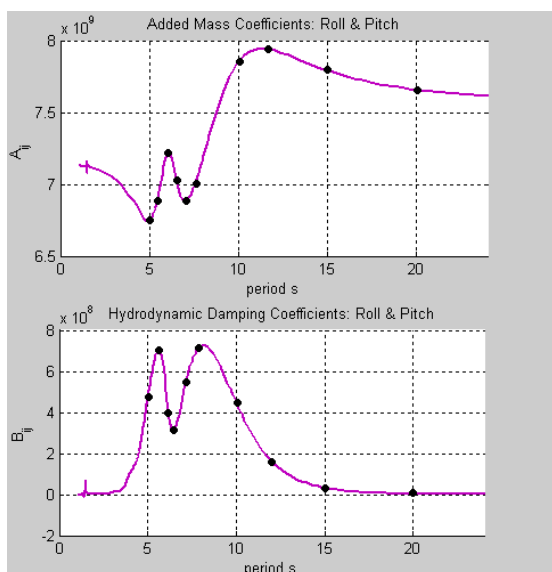


Figure 4-6 Roll & Pitch Added Mass and Damping

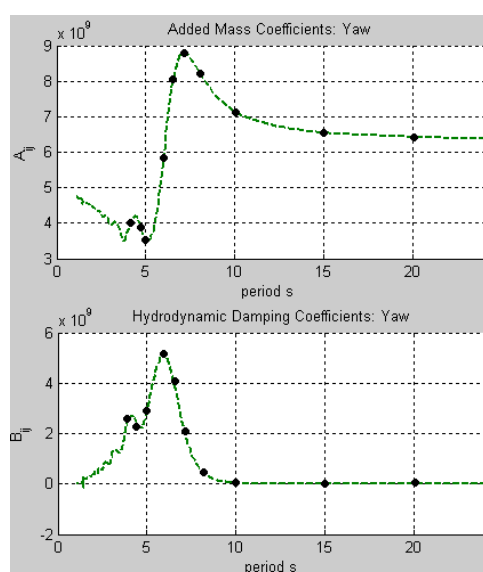


Figure 4-7 Yaw Added Mass and Damping

Table 4-13 collects all the periods selected for the forced oscillation tests in each degree of freedom. Amplitude 1 for the oscillations will be tested with all the periods. Only the periods shown in Table 4-13 in red font will be tested again with the amplitude 2 for verification purposes.

	Forced Oscillations					
	Surge	Sway	Heave	Roll	Pitch	Yaw
Amplitude #1	1.125m	1.125m	1.125m	5°	5°	5°
Amplitude #2	2.25m	2.25m	2.25m	10°	10°	10°
Periods (s)	5	5	5	5	5	4
	6	6	6	5.5	5.5	4.5
	6.4	6.4	7	6	6	5
	7	7	8	6.5	6.5	6
	8	8	8.4	7	7	6.5
	9	9	9	8	8	7
	10	10	10.5	10	10	8
	12	12	11.5	11.5	11.5	10
	15	15	13	15	15	15
	20	20	20	20	20	20

Table 4-13 Periods for the Forced Oscillation Tests

### 4.3.2 Regular Waves with Fixed Hull

B is a group of cases where the platform is fixed and the forces induced by incoming regular waves with different periods are measured. This will allow obtaining the force RAO's of the platform. The periods of the regular waves are shown in Table 4-14. These tests have been chosen based on WAMIT computations of the Exciting Force Coefficients that are shown in Figure 4-8 (X1, X2, X3, X4, X5, and X6 correspond to the coefficients in surge, sway, heave, roll, pitch and yaw).

Regular Waves Fixed Hull	
Amplitude (m)	6.75
Periods (s)	5
	6
	7
	8
	9
	10
	11
	15
	20
	25

Table 4-14 Regular Waves Periods in Fixed Hull Tests

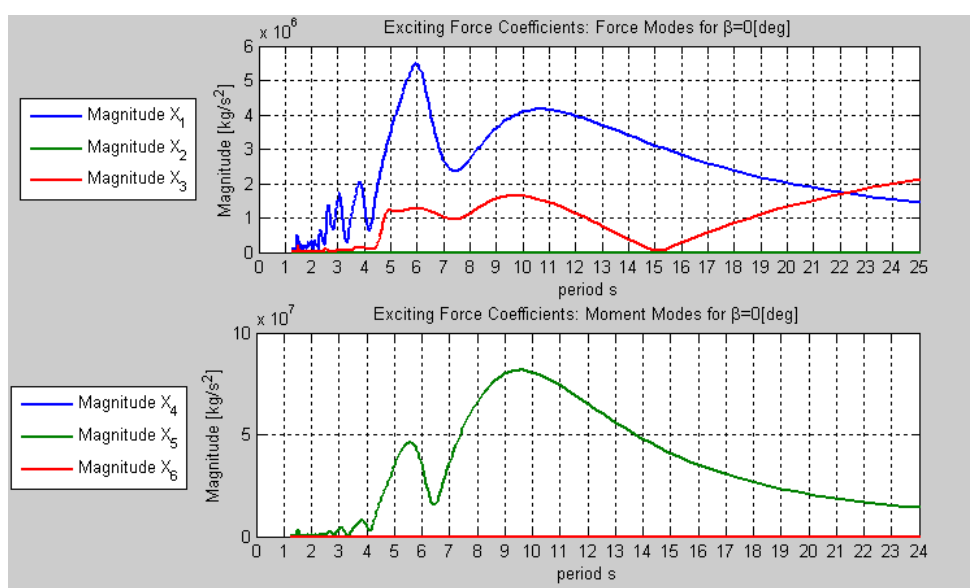


Figure 4-8 Exciting Force Coefficients Computed with WAMIT

The force RAO's can be obtained also by testing the fixed platform under a White Noise wave spectrum. This is done in the group of cases C with two different significant wave heights (4.5m and 9m).

### 4.3.3 Free Decay Tests

Free decay tests are performed in the group of cases D. These cases include free decay experiments with the platform free (heave, roll and pitch) and moored (surge, sway, heave, roll, pitch and yaw). Therefore, the platform, unmoored for the first part of the test campaign will be moored during the execution of this group of cases for the free decay tests with "moored hull". Then, it will stay moored for the rest of the campaign. All the free decay tests are performed twice, with two different initial displacements.

Free Decay Tests			
Initial Displacement			
	Test Repetition	Free Hull	Moored Hull
Surge	#1		13.5m
	#2		6.75m
Sway	#1		13.5m
	#2		6.75m
Heave	#1	4.5m	4.5m
	#2	2.25m	2.25m
Roll	#1	10°	10°
	#2	5°	5°
Pitch	#1	10°	10°
	#2	5°	5°
Yaw	#1		10°
	#2		5°

Table 4-15 Initial Displacements for the Free Decay Tests

### 4.3.4 Moored Platform Static Displacement

In this test, a static displacement on the moored platform in surge and sway is introduced with the objective of verifying the stiffness of the mooring system installed in the wave tank. The forces and moments on the 6 degrees of freedom of the platform will be measured. The relationships between restoring forces and moments with respect to the surge and sway displacements are provided in [1]:

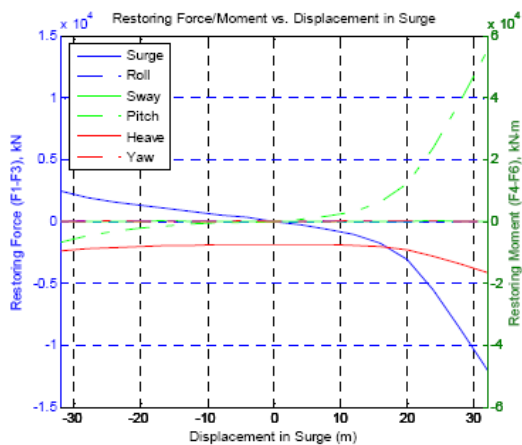


Figure 4-9 Restoring Force/Moment vs. Surge [1]

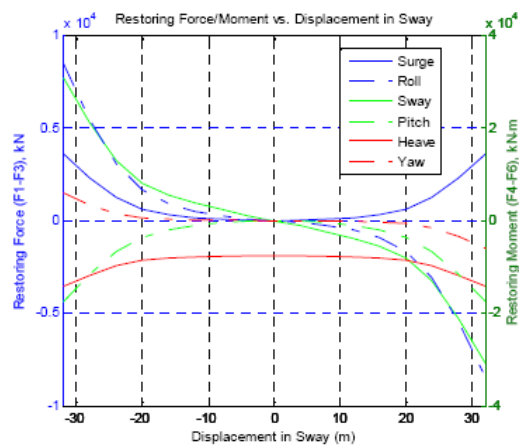


Figure 4-10 Restoring Force/Moment vs. Sway [1]

Based on Figure 4-9 and Figure 4-10, the following static displacements to be introduced to the platform in surge and sway have been chosen:

Static Displacement Surge (m)
-20
-10
10
20
25
30

Table 4-16 Surge Displacements

Static Displacement Sway (m)
-10
-5
10
5

Table 4-17 Sway Displacements

#### 4.3.5 Regular Waves with Moored Hull

The groups of cases F and G are similar to B and C, but with the platform moored and floating, instead of being fixed. The motion RAO's of the platform can be obtained from these experiments. The periods of the regular waves for the execution of the F group of cases are shown in Table 4-18:



Regular Waves Moored Hull	
Amplitude (m)	6.75
Periods (s)	5
	6
	7
	8
	9
	10
	11
	15
	20
	25

**Table 4-18 Periods for the Regular Waves with Moored Hull Tests**

#### 4.3.6 Environmental Conditions Definition

The last part of the test matrix consists of cases representatives of different sea states and also different sea states in combination with winds. These environmental conditions (irregular sea states, regular sea states and wind conditions) are presented in Table 4.19, Table 4.20 and Table 4.21. A more detailed description of the cases involving these environmental conditions is provided in Sections 4.3.6, 4.3.7, 4.3.8 and 4.3.9.

Irregular Sea States		
Sea State	Hs (m)	Tp (s)
1	2.75	5.5
2	3.14	6.5
3	4.13	7.3
4	4.88	8.9
5	6	10

**Table 4-19 Irregular Sea Conditions**

Regular Sea States		
Sea State	Height (m)	Period (s)
1	2.75	5.5
2	3.14	6.5
3	4.13	7.3
4	4.88	8.9
5	6	10

Table 4-20 Regular Sea Conditions

Wind Conditions		
Wind State	Steady Wind Speeds (m/s)	Turbulent Wind Speeds (m/s)
1	7	7
2	8.5	8.5
3	11.4	11.4
4	18	18
5	25	25

Table 4-21 Wind Conditions

#### 4.3.7 Irregular Waves Cases

The group of cases H consists of irregular waves with the  $H_s$  and  $T_p$  defined in Table 4-19 with  $0^\circ$  and  $45^\circ$  of heading direction.

#### 4.3.8 Wind Loading Characterization

The group of cases I consist of wind only cases with the platform moored and still water. Constant and turbulent winds with the wind speeds from Table 4-21 are reproduced. These cases allow characterizing the wind loading system and verifying that it is correctly tuned and that the displacements in surge and pitch correspond to the expected values.

The group of cases J consists of free decay tests in surge and pitch combined with constant winds (see Table 4-22). These cases are useful for the characterization of the damping introduced by the aerodynamic loading.

		Free Decay + Constant Wind	
		Initial Displacement	Wind Speed (m/s)
Surge	# 1	6.75m	8.5
	# 2	6.75m	11.4
	# 3	6.75m	18
Pitch	# 1	5°	8.5
	# 2	5°	11.4
	# 3	5°	18

Table 4-22 Free Decay + Constant Wind Conditions

#### 4.3.9 Combined Wave and Wind Tests

The groups of cases K, L, M and N consist of combinations of regular and irregular waves with steady and turbulent winds according to the conditions described in Table 4-19, Table 4-20 and Table 4-21.

#### 4.4 Practical Recommendations

- For the experimental verification of the RAO's there is a need of more than 5 tests. For the semi-submersible type e.g. there are complicated ROA curves with frequencies where the response almost vanishes depending on the distance between the legs.
- In experiments for the fairlead positions of the mooring lines the relation between the fairlead position and the motion of the platform in waves should be defined and the influence of the pitch angle of the blades on the motion of the platform should be investigated. A mechanism to control the pitch angle of the blades of the scale model should be modelled.
- The method of excitation for the decay tests should consider structural properties. Pushing e.g. the top of the tower in the pitch direction causes substantial changes on the initial tower bending. It is recommended to combine the tuning of the pitch and the tower bending frequency, see paragraph 4.3.3 Free Decay Tests.
- The gyroscopic effect of the rotor blades is an important effect on floating wind turbine platforms that must be modelled in scale-model experiments as discussed in detail in chapter 2 and chapter 3.
- The rotating wind turbine has an angular momentum about the surge axis, leading to platform motion in pitch direction. As a result of this, the rotating wind turbine creates a new component of angular momentum yaw. A very clear explanation is given in [8]. The following is a citation from this Master Thesis:  
*"This new component of angular momentum may either enhance or decrease the yaw motions of the platform (depending on the relative phase of the pitch and yaw motions). Similarly, initial yaw motions can also induce torque and motions in pitch. The angular velocity induced by pitch motion can also enhance or decrease pitch motions of the platform. As a result of yaw motions created on the platform, a secondary gyroscopic effect*

*may also occur. Forces in the sway axis occur on a yawed rotor disc. These forces may also induce torque and motions in roll. The gyroscopic effect (and resulting torques) depends on the angular velocity and moment of inertia of the spinning rotor. Platform motions induced in yaw, pitch, and roll as a result of gyroscopic forces are directly proportional to the angular velocity and moment of inertia of the spinning rotor that creates these gyroscopic forces.”*

- The final definition of wave heights, periods and directions as well as wind conditions should be made after some pre-calculations as shown in paragraph 4.3.6 Environmental Conditions Definition.
- Hybrid Model Tests are employed in general when the mooring lines of a deep water structure are required to be replaced by an active or passive system which provides an approximation of the mooring line response. The purpose of the procedure from ITTC [9] is to ensure that Hybrid Model Tests are conducted according to the best available techniques and to provide an indication of where improvements in techniques might be made. The procedure also tempts to insure that any compromises, inherent in a particular Hybrid System model test, are identified and their effect on the measured results is under-stood.

## References Chapter 4

- [1] A. Robertson, J. Jonkman, M. Masciola, H. Song, A. Goupee, A. Coulling, and C. Luan, *Definition of the Semisubmersible Floating System for Phase II of OC4* IEA Annex 30 Internal Report, 2012
- [2] A. J. Goupee, B. J. Koo, K. F. Lamrakos, R. Kimball, *Offshore Wind Energy: Model Tests for Three Floating Wind Turbine Concepts* Proceedings of the Offshore Technical Conference, April 30 – May 3, 2012, Houston, TX.
- [3] J. Jonkman, S. Butterfield, W. Musial, and G. Scott, *Definition of a 5-MW Reference Wind Turbine for Offshore System Development* NREL, 2009
- [4] J. Jonkman, *Dynamics Modeling and Loads Analysis of an Offshore Floating Wind Turbine* NREL/TP-500-41958. Golden, CO.
- [5] H. Bredmose , S. E. Larsen, D. Matha, A. Rettenmeier, E. Marino and L. Saettran *Collation of offshore wind-wave dynamics*, MARINET, 2012.
- [6] J. Azcona, F. Bouchotrouch, M. González, J. Garcíandía, X. Munduate, F. Kelberlau, T. A. Nygaard *Aerodynamic Thrust Modelling in Wave Tank Tests of Offshore Floating Wind Turbines Using a Ducted Fan* 2014 J. Phys.: Conf. Ser. 524 012089
- [7] C. H. Lee, *WAMIT Theory Manual* Report 95-2, Dept. of Ocean Engineering, MIT, 1995
- [8] *Scale model experiments on floating offshore wind turbines*, Thesis Syed Kazim Naqvi, May 2012
- [9] ITTC – Recommended Procedures, *Testing and Extrapolation Methods Loads and Responses*, Ocean Engineering, Stationary Floating Systems Hybrid Mooring Simulation Model Test Experiments, 2002

## APPENDIX TEST CAMPAIGN 10MW FLOATING WIND TURBINE

Priority	Test ID	Case		Description	Wave Height (m)	Period (s)	Wave Height (Full Scale) (m)	Period (Full Scale) (s)	Wave Direction (deg)	Measurements	Duration (s)	Duration (Full scale) (s)	Comments
1	S2F1	Regular waves / moored hull			0,119	0,664	6,75	5	0	V Wv ML PM	37,3	250,0	For displacement RAO's
1	S2F2	Regular waves / moored hull			0,119	0,797	6,75	6	0	V Wv ML PM	44,7	300,0	For displacement RAO's
1	S2F3	Regular waves / moored hull			0,119	0,930	6,75	7	0	V Wv ML PM	52,2	350,0	For displacement RAO's
1	S2F4	Regular waves / moored hull			0,119	1,062	6,75	8	0	V Wv ML PM	59,6	400,0	For displacement RAO's
1	S2F5	Regular waves / moored hull			0,119	1,195	6,75	9	0	V Wv ML PM	67,1	450,0	For displacement RAO's
1	S2F6	Regular waves / moored hull			0,119	1,328	6,75	10	0	V Wv ML PM	74,5	500,0	For displacement RAO's
1	S2F7	Regular waves / moored hull			0,119	1,461	6,75	11	0	V Wv ML PM	82,0	550,0	For displacement RAO's
1	S2F8	Regular waves / moored hull			0,119	1,992	6,75	15	0	V Wv ML PM	111,8	750,0	For displacement RAO's
1	S2F9	Regular waves / moored hull			0,119	2,656	6,75	20	0	V Wv ML PM	149,1	1000,0	For displacement RAO's
1	S2F10	Regular waves / moored hull			0,119	3,320	6,75	25	0	V Wv ML PM	186,3	1250,0	For displacement RAO's
1	S2G1	White Noise / moored hull		Two different Hs (low and high) will be tested	0,079	-	4,5	-	0	V Wv ML PM	536,7	3600	For displacement RAO's
1	S2G2	White Noise / moored hull		Two different Hs (low and high) will be tested	0,159	-	9	-	0	V Wv ML PM	536,7	3600	For displacement RAO's
2	S2H1	Irregular waves / moored hull		Wave Direction #1	0,049	0,730	2,75	5,5	0	V Wv ML PM	536,7	3600,0	JONSWAP gamma 2.87
2	S2H2	Irregular waves / moored hull		Wave Direction #1	0,055	0,863	3,14	6,5	0	V Wv ML PM	536,7	3600,0	JONSWAP gamma 2.87
2	S2H3	Irregular waves / moored hull		Wave Direction #1	0,073	0,969	4,13	7,3	0	V Wv ML PM	536,7	3600,0	JONSWAP gamma 2.87
2	S2H4	Irregular waves / moored hull		Wave Direction #1	0,086	1,182	4,88	8,9	0	V Wv ML PM	536,7	3600,0	JONSWAP gamma 2.87
2	S2H5	Irregular waves / moored hull		Wave Direction #1	0,106	1,328	6	10	0	V Wv ML PM	536,7	3600,0	JONSWAP gamma 2.87
3	S2H6	Irregular waves / moored hull		Wave Direction #2	0,049	0,730	2,75	5,5	45	V Wv ML PM	536,7	3600,0	JONSWAP gamma 2.87
3	S2H7	Irregular waves / moored hull		Wave Direction #2	0,055	0,863	3,14	6,5	45	V Wv ML PM	536,7	3600,0	JONSWAP gamma 2.87
3	S2H8	Irregular waves / moored hull		Wave Direction #2	0,073	0,969	4,13	7,3	45	V Wv ML PM	536,7	3600,0	JONSWAP gamma 2.87
3	S2H9	Irregular waves / moored hull		Wave Direction #2	0,086	1,182	4,88	8,9	45	V Wv ML PM	536,7	3600,0	JONSWAP gamma 2.87
3	S2H10	Irregular waves / moored hull		Wave Direction #2	0,106	1,328	6	10	45	V Wv ML PM	536,7	3600,0	JONSWAP gamma 2.87

Priority	Test ID	Case		Description	Wind speed (m/s)	Wind speed (m/s) (Full scale)	Measurements	Duration (s)	Duration (Full scale) (s)	Comments
1	S2I1	Wind tests / moored platform / <b>still water</b>		Steady Wind	0,9	7	V Wi ML PM	79,7	600	Wind ID
1	S2I2	Wind tests / moored platform / <b>still water</b>		Steady Wind	1,1	8,5	V Wi ML PM	79,7	600	Wind ID
1	S2I3	Wind tests / moored platform / <b>still water</b>		Steady Wind	1,5	11,4	V Wi ML PM	79,7	600	Wind ID
1	S2I4	Wind tests / moored platform / <b>still water</b>		Steady Wind	2,4	18	V Wi ML PM	79,7	600	Wind ID
1	S2I5	Wind tests / moored platform / <b>still water</b>		Steady Wind	3,3	25	V Wi ML PM	79,7	600	Wind ID
2	S2I6	Wind tests / moored platform / <b>still water</b>		Turbulent wind	0,9	7	V Wi ML PM	478,1	3600	Wind ID
2	S2I7	Wind tests / moored platform / <b>still water</b>		Turbulent wind	1,1	8,5	V Wi ML PM	478,1	3600	Wind ID
2	S2I8	Wind tests / moored platform / <b>still water</b>		Turbulent wind	1,5	11,4	V Wi ML PM	478,1	3600	Wind ID
2	S2I9	Wind tests / moored platform / <b>still water</b>		Turbulent wind	2,4	18	V Wi ML PM	478,1	3600	Wind ID
2	S2I10	Wind tests / moored platform / <b>still water</b>		Turbulent wind	3,3	25	V Wi ML PM	478,1	3600	Wind ID

Priority	Test ID	Case		Description	Initial Displacement (m/deg)	Initial Displacement (Full Scale) (m/deg)	Wind speed (m/s)	Wind speed (m/s) (Full scale)	Measurements	Duration (s)	Duration (Full scale) (s)	Comments
1	S2J1	Free decay tests + steady wind / moored hull		Surge + Steady wind	0,12	6,75	1,13	8,50	V Wi ML PM	143,3	1079	
1	S2J2	Free decay tests + steady wind / moored hull		Surge + Steady wind	0,12	6,75	1,51	11,40	V Wi ML PM	143,3	1079	
1	S2J3	Free decay tests + steady wind / moored hull		Surge + Steady wind	0,12	6,75	2,39	18,00	V Wi ML PM	143,3	1079	
1	S2J4	Free decay tests + steady wind / moored hull		Pitch + Steady wind	5,00	5,00	1,13	8,50	V Wi ML PM	33,9	255,4	
1	S2J5	Free decay tests + steady wind / moored hull		Pitch + Steady wind	5,00	5,00	1,51	11,40	V Wi ML PM	33,9	255,4	
1	S2J6	Free decay tests + steady wind / moored hull		Pitch + Steady wind	5,00	5,00	2,39	18,00	V Wi ML PM	33,9	255,4	

Priority	Test ID	Case	Description	Wave Height (m)	Period (s)	Wave Height (Full Scale) (m)	Period (Full Scale) (s)	Wave Direction (deg)	Wind speed (m/s)	Wind speed (m/s) (Full scale)	Measurements	Duration (s)	Duration (Full scale) (s)	Comments
1	S2K1	Regular wave + steady wind	Wave Direction #1	0,049	0,730	2,75	5,50	0,0	0,9	7,0	V Wv Wi ML PM	36,5	275	Wind & Wave
1	S2K2	Regular wave + steady wind	Wave Direction #1	0,055	0,863	3,14	6,50	0,0	1,1	8,5	V Wv Wi ML PM	43,2	325	Wind & Wave
1	S2K3	Regular wave + steady wind	Wave Direction #1	0,073	0,969	4,13	7,30	0,0	1,5	11,4	V Wv Wi ML PM	48,5	365	Wind & Wave
1	S2K4	Regular wave + steady wind	Wave Direction #1	0,086	1,182	4,88	8,30	0,0	2,4	18,0	V Wv Wi ML PM	59,1	445	Wind & Wave
1	S2K5	Regular wave + steady wind	Wave Direction #1	0,106	1,328	6,00	10,00	0,0	3,3	25,0	V Wv Wi ML PM	66,4	500	Wind & Wave
2	S2K6	Regular wave + steady wind	Wave Direction #2	0,049	0,730	2,75	5,50	45,0	0,9	7,0	V Wv Wi ML PM	36,5	275	Wind & Wave
2	S2K7	Regular wave + steady wind	Wave Direction #2	0,055	0,863	3,14	6,50	45,0	1,1	8,5	V Wv Wi ML PM	43,2	325	Wind & Wave
2	S2K8	Regular wave + steady wind	Wave Direction #2	0,073	0,969	4,13	7,30	45,0	1,5	11,4	V Wv Wi ML PM	48,5	365	Wind & Wave
2	S2K9	Regular wave + steady wind	Wave Direction #2	0,086	1,182	4,88	8,30	45,0	2,4	18,0	V Wv Wi ML PM	59,1	445	Wind & Wave
2	S2K10	Regular wave + steady wind	Wave Direction #2	0,106	1,328	6,00	10,00	45,0	3,3	25,0	V Wv Wi ML PM	66,4	500	Wind & Wave
1	S2L1	Irregular wave + steady wind	Wave Direction #1	0,049	0,730	2,75	5,50	0	0,93	7,0	V Wv Wi ML PM	478,1	3600	Wind & Wave
1	S2L2	Irregular wave + steady wind	Wave Direction #1	0,055	0,863	3,14	6,50	0	1,13	8,5	V Wv Wi ML PM	478,1	3600	Wind & Wave
1	S2L3	Irregular wave + steady wind	Wave Direction #1	0,073	0,969	4,13	7,30	0	1,51	11,4	V Wv Wi ML PM	478,1	3600	Wind & Wave
1	S2L4	Irregular wave + steady wind	Wave Direction #1	0,086	1,182	4,88	8,30	0	2,39	18,0	V Wv Wi ML PM	478,1	3600	Wind & Wave
1	S2L5	Irregular wave + steady wind	Wave Direction #1	0,106	1,328	6,00	10,00	0	3,32	25,0	V Wv Wi ML PM	478,1	3600	Wind & Wave
2	S2L6	Irregular wave + steady wind	Wave Direction #2	0,049	0,730	2,75	5,50	45	0,93	7,0	V Wv Wi ML PM	478,1	3600	Wind & Wave
2	S2L7	Irregular wave + steady wind	Wave Direction #2	0,055	0,863	3,14	6,50	45	1,13	8,5	V Wv Wi ML PM	478,1	3600	Wind & Wave
2	S2L8	Irregular wave + steady wind	Wave Direction #2	0,073	0,969	4,13	7,30	45	1,51	11,4	V Wv Wi ML PM	478,1	3600	Wind & Wave
2	S2L9	Irregular wave + steady wind	Wave Direction #2	0,086	1,182	4,88	8,30	45	2,39	18,0	V Wv Wi ML PM	478,1	3600	Wind & Wave
2	S2L10	Irregular wave + steady wind	Wave Direction #2	0,106	1,328	6,00	10,00	45	3,32	25,0	V Wv Wi ML PM	478,1	3600	Wind & Wave
1	S2M1	Regular wave + turbulent wind	Wave Direction #1	0,049	0,730	2,75	5,5	0	0,9	7,0	V Wv Wi ML PM	478,1	3600	Wind & Wave
1	S2M2	Regular wave + turbulent wind	Wave Direction #1	0,055	0,863	3,14	6,5	0	1,1	8,5	V Wv Wi ML PM	478,1	3600	Wind & Wave
1	S2M3	Regular wave + turbulent wind	Wave Direction #1	0,073	0,969	4,13	7,3	0	1,5	11,4	V Wv Wi ML PM	478,1	3600	Wind & Wave
1	S2M4	Regular wave + turbulent wind	Wave Direction #1	0,086	1,182	4,88	8,3	0	2,4	18,0	V Wv Wi ML PM	478,1	3600	Wind & Wave
1	S2M5	Regular wave + turbulent wind	Wave Direction #1	0,106	1,328	6	10	0	3,3	25,0	V Wv Wi ML PM	478,1	3600	Wind & Wave
2	S2M6	Regular wave + turbulent wind	Wave Direction #2	0,049	0,730	2,75	5,5	45	0,9	7,0	V Wv Wi ML PM	478,1	3600	Wind & Wave
2	S2M7	Regular wave + turbulent wind	Wave Direction #2	0,055	0,863	3,14	6,5	45	1,1	8,5	V Wv Wi ML PM	478,1	3600	Wind & Wave
2	S2M8	Regular wave + turbulent wind	Wave Direction #2	0,073	0,969	4,13	7,3	45	1,5	11,4	V Wv Wi ML PM	478,1	3600	Wind & Wave
2	S2M9	Regular wave + turbulent wind	Wave Direction #2	0,086	1,182	4,88	8,3	45	2,4	18,0	V Wv Wi ML PM	478,1	3600	Wind & Wave
2	S2M10	Regular wave + turbulent wind	Wave Direction #2	0,106	1,328	6	10	45	3,3	25,0	V Wv Wi ML PM	478,1	3600	Wind & Wave
1	S2N1	Irregular wave + turbulent wind	Wave Direction #1	0,049	0,730	2,75	5,50	0	0,93	7,0	V Wv Wi ML PM	478,1	3600	Wind & Wave
1	S2N2	Irregular wave + turbulent wind	Wave Direction #1	0,055	0,863	3,14	6,50	0	1,13	8,5	V Wv Wi ML PM	478,1	3600	Wind & Wave
1	S2N3	Irregular wave + turbulent wind	Wave Direction #1	0,073	0,969	4,13	7,30	0	1,51	11,4	V Wv Wi ML PM	478,1	3600	Wind & Wave
1	S2N4	Irregular wave + turbulent wind	Wave Direction #1	0,086	1,182	4,88	8,30	0	2,39	18,0	V Wv Wi ML PM	478,1	3600	Wind & Wave
1	S2N5	Irregular wave + turbulent wind	Wave Direction #1	0,106	1,328	6,00	10,00	0	3,32	25,0	V Wv Wi ML PM	478,1	3600	Wind & Wave
2	S2N6	Irregular wave + turbulent wind	Wave Direction #2	0,049	0,730	2,75	5,50	45	0,93	7,0	V Wv Wi ML PM	478,1	3600	Wind & Wave
2	S2N7	Irregular wave + turbulent wind	Wave Direction #2	0,055	0,863	3,14	6,50	45	1,13	8,5	V Wv Wi ML PM	478,1	3600	Wind & Wave
2	S2N8	Irregular wave + turbulent wind	Wave Direction #2	0,073	0,969	4,13	7,30	45	1,51	11,4	V Wv Wi ML PM	478,1	3600	Wind & Wave
2	S2N9	Irregular wave + turbulent wind	Wave Direction #2	0,086	1,182	4,88	8,30	45	2,39	18,0	V Wv Wi ML PM	478,1	3600	Wind & Wave
2	S2N10	Irregular wave + turbulent wind	Wave Direction #2	0,106	1,328	6,00	10,00	45	3,32	25,0	V Wv Wi ML PM	478,1	3600	Wind & Wave



## 5 INTEGRATION OF POLIMI AERO-SERVO-ELASTIC SCALED MODEL WITH A FROUDE-SCALED FLOATING PLATFORM

Filippo Campagnolo, Poli-Wind – Laboratory of the Dipartimento de Ingegneria Aerospaziale of the Politecnico di Milano (DIA-PoliMI)

### FOWT MODEL SCALE TESTING



#### MAIN ISSUE

Performing wave-tank testing with the POLIMI aero-servo-elastic model requires investigating HOW to couple the POLIMI model with a Froude-scaled floating platform.

#### APPROACH

Numerical simulation of full-scale FOWT dynamics and POLIMI model+scaled floating platform dynamics and comparison of simulation results (time series & RAOs)

## POLIMI AEROELASTIC SCALING LAWS

**Criteria for definition of scaling** (using Buckingham  $\Pi$  Theorem):

- **Exactly matched quantities:** TSR, Lock number, relative placement of frequencies wrt rev harmonics (same Campbell diagram)
- **Best compromise between:**
  - Reynolds mismatch (quality of aerodynamics)
  - Speed-up of scaled time (avoid excessive increase of control bandwidth)

Quantity	Scaling factor
Length Ratio	1/45
Time Ratio	1/22.84
Velocity Ratio	1/1.97
Rotor Speed Ratio	22.84/1
Torque Ratio	1/353574
Reynolds Ratio	1/88.64
Froude Ratio	11.6/1
Mach Ratio	1/1.97

### POLIMI SCALING

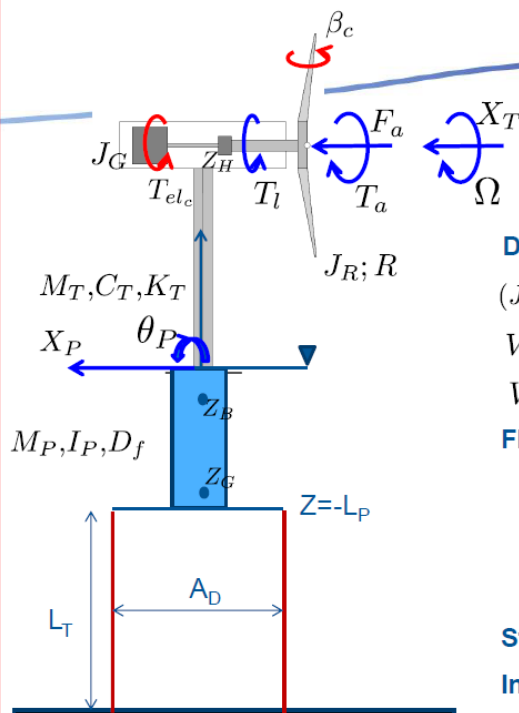
**+Pros:**

- Realistic model aerodynamic performance (thrust, power, TSR, wave geometry/deficit, etc...)

**-Cons:**

- Model aerodynamic/gravity forces ratio is  $\approx 11$  times the full scale one. This could be a hurdle when gravity plays an important role in determining the system dynamics!!

## FOWT MATHEMATICAL MODEL



### Simple 4 DOF non-linear model for TLP platform

**Drive -train shaft dynamics**

$$(J_R + J_G)\dot{\Omega} + T_l(\Omega) + T_{elc} - T_a(\Omega, \beta_c V_r, V_t) = 0$$

$$V_w = V_m + V_t \quad \text{Wind: mean wind + turbulence}$$

$$V_r = V_w - \dot{X}_T - \dot{X}_P - \dot{\theta}_P Z_H$$

**Flex. tower and platform dynamics:**

- Elastic tower fore-aft motion
- Platform pitch dynamics
- Platform surge dynamics

**States:**  $X_T, \dot{X}_T, \Omega, \theta_P, \dot{\theta}_P, X_P, \dot{X}_P$

**Inputs:**  $\beta_c, T_{elc}$

## TOWER/PLATFORM DYNAMICS EQUATIONS

SMALL ROTATION/DISPLACEMENT

$$\mathbf{M}\ddot{\eta} + \mathbf{C}_T\dot{\eta} + (\mathbf{K}_H + \mathbf{K}_G + \mathbf{K}_T)\eta = \mathbf{F}^{W\&W} + \mathbf{F}^M$$

$$\eta = \{X_T, X_P, \theta_P\}^T$$

Hydrostatic restoring

Gravity contribution

Tower stiffness contribution

Moorings forces

Wind & Waves forces

### WAVE FORCES

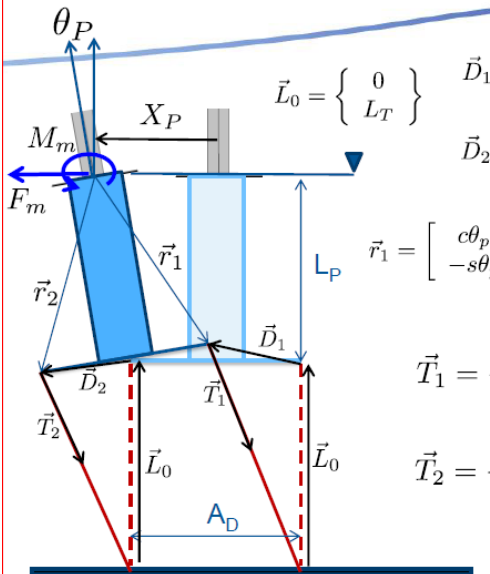
Morison equation, under the assumption of small floater diameter to wave length

$$dF_m = \rho(C_m + 1)\frac{\pi}{4}D_f^2\dot{u}(z)dz + \frac{1}{2}\rho C_D D_f(u(z) - \dot{X}_P)|u(z) - \dot{X}_P|dz$$

$$\mathbf{F}^{W\&W} = \begin{Bmatrix} F_a(\Omega, \beta_e, V_r) \\ F_a(\Omega, \beta_e, V_r) + \int_{z=-L}^0 dF_m dz \\ F_a(\Omega, \beta_e, V_r)Z_H + \int_{z=-L}^0 dF_m z dz \end{Bmatrix}$$

## MOORINGS FORCES

NON-LINEAR STATIC MODEL



$$\vec{L}_0 = \begin{Bmatrix} 0 \\ L_T \end{Bmatrix}$$

$$\vec{D}_1 = \begin{bmatrix} c\theta_p - 1 & s\theta_p \\ -s\theta_p & c\theta_p - 1 \end{bmatrix} \begin{Bmatrix} -\frac{A_D}{2} \\ -L_P \end{Bmatrix} + \begin{Bmatrix} x_P \\ 0 \end{Bmatrix}$$

$$\vec{D}_2 = \begin{bmatrix} c\theta_p - 1 & s\theta_p \\ -s\theta_p & c\theta_p - 1 \end{bmatrix} \begin{Bmatrix} \frac{A_D}{2} \\ -L_P \end{Bmatrix} + \begin{Bmatrix} x_P \\ 0 \end{Bmatrix}$$

$$\vec{r}_1 = \begin{bmatrix} c\theta_p & s\theta_p \\ -s\theta_p & c\theta_p \end{bmatrix} \begin{Bmatrix} -\frac{A_D}{2} \\ -L_P \end{Bmatrix} \quad \vec{r}_2 = \begin{bmatrix} c\theta_p & s\theta_p \\ -s\theta_p & c\theta_p \end{bmatrix} \begin{Bmatrix} \frac{A_D}{2} \\ -L_P \end{Bmatrix}$$

$$\vec{T}_1 = - \left[ \frac{AE}{|\vec{L}_0|} \left( |\vec{L}_0 + \vec{D}_1| - |\vec{L}_0| \right) + \frac{T_e}{2} \right] \frac{\vec{L}_0 + \vec{D}_1}{|\vec{L}_0 + \vec{D}_1|}$$

$$\vec{T}_2 = - \left[ \frac{AE}{|\vec{L}_0|} \left( |\vec{L}_0 + \vec{D}_2| - |\vec{L}_0| \right) + \frac{T_e}{2} \right] \frac{\vec{L}_0 + \vec{D}_2}{|\vec{L}_0 + \vec{D}_2|}$$

$$\mathbf{F}^M = \begin{Bmatrix} 0 \\ F_m \\ M_m \end{Bmatrix} = \begin{Bmatrix} 0 \\ \vec{T}_1^{(1)} + \vec{T}_2^{(1)} \\ -\vec{r}_1 \times \vec{T}_1 - \vec{r}_2 \times \vec{T}_2 \end{Bmatrix}$$

**Buoyancy force**

$$T_e = \rho g V_B - (M_P + M_T)g$$

## TOWER/PLATFORM DYNAMICS EQUATIONS

SMALL ROTATION/DISPLACEMENT

$$\mathbf{M} = \begin{pmatrix} M_T & M_T & M_T Z_H \\ M_T & M_P + M_T + A_{11} & M_P Z_G + M_T Z_H + A_{12} \\ M_T Z_H & M_P Z_G + M_T Z_H + A_{21} & M_P Z_G^2 + M_T Z_H^2 + I_P + A_{22} \end{pmatrix}$$

$$\mathbf{K}_H = \begin{pmatrix} 0 & 0 & 0 \\ 0 & 0 & 0 \\ 0 & 0 & \rho g I_{wl} + \rho g V_B Z_B \end{pmatrix} \quad \mathbf{K}_G = \begin{pmatrix} 0 & 0 & -M_T g \\ 0 & 0 & 0 \\ -M_T g & 0 & M_P g Z_G - M_T g Z_H \end{pmatrix}$$

Hydrostatic restoring

$$I_{wl} = \frac{\pi D_f^4}{64}$$

Gravity effect on system restoring properties

$$\mathbf{K}_T = \begin{pmatrix} K_T & 0 & 0 \\ 0 & 0 & 0 \\ 0 & 0 & 0 \end{pmatrix} \quad \mathbf{C}_T = \begin{pmatrix} C_T & 0 & 0 \\ 0 & 0 & 0 \\ 0 & 0 & 0 \end{pmatrix}$$

$$A_{11} = \int_{z=-L_P}^0 \rho C_m \frac{\pi}{4} D_f^2 dz; \quad A_{22} = \int_{z=-L_P}^0 \rho C_m \frac{\pi}{4} D_f^2 z^2 dz$$

$$A_{12} = A_{21} = \int_{z=-L_P}^0 \rho C_m \frac{\pi}{4} D_f^2 z dz; \quad \text{Hydrodynamic added mass/inertia}$$

## FULL SCALE & SCALED MODEL DATA

### WIND TURBINE

	FULL-SCALE	POLIMI MODEL
R[m]	46,57	1,0162
Z <sub>H</sub> [m]	80	1,786
M <sub>T</sub> [Kg]	4.312E+05	6.017
K <sub>T</sub> [N/m]	9.409E+05	11560
C <sub>T</sub> [Ns/m]	2.548E+04	10,55
J <sub>G</sub> [Kgm <sup>2</sup> ]	1.172E+06	0.0026
J <sub>R</sub> [Kgm <sup>2</sup> ]	1.021E+07	0,06
C <sub>P</sub> <sup>II</sup> [-]	0,4864	0,343
C <sub>F</sub> <sup>II</sup> [-]	0,9534	0,734
Ω <sub>R</sub> [rpm]	16	365

### FLOATING PLATFORM (MIT TLP)

	FULL-SCALE	1/45 SCALED MODEL
L <sub>P</sub> [m]	48	1.067
L <sub>T</sub> [m]	152,11	3.38
D <sub>f</sub> [m]	18	0,4
C <sub>D</sub> [-]	0,7	0,7
C <sub>m</sub> [-]	0,8	0,8
I <sub>P</sub> [Kgm <sup>2</sup> ]	5.716E+08	3.0976
M <sub>P</sub> [Kg]	8.774E+06	96.286
Z <sub>B</sub> [m]	-24	-0,533
Z <sub>G</sub> [m]	-40,61	-0.902
A <sub>D</sub> [m]	27	0.6
EA [N]	1.5E+09	1.909E+05

## POLIMI-MODEL Froude MISMATCH

$$T_e = g(\rho V_B - M_P - M_T)$$

Model leg tension  $\approx 11$  times lower than desired

$$g \approx \frac{1}{11} g^{(desired)} !!!$$

$$\mathbf{K}_H^{33} + \mathbf{K}_G^{33} = g(\rho I_{wl} + \rho V_B Z_B - M_P Z_G - M_T Z_H)$$

Hydrostatic/gravity restoring  $\approx 11$  times lower than desired

Linearized moorings  $\left. \frac{\partial F_i^M}{\partial \eta_j} \right|_{\eta=0} = \mathbf{K}_{TLP} = \begin{bmatrix} 0 & 0 & 0 \\ 0 & \frac{T_e}{L_T} & -T_e \frac{L_P}{L_T} \\ 0 & -T_e \frac{L_P}{L_T} & T_e L_P \left( \frac{L_P}{L_T} + 1 \right) + \frac{A_D^2}{2} \frac{EA}{L_T} \end{bmatrix}$

Only the restoring effect provided by the moorings extension can be correctly scaled

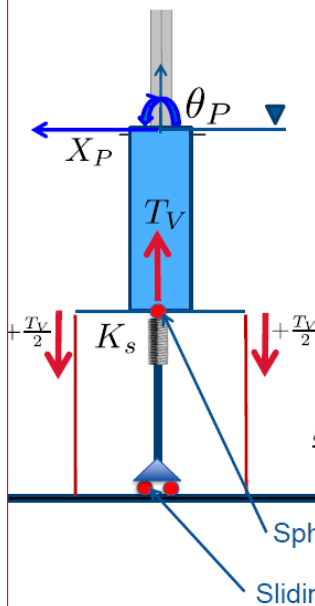
Undisplaced moorings surge-restoring  $\approx 11$  times lower than desired

## HOW TO GET DESIRED PLATFORM RESTORING PROPERTIES?

### 1° SOLUTION:

Get the desired restoring properties by fixing a pre-compressed spring at the platform base.

The constraints system (sliding+spherical joint) allows to kept the spring-load direction fixed



Negative effect on pitch stability

Increased leg tension

$$\mathbf{K}_S \approx \begin{bmatrix} 0 & 0 & 0 \\ 0 & 0 & 0 \\ 0 & 0 & -T_V L_P \end{bmatrix}$$

$$\left. \frac{\partial F_i^M}{\partial \eta_j} \right|_{\eta=0} = \mathbf{K}_{TLP} = \begin{bmatrix} 0 & 0 & 0 \\ 0 & \frac{T_e + T_V}{L_T} & -(T_e + T_V) \frac{L_P}{L_T} \\ 0 & -(T_e + T_V) \frac{L_P}{L_T} & (T_e + T_V) L_P \left( \frac{L_P}{L_T} + 1 \right) + \frac{A_D^2}{2} \frac{EA}{L_T} \end{bmatrix}$$

Tune the cable stiffness to balance the reduction of pitch stability due to the spring pre-load

## SIZING OF SPRING PRE-LOAD

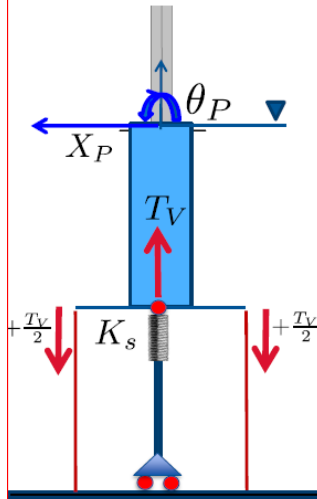
Optimize pre-load and line stiffness to get desired platform natural modes/displacements (or combinations)

$$\mathbf{p} = \{T_V, EA\} \quad \mathbf{p}^* = \arg \min_{\mathbf{p}} J$$

$$J = \sum_{i=1}^{N_m} \frac{\omega^{(i)}(\mathbf{p}) - \omega_r^{(i)}}{\omega_r^{(i)}} \quad \text{or} \quad J = \sum_{i=1}^{N_m} \frac{\bar{\eta}^{(i)}(\mathbf{p}) - \eta_r^{(i)}}{\eta_r^{(i)}}$$

Reference modes

Reference disp.



Non-linear moorings behaviour included in the evaluation of the cost function

$$(\mathbf{K}_S(\mathbf{p}) + \mathbf{K}_H + \mathbf{K}_G + \mathbf{K}_T)\bar{\eta} = \bar{\mathbf{F}}^{W\&W} + \mathbf{F}^M(\mathbf{p})$$

$$-\omega^2 \mathbf{M} + \left( \frac{\partial \mathbf{F}_i^M(\mathbf{p})}{\partial \eta_j} \right)_{\eta=\bar{\eta}} + \mathbf{K}_S(\mathbf{p}) + \mathbf{K}_H + \mathbf{K}_G + \mathbf{K}_T = \mathbf{0}$$

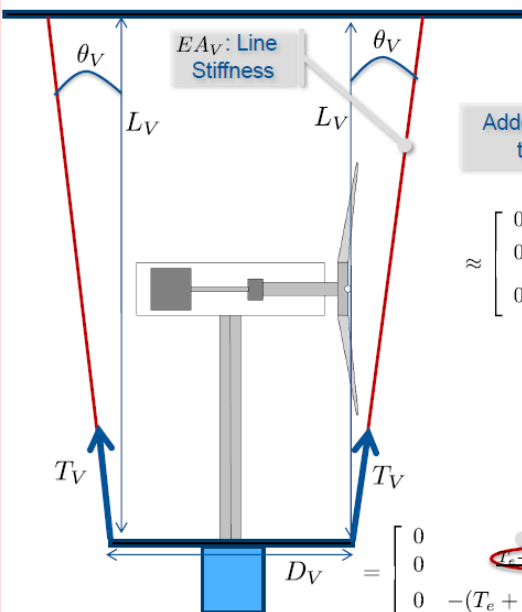
Static wind condition

$$\bar{\mathbf{F}}^{W\&W} = \begin{Bmatrix} F_a(\Omega, \beta_e, V_m) \\ F_a(\Omega, \beta_e, V_m) \\ F_a(\Omega, \beta_e, V_m) Z_H \end{Bmatrix}$$

## HOW TO GET DESIRED PLATFORM RESTORING PROPERTIES?

### 2° Solution:

Get desired restoring properties adding upward moorings



Added upward tension

$$\frac{\partial F_i^V}{\partial \eta_j} \bigg|_{\eta=0} = \mathbf{K}_{TV} \approx$$

$$\approx \begin{bmatrix} 0 & 0 & 0 \\ 0 & \frac{2EA_V t^2}{L_V(1+t^2)^{3/2}} + \frac{2T_V}{L_V(1+t^2)} \left( \sqrt{1+t^2} - \frac{t^2}{\sqrt{1+t^2}} \right) & -\frac{D_V EA_V t}{L_V(1+t^2)^{3/2}} \\ 0 & -\frac{D_V EA_V t}{L_V(1+t^2)^{3/2}} & \frac{D_V^2 EA_V}{2L_V(1+t^2)^{3/2}} \end{bmatrix}$$

$$t = \tan \theta_V$$

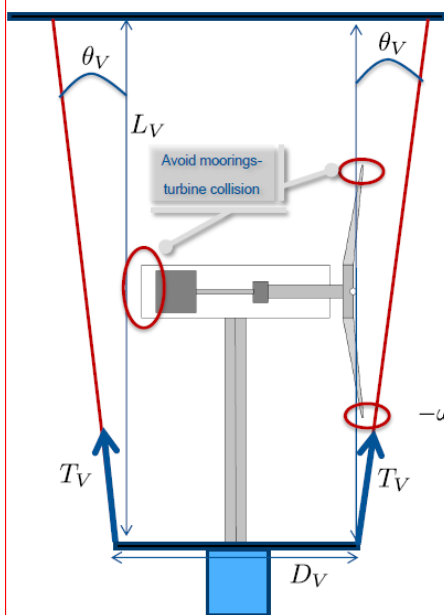
Increased leg tension

$$\frac{\partial F_i^M}{\partial \eta_j} \bigg|_{\eta=0} = \mathbf{K}_{TLP} =$$

$$= \begin{bmatrix} 0 & 0 & 0 \\ 0 & \frac{L_e + 2T_V \cos \theta_V}{L_T} & -(T_e + 2T_V \cos \theta_V) \frac{L_P}{L_T} \\ 0 & -(T_e + 2T_V \cos \theta_V) \frac{L_P}{L_T} & (T_e + 2T_V \cos \theta_V) L_P \left( \frac{L_P}{L_T} + 1 \right) + \frac{A_P^2}{2} \frac{EA}{L_T} \end{bmatrix}$$



## SIZING OF UPWARD MOORINGS



Optimize upward moorings properties to get desired platform natural modes/displacements (or combinations).

Constrained optimization: avoid turbine/moorings collision for the overall model operating envelope

$$\mathbf{p} = \{T_V, D_V, EA_V, L_V, \theta_V\}$$

$$\mathbf{p}^* = \arg \min_{\mathbf{p}} J$$

Non-linear moorings behaviour included in the evaluation of the cost function

$$(\mathbf{K}_H + \mathbf{K}_G + \mathbf{K}_T)\bar{\eta} = \bar{\mathbf{F}}^{W\&W} + \mathbf{F}^M(\mathbf{p}) + \mathbf{F}^V(\mathbf{p})$$

$$-\omega^2 \mathbf{M} + \left( \frac{\partial \mathbf{F}_i^V(\mathbf{p})}{\partial \eta_j} \bigg|_{\eta=\bar{\eta}} + \frac{\partial \mathbf{F}_i^M(\mathbf{p})}{\partial \eta_j} \bigg|_{\eta=\bar{\eta}} + \mathbf{K}_H + \mathbf{K}_G + \mathbf{K}_T \right) = 0$$

$$\bar{\mathbf{F}}^{W\&W} = \begin{Bmatrix} F_a(\Omega, \beta_e, V_m) \\ F_a(\Omega, \beta_e, V_m) \\ F_a(\Omega, \beta_e, V_m) Z_H \end{Bmatrix}$$

Static wind condition

## NUMERICAL SIMULATIONS

### DEFINITION OF CLIMATE FOR FULL-SCALE SIMULATIONS

#### Wind&Wave

- Constant wind: 17 [m/s]
- Irregular waves: JONSWAP spectrum  $H_s$  3,37 [m];  $T_p$  7,03 [s]



Simulation wind&wave climate based on indication found in MARINET deliverable 4.2

### INCLUSION OF CLOSED LOOP CONTROL

#### Closed Loop Control

Wind-scheduled LQR-MIMO controller based on linearized state-space model

Bottasso, C.L. and Croce, A. and Riboldi, C.E.D. and Nam, Y. Power curve tracking in the presence of a tip speed constraint. Renewable Energy (2012)

$$\mathbf{u} = (\beta_c, T_{elc})^T \quad \mathbf{x} = (\eta^T, \dot{\eta}^T, \Omega, \int \Omega)$$

$$\dot{\mathbf{x}} = \mathbf{f}(\mathbf{x}, \mathbf{u}, V_m) \quad \text{Non-linear dynamic equations}$$

$$\Delta \dot{\mathbf{x}} = \mathbf{A}(\mathbf{x}^*, \mathbf{u}^*, V_m^*) \Delta \mathbf{x} + \mathbf{B}(\mathbf{x}^*, \mathbf{u}^*, V_m^*) \Delta \mathbf{u}$$

$$\Delta \mathbf{x} = \mathbf{x} - \mathbf{x}^* \quad \Delta \mathbf{u} = \mathbf{u} - \mathbf{u}^*$$

Trim state

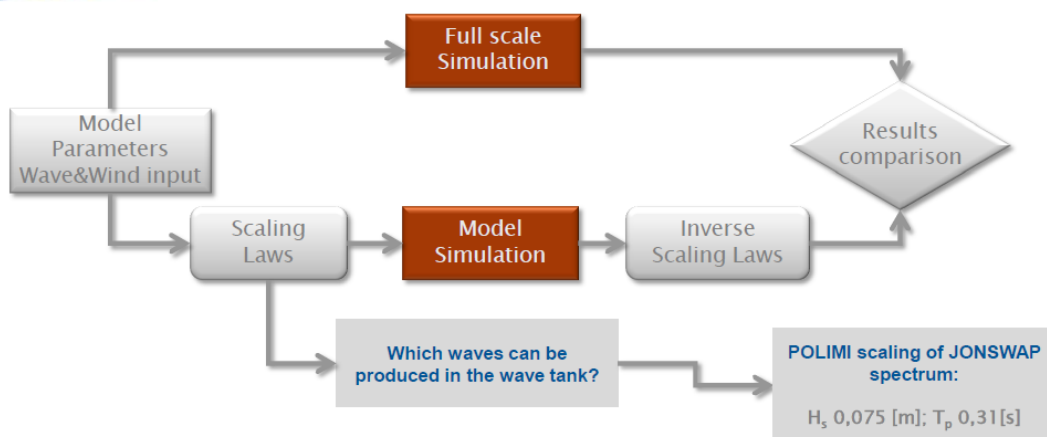
Trim control action

$$\Delta \mathbf{u} = \mathbf{K}_G \Delta \mathbf{x}$$

$\mathbf{K}_G$ : control gains



## COMPARISON OF NUMERICAL SIMULATION RESULTS



**POLIMI scaling requires wave forces  $\approx 11$  times higher than Froude scaled ones.**

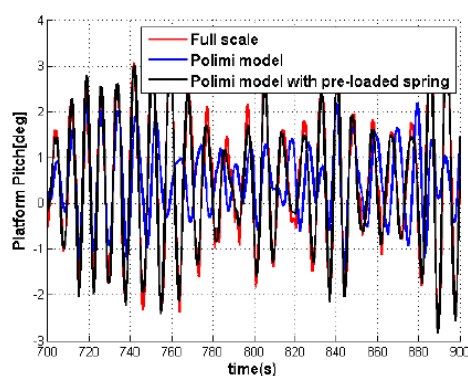
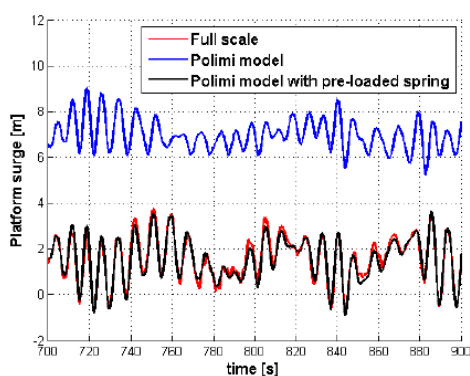
The waves generated in the tank must be faster than Froude scaled ones (same height, but wave celerity  $\approx 3.4$  times higher)

## SIMULATION RESULTS

**Simulation of Full-scale dynamics and POLIMI Model dynamics without and with additional spring pre-load(1° solution)**

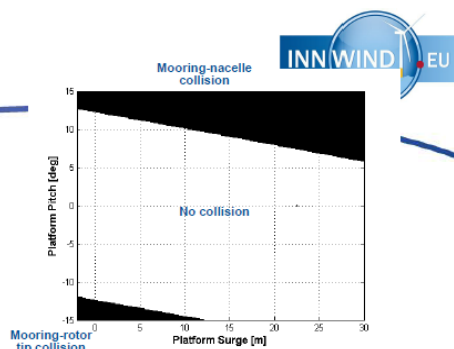
**Additional upward tension determined with the goal of matching the full scale platform dynamics:**

$T_V \approx 11T_e \approx 3700$  [N],  $EA \approx +50\%$



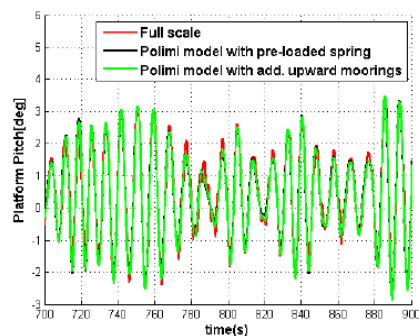
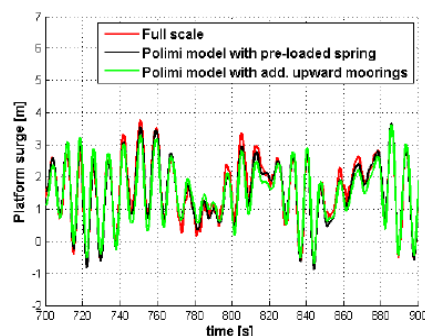
## SIMULATION RESULTS

Simulation of Full-scale dynamics and POLIMI Model dynamics with additional spring pre-load(1° solution) and additional upward moorings (2° solution)



Additional upward moorings prop. determined with the goal of matching the full scale platform dynamics and avoiding any collision between the turbine and the upward moorings

$T_V \approx 3T_e \approx 1000$  [N],  $L_V \approx 5.9$  [m],  $EA_V \approx 25\%$  EA,  $DV \approx 0.5$  [m],  $\theta_V \approx 5$  [deg]



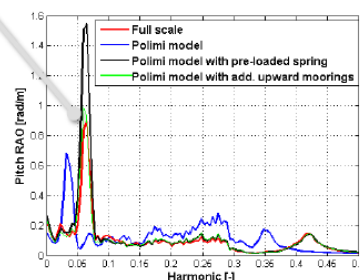
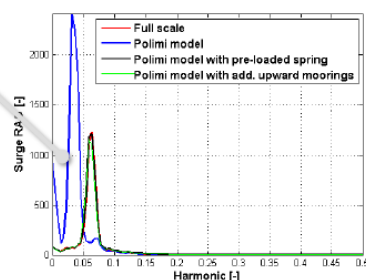
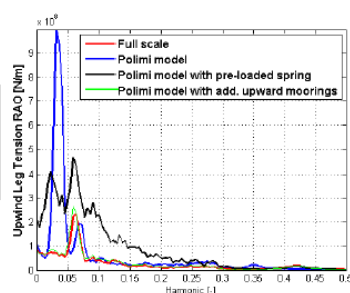
## SIMULATION RESULTS COMPARISON

Time histories and RAOs plots highlight the realistic POLIMI model platform dynamics when upward tension is added

Lower model platform natural modes due to lower restoring properties when NO upward tension is added

Better match of model-full scale platform pitch RAO when additional vertical moorings are added

The match between the upwind tension leg RAO, when pre-loaded spring is added, is poor due to the increased line stiffness (+50%)



## CONCLUSIONS

Combine POLIMI model and Froude scaled model platform is possible, but it is necessary to adjust the platform restoring properties; this can be achieved by adding upward tension and two different ways have been shown.

**POLIMI model can provide unique capabilities:**

- Realistic aerodynamic performances
- Close loop pitch&torque control, with individual pitch control capabilities
- 2 Models: wakes condition testing      One model assembled on the floating platform, the other, located upstream and ground-fixed, generates wakes of realistic geometry/deficit

## 6 MOORING LINES: ISSUES FOR DESIGN, MODELLING AND DYNAMIC ANALYSIS

### 6.1 Description of Mooring Lines

Mooring lines are defined as mechanical members that connect and attach floating structures to its anchoring points. They can have a strong influence on the behaviour of the attached structures and therefore also on the motion characteristics of the floating device. This section gives an overview on the types of mathematical descriptions of mooring lines. At DNV GL ANSYS AQWA is used for the simulation of dynamic mooring behavior. In AQWA-NAUT (ANSYS, Inc.) line types of mooring lines include both linear and non-linear cables:

#### Linear cables

- Linear elastic cables
- Winch cables
- Constant force cables
- Pulleys
- Drum winch cable

#### Non-linear cables

- Steel wire cables

#### Composite catenary cables

- Intermediate buoys and clump weights
- Non-linear cables described by a polynomial of up to fifth order

Finally, fixed and floating fenders can be defined. These are classified as a type of mooring line and have non-linear properties.

The linear cables represent a simple type of mooring line description. The simplest models are the constant force cables that act at the centre of gravity of the body and their force magnitude and direction are fixed. The winch cables maintain a constant tension provided the distance between the end of the mooring line is greater than the specified unstretched length. For the linear elastic cables the tension is proportional to its extension. The structures attached to the cable experience a force varying magnitude and direction.

A more realistic description of mooring lines is provided by the non-linear cables. One of the methods consists in a polynomial equation that describes the tension force as a function of extension. Beside of this, the mooring line also can be described as a multiple degrees of freedom spring-mass system where the cable is represented by a series of straight segments each with a constant stiffness and mass.

### 6.2 Evaluation of Mooring Lines and Anchors for Floating Offshore Wind Turbines

#### Mooring types to be considered

- Spread moorings (catenary, taut line and semi taut-line)
- Single point moorings, anchored by spread mooring arrangements
- Mooring material, steel and synthetic fibre ropes

#### **Defining design situations**

- Service requirements
- Design service life
- Hazards to which the station keeping system and the connected floating structure can be exposed during service life
- Potential consequences of partial or complete station keeping system failure
- Nature and severity of environmental to be expected during the design service life
- Parameters needed for the environmental design assessment should be estimated from the available environmental information. This can be based on a risk analysis, if not enough information are available.
- Definition of specific design situations, calculation process and design criteria are interrelated

#### **Design situations for ULS (ISO 19901-7, GL and DNV Guidelines and Technical Notes or Recommended Practices)**

##### **Permanent moorings:**

- permanent moorings with short design service (service life design < 20 year, return period for environmental design situations can be less than the 100 years used in the oil and gas industry. 50y years could be a compromise)
- permanent moorings designed for disconnection
- permanent moorings in proximity to other installations (possible consequences to contact sea surface with sea floor infrastructures and installations)
- permanent moorings redundancy check condition (should be designed with redundancy to withstand the assumed design situations even with a failure of one line. This can be consequence breakage, planned maintenance or local failure. This requirement should be different for different type of structures and the consequences of a failure should be evaluated a priori using FMEA – Failure Mode and Effect Analysis. Strength on mooring lines to be compared to the minimum break strengths (certified strength for a chain, wire rope, fibre rope or accessories)

#### **Design situations for FLS**

##### **Site specific data requirements:**

- Water depth for the mooring system at each anchor location considering tidal and storm surges
- Soil and sea floor conditions
- Wave statistics: Wave period, height and direction

- Wind statistics: wind speed and direction
- Current speed, profile and direction and the frequency of occurrence of each environmental state
- Frequency of occurrence of each environmental state
- Atmospheric Icing
- Marine growth

#### **Environmental impacts on mooring lines.**

- Current induced loads
- Ice-induced loads
- Vortex induced vibrations of mooring lines

#### **Indirect impacts**

Wave-induced impacts:

- The actions on floating structures categorized according frequency range:
- Steady actions: wind, current and wave drift that are constant in magnitude and direction for the duration of interest
- Low-frequency cyclic actions (slow drift) – periods between 1 min and 10 min causing induced dynamic excitation in the range of the dynamic excitation of their natural periods of surge, sway and yaw. The type of platform should be taken into account for this consideration. For spar platforms wave- induced actions can induce dynamic excitation at the pitch and natural periods.
- Wave-frequency cyclic actions with characteristics periods ranging from 3s to 30 s

#### **Current-induced impacts (steady and low-frequency)**

- Should be determined by model tests and or empirical analysis tools.

#### **Directional distribution**

- Floating structures offsets and motions have to be used in the station keeping design considering the most unfavourable combination of wind, wave and current directions consistent with the site-specific metocean conditions.

#### **Vortex-induced motions**

- Relevant for TLP designs in deeper water. Additional information and guidance on VIM is contained in API RP 2SK.

#### **Mooring Analysis**

- Floating structure offset
- Floating structure response
- Mooring line response
- Line tension limit
- Grounded line length
- Line length and geometry constraints
- Anchor forces
- Typical mooring configuration analysis and assessment
- Transient analysis of floating structure motions
- Fatigue analysis

### 6.3 Standards and Guidelines for mooring systems

Enclose a summary of state-of-the-art offshore standards is given dealing directly with mooring systems or floating structures including application of mooring systems. In column three the applicability for Floating Offshore Wind Turbines (FOWT) has been appointed in line with restrictions regarding specific requirements for FOWT.

Abbreviations	
MOU	Mobile Offshore Unit
FOI	Floating Offshore Installations
FPS	Floating Production Systems
FPU	Floating Production Units
OLS	Offshore Loading Systems
LRFD	Load and Resistance Factor Design
WSD	Working Stress Design
OS	Offshore Standards
OSS	Offshore Service Specifications

	Standard	Scope	Applicability for FOWT
1	<b>GL Industrial Services</b> , "Guideline for the Certification of Offshore Wind Turbines", Edition 2012	Guideline applies to the design assessment and certification of offshore wind turbines and offshore wind farms	- Detailed requirements for design calculations - Description of load cases which cover design situations and external conditions  Restrictions: No specific requirement for FOWT (e.g. floating units, mooring)



2	<b>GL Industrial Services</b> , "Part 6: Offshore Technology – Chapter 2: Mobile Offshore Units", Edition 2007	Requirements for different types of mobile offshore units (MOU) as: - units connected to the sea bed by anchoring (mooring) - units kept on position by dynamic positioning/propelling system (active) - units connected by legs in jacked up position	Section 8 "Mooring Equipment" contains requirements for design and approval for different types of mobile offshore units, such as: - Units connected to the sea bed by anchoring (mooring) - Units kept on position by dynamic positioning/propelling system - Units connected by legs in jacked up condition  Restrictions: No specific design load case requirements
3	<b>GL Noble Denton</b> , "Technical Policy Board – Guidelines for Moorings, 0032/ND", Rev. 0, Issued 2010-12-06	Guidelines for different types of mooring such as: - catenary/taut leg mooring of MOU - catenary/taut leg mooring for FOI - Quayside/ Inshore mooring for MOU/FOI  Provides information on different codes/ standards, design requirements, design environmental conditions, mooring design and analysis	- Information on general design requirements -for more Detailed Information codes/standards are referenced  Restrictions: No Detailed requirements for design calculation
4	<b>IEC 61400-3-Ed.1</b> , "Wind Turbines - Part 3: Design requirements for offshore wind turbines", International Electro-technical Commission (IEC), 1st Edition 1.0, Issued 2009	Guidelines for Offshore Wind Turbines with detailed requirements on design assessment, load calculation and certification	- Detailed requirements for design calculations - Description of load cases which cover design situations and external conditions  Restrictions: No specific requirement for FOWT (e.g. floating units, mooring)
5	<b>ISO 1704</b> , "Ships and marine technology - Stud-link anchor chains"		

6	<b>ISO 19900</b> , "Petroleum and natural gas industries - General requirements for offshore structures - Part 1: Metocean design and operating considerations", 1st Edition, Issued December 2002	Standard specifies general principles for the design and assessment of offshore structures	
7	<b>ISO 19901-7</b> , "Petroleum and natural gas industries – Specified requirements for offshore structures – Part 7:2011 Station keeping systems for floating offshore structures and mobile offshore units"	Design, Analysis and Evaluation of Station keeping systems for Floating Structures used by the Oil and Gas Industry. And the Assessment of Station keeping Systems for Site-Specific Applications of MOU.	<p>- Recommended analysis methods and conditions</p> <p>In Part 7 specific requirements for station keeping systems for floating offshore structures and mobile offshore units.</p> <p>ISO19901-7 to be the preferred code for the design of all mooring systems.</p>
8	<b>ISO 19904-1</b> , "Petroleum and natural gas industries - Floating Offshore Structures - Part 1: Monohulls, semi submersibles and spars", Issued February 2006	Requirements and guidance for the structural design and/or assessment of floating offshore platforms used by the petroleum and natural gas industries. Reference to DNV-OS-C101	<p>General requirements for floating offshore platforms</p> <p>Restrictions: No specific design load case requirements</p>
9	<b>API RP 2FPS</b> , "Recommended Practice for Planning, Designing, and Constructing Floating Production Systems", 1st Edition, American Petroleum Institute, Issued March 2001	Recommended practice provides guidance for design, fabrication, installation, inspection and operation of FPSs.	<p>Precise Chapter for Station Keeping and Anchoring Systems</p> <p>Restrictions: No detailed information on design requirements for FOWT</p>
10	<b>API RP 2SK</b> , "Design and Analysis of Stationkeeping Systems for Floating Structures", 3rd Edition, American Petroleum Institute, Issued October 2005	Recommended practice provides methods for analysing, designing and/or evaluating station-keeping systems used for floating units.	Includes extensive guidance that is not covered within the ISO19901-7

11	<b>DNV</b> , "Energy Report - Guideline for offshore floating wind turbine structures", Rev.0, Report no: 129G6V8-7, Issued December 2009	Requirements and recommendations for design of floating support structures for offshore wind turbines. Serves as a supplement to DNV-OS-J101 for topics not covered by in this guideline.	<ul style="list-style-type: none"> <li>- Covers most design requirements for wind turbine support structures briefly including corresponding standards.</li> <li>- Overview about design types</li> </ul> <p>Restrictions: No specific requirements for the design assessment or calculation</p>
12	<b>DNV-OS_F201</b> , "Dynamic Risers", Rev. 2, Issued October 2010		<p>Coupled analysis may be found in here</p> <p>Restrictions: No specific requirements for mooring or FOWT</p>
13	<b>DNV-OS-C101</b> , "Design of Offshore Steel Structures, General (LRFD Method)", Issued October 2008	Offshore standard provides design principles, technical requirements and guidance for the structural design of offshore structures. OS-C101 is general part of DNV offshore standards (OS) for structures	<ul style="list-style-type: none"> <li>- General requirements for all offshore structures</li> </ul> <p>Restrictions: No specific design load case requirements</p>
14	<b>DNV-OS-C201</b> , "Structural Design of Offshore Units (WSD method)"		
15	<b>DNV-OS-C401</b> , "Fabrication and Testing of Offshore Structures", Rev. 1, Issued April 2005		
16	<b>DNV-OS-E301</b> , "Position Mooring", Rev. 1, Issued October 2010	This standard is applicable to all types of floating offshore units including buoys relying on catenary mooring, semi-taut and taut leg mooring systems as well as soft yoke systems.	<ul style="list-style-type: none"> <li>- Specific guideline for mooring systems, e.g. applicable for FOWT</li> </ul> <p>Restrictions: n/a</p> <p>An acceptable alternative to ISO19901-7 when used in conjunction with DNV RP C205</p>

17	<b>DNV-OS-E302</b> , "Offshore Mooring Chain", Rev.1, Issued October 2009	This offshore standard contains criteria, technical requirements and guidance on materials, design, manufacture and testing of offshore mooring chain and accessories.	- Defines requirements for offshore mooring chain and accessories for position mooring applications such as: mooring of MOUs, FPU's, OLS and gravity base structures (during fabrication)
18	<b>DNV-OSS-312</b> , "Certification of Tidal and Wave Energy Converters", Issued October 2008	Offshore Service Specification with general information about Tidal and Wave Energy Converters	Refers to Standards for Certification: - No.2.6 Certification of Offshore Mooring Chains - No. 2.9 Approval Programs - related to components, manufacturers, service suppliers  Restrictions: No specific requirement for FOWT (e.g. floating units, mooring)
19	<b>DNV-OSS-901</b> "Project Certification of Offshore Wind Farms", Issued June 2012	OSS applies to project certification and related verification tasks during the design, construction and operation of offshore wind farms	- Specifications for wind turbines and their support structures, and substations including topsides and support structures  Restrictions: No requirements on mooring lines
20	<b>DNV-RP-C205</b>	Recommended practice provides design criteria and guidance for assessment of loads on marine structures subjected to wind, wave, and current loading.	- general requirements for all offshore structures  Restrictions: No specific design load case requirements
21	<b>ABS</b> , "ABS - Final Report - Floating Wind Turbines", 1st Edition, American Bureau of Shipping, Issued May 2012	Design and Code Study, different design concepts and challenges	

22	<p><b>ABS</b>, "ABS - Guide for the Certification of offshore mooring chain", 3rd Edition, American Bureau of Shipping, Issued December 2009</p>		<p>Requirements for the manufacturing of mooring chains such as materials, design, manufacture, testing; Included additional requirements for the qualification of manufacturers, especially with respect to forged and cast accessories</p> <p>Restrictions: No specific requirements on the demands for FOWT</p>
----	--	--	--

## 6.4 Definition of Load Cases - Extract from chapter 4 from GL 2012 -Guideline for the Certification of Offshore Wind Turbines

### Section 4.4.6.5 Load assumptions for floating offshore Units

The load cases and design conditions for floating offshore wind turbines shall follow the definitions made under 4.4.3 for fixed offshore wind turbines. Additional considerations from particular aspects of floating and moored structures, as listed in sections 4.4.2.10 and 4.4.2.11 [1], shall be considered in the specification of the design and operative conditions.

Additional specific load cases for floating wind turbines given in Table 4.4.4 [1] shall be observed.

Mooring and riser systems shall be considered as additional component with associated failure modes in the concept design. For special cases (e.g. TLP platforms) additional requirements in design, operation and maintenance may apply and have to be agreed upon in consultation with GL. The anchoring system shall be designed such that a sudden failure of any single anchor line will not cause progressive failure of the remaining lines.

Note:

In general, if the requirement is not met a risk analysis shall be performed. As a result of the analysis monitoring and measures to prevent mooring line loss or collisions with neighbour turbines shall be formulated.

Mooring analysis shall be performed to predict extreme values of action effects such as floating structure offsets, line tensions and anchor forces.

A dynamic analysis of the complete system shall be performed for all load cases.

DLC 10.1 and 10.4 correspond to a transient situation between the intact condition (all mooring lines are intact) and the redundancy check situation. This is the situation after one line breaks and the structure has reached a new mean position (DLC 10.2 and 10.5). The transient load cases DLC 10.1 and 10.4 shall be investigated only if the platform is close to other devices or collision with them is possible.

Additional load cases DLC 10.3 and 10.6 shall be investigated for all relevant leakages. The leakage conditions shall be chosen according to damage stability requirements specified in 4.4.2.11 [1].

The definition of the design load cases DLC 10.4 to DLC 10.6 are the same as the ones from DLC 10.1 to DLC 10.3, with the exception of the wind conditions. In the first group (DLC 10.1 to DLC 10.3) the NTM wind model shall be used while in the second group (DLC 10.4 to 10.6) the extreme wind model EWM shall be used. Yaw system misalignment and the hysteresis shall be considered for yaw movement.

If the wind turbine is subject to large yaw movements, changes in the operating condition or stand-by condition during the increase in the wind speed from normal operation to the extreme condition, this behaviour shall be considered in the analysis of load cases 10.1 to 10.6.

If wind, wave and current misalignment can lead to higher loading this shall be considered.

Design situation	DLC	Wind conditions	Marine conditions	Other conditions	Type of Analysis	Partial safety factors
Power production	10.1	NTM $V_{hub} = V_r$ or $V_{out}$	Irregular sea state with $H_s(V)$	transient condition between intact and redundancy check condition	U	A
	10.2	NTM $V_{in} \leq V_{hub} \leq V_{out}$	Irregular sea state with $H_s(V)$	One single line break, redundancy check MIS	U	A
	10.3	NTM $V_{in} \leq V_{hub} \leq V_{out}$	Irregular sea state with $H_s(V)$	Leakage (damage stability) MIS	U	A
Parked (standstill or idling)	10.4	EWM $V_{hub} = V_{ref}$	Irregular sea state with $H_s(V)$	transient condition between intact and redundancy check condition	U	A
	10.5	EWM $V_{hub} = V_{ref}$	Irregular sea state with $H_s(V)$	One single line break, redundancy check MIS	U	A
	10.6	EWM $V_{hub} = V_{ref}$	Irregular sea state with $H_s(V)$	Leakage MIS	U	A

Table 4.4.4 of [1] Design load cases for floating offshore wind turbines.

Meaning of the abbreviations in Table 4.4.4:

DLC	Design load case
ECD	Extreme coherent gust with direction change
EOG	Extreme operating gust
ETM	Extreme turbulence model
EWM	Extreme wind speed model
EWS	Extreme wind shear
NTM	Normal turbulence model



NWP	Normal wind profile model
MIS	Wind, wave and current misalignment to be considered
MUL	Multidirectionality of metocean conditions to be considered
$H_s(V)$	Significant wave height corresponding to $V_{hub}$
$H_{max}(V)$	Maximum wave height corresponding to $V_{hub}$
$H_{s1}$	Significant wave height with the recurrence period of 1 year
$H_{s50}$	Significant wave height with the recurrence period of 50 year
$H_{max1}$	Maximum wave height with the recurrence period of 1 year
$H_{max50}$	Design wave height with the recurrence period of 50 years
F	Fatigue strength
U	Ultimate strength
N	Normal
E	Extreme
A	Abnormal
T	Transport, erection, installation and maintenance

## Reference Chapter 6

[1] GL Industrial Services, "Guideline for the Certification of Offshore Wind Turbines", Edition 2012

## 7 CONCLUSIONS

Starting with a global review of the tank test experiments of floating wind turbines over the last decade, a comprehensive literature and publication collection on floating tank tests and their approaches is provided.

The literature review shows how various institutions have addressed this specific scaling problem along with presenting the numerous attempts to gain insight into the complex dynamics of floating wind turbines in order to build full scale systems and increase fidelity of numerical models. Following the detailed description of the projects an overview table shows a short summary of the findings of each study.

This overview is followed by a theoretical excursion on scaling laws with respect to the optimal aerodynamic and hydrodynamic representation of full scale floating wind turbines in the range of 10 - 20 MW. Tables with scaling factors for all significant dimensions and forces for designing and analysing floating wind turbine models are given.

Based on these scaling laws practical recommendations are given for the building of a test model, the usage of different materials and the testing instrumentation. On a real example it is illustrated how to define a test campaign and its load case definitions. A comprehensive test matrix with a detailed definition of all the test cases for a full scale 10 MW wind turbine is given in a spreadsheet. A description of each group of test cases, including the objective of each test and an explanation of how they have been defined is also provided.

The correct design of experimental floating wind turbine models is a difficult procedure due to the interaction of the regarded system with two different environments, wind and waves, which ask for counteracting scaling procedures. For the scaling of aerodynamic loading during combined wave and wind scaled tests at wave tank a new methodology has been presented. The introduced method uses a ducted fan governed by a real time computation of the full rotor coupled with the platform motions during the test. The so-called “Software-in-the-Loop” (SIL) approach enables to apply varying rotor thrust at the tower top of the floating model. Turbine control behaviour from previous simulations can be applied as well as wind gust loading. The SIL methodology has been applied to a semi-submersible floating wind turbine design in the ECN (Nantes) wave tank to verify its performance. The experimental results have been compared with computations and deliver in general good correspondence.

It is planned to apply it in the future test campaigns that will be carried out as part of the INN WIND.EU activities. The results obtained in these future experiments will be useful to further validate the method. The methodology is very promising, furthermore, considering the low cost of the system and its versatility to be used in different test campaigns.

Another approach for modelling aerodynamic forces and coupled rotor dynamic effects is the application of a specific test rotor for low Reynolds numbers which keeps roughly the tip-speed ratio and the Froude number. While the hydrodynamic interactions can be correctly scaled using a constant ratio of the gravitational and inertial forces, aerodynamic interactions are usually scaled using a constant Reynolds number and thus maintaining the ratio between viscous and inertial forces. Because both scaling methods cannot be satisfied in one and the same system, the rotor has been adjusted so that the dynamic response of the rotor is scaled adequately. This report presents an analysis of this optimisation task. Further tests performed at Polimi Laboratories with a low Reynolds number rotor in a wind tunnel showed good agreements with the simulations.

Finally requirements and recommendations for the design and numerical modelling of mooring and station keeping systems are given. A selection of standards from the offshore wind and oil&gas is provided which are suitable for certification.